AD NUMBER

ADB955265

NEW LIMITATION CHANGE

TO

Approved for public release, distribution unlimited

FROM

Distribution limited to DoD only; Software Documentation; Oct 83. Other requests must be referred to AFWAL/FIBED, Wright-Patterson AFB, OH 45433.

AUTHORITY

AFRL ltr., 14 Sep 99

AFWAL-TR-83-3072

DYNAMIC STABILITY OF BEAMS IN A COMBINED THERMAL-ACOUSTIC ENVIRONMENT

Paul Seide and Cyrous Adami

Department of Civil Engineering
University of Southern California
Los Angeles CA 90007

Oct 1983

SUBJECT TO EXPORT CONTROL LAWS

This document contains information for manufacturing or using munitions of war. Export of the information contained herein, or release to foreign nationals within the United States, without first obtaining an export license, is a violation of the International Traffic-in-Arms Regulations. Such violation is subject to a penalty of up to 2 years imprisonment and a fine of $100,000 under 22 USC 2778.

Include this notice with any reproduced portion of this document.

Distribution limited to DOD components only: ~~computer~~ software; October 1983. Non-DOD requests for this document must be referred to AFWAL/FIBEC, WPAFB, OH 45433, and must include the statement of terms and conditions contained in Atch 21 to AFR 300-6.

FLIGHT DYNAMICS LABORATORY
AIR FORCE WRIGHT AERONAUTICAL LABORATORIES
AIR FORCE SYSTEMS COMMAND
WRIGHT-PATTERSON AIR FORCE BASE, OHIO 45433

NOTICE

When Government drawings, specifications, or other data are used for any purpose other than in connection with a definitely related Government procurement operation, the United States Government thereby incurs no responsibility nor any obligation whatsoever; and the fact that the government may have formulated, furnished, or in any way supplied the said drawings, specifications, or other data, is not to be regarded by implication or otherwise as in any manner licensing the holder or any other person or corporation, or conveying any rights or permission to manufacture use, or sell any patented invention that may in any way be related thereto.

This technical report has been reviewed and is approved for publication.

Howard F. Wolfe

HOWARD F. WOLFE, Technical Manager
Acoustics and Sonic Fatigue Group
Structural Integrity Branch

Davey L. Smith

DAVEY L. SMITH, Chief
Structural Integrity Branch
Structures and Dynamics Division

FOR THE COMMANDER

Ralph L. Kuster, Jr.

RALPH L. KUSTER, JR., COL, USAF
Chief, Structures and Dynamics Division
Flight Dynamics Laboratory

"If your address has changed, if you wish to be removed from our mailing list, or if the addressee is no longer employed by your organization please notify AFWAL/FIBED *W-PAFB, OH 45433 to help us maintain a current mailing list".*

Copies of this report should not be returned unless return is required by security considerations, contractual obligations, or notice on a specific document.

SECURITY CLASSIFICATION OF THIS PAGE (When Data Entered)

REPORT DOCUMENTATION PAGE

READ INSTRUCTIONS BEFORE COMPLETING FORM

1 REPORT NUMBER	2. GOVT ACCESSION NO.	3. RECIPIENT'S CATALOG NUMBER
AFWAL-TR-83-3072		

4. TITLE (and Subtitle)	5. TYPE OF REPORT & PERIOD COVERED
DYNAMIC STABILITY OF BEAMS IN A COMBINED THERMAL-ACOUSTIC ENVIRONMENT	Final Technical Report Oct 1978 - Oct 1982
	6. PERFORMING ORG. REPORT NUMBER
7. AUTHOR(s)	8. CONTRACT OR GRANT NUMBER(s)
Paul Seide, Cyrous Adami	AFOSR-79-0013
9. PERFORMING ORGANIZATION NAME AND ADDRESS Department of Civil Engineering University of Southern Califronia Los Angeles CA 90007	10. PROGRAM ELEMENT, PROJECT, TASK AREA & WORK UNIT NUMBERS P.E. 61102F 2307N113
11 CONTROLLING OFFICE NAME AND ADDRESS Air Force Wright Aeronautical Laboratory Air Force Systems Command Wright-Patterson Air Force Base OH 45433	12. REPORT DATE Oct 1983 13. NUMBER OF PAGES 126
14 MONITORING AGENCY NAME & ADDRESS(if different from Controlling Office)	15. SECURITY CLASS. (of this report) Unclassified 15a. DECLASSIFICATION/DOWNGRADING SCHEDULE

16 DISTRIBUTION STATEMENT (of this Report)

Distribution limited to DOD components only: ~~computer~~ software DOCUMENTATION Oct 1983. Non DOD requests for this document must be referred to AFWAL/FIBED, WPAFB OH 45433, and must include the statement of terms and conditions contained in Atch 21 to AFR 300-6.

17 DISTRIBUTION STATEMENT (of the abstract entered in Block 20, if different from Report)

18 SUPPLEMENTARY NOTES

19. KEY WORDS (Continue on reverse side if necessary and identify by block number)

thermal loads	beam snap through
acoustic loads	random loading
oil canning	RMS beam response
beam buckling	nonlinear structures

20. ABSTRACT (Continue on reverse side if necessary and identify by block number)

The present report describes a number of studies carried out to further understanding of the phenomenon of snap-through of initially buckled beams under random loading. The most significant of these involves the numerical integration of the equations of motion with the use of a computer generated random loading function. The results lead to a definition of a critical power spectral density of th loading as the value for which the average zero-crossing frequency of sponse becomes very small or zero and to an

DD FORM 1 JAN 73 1473 EDITIO

SECURITY CLASSIFICATION OF THIS PAGE (When Data Entered)

Block #20

estimate of the critical value. The required calculations are lengthy and costly and point up the need for better analytical techniques for highly nonlinear structures.

E-4

TABLE OF CONTENTS

NOMENCLATURE

A	area of beam cross-section
d	amount by which beam ends are moved together
d_{cr}	end shortening which first produces beam buckling
E	Young's modulus of beam material
f	average zero-crossing frequency of beam
h	distance from centroidal axis to outermost beam fibers
I	moment of inertia of beam cross-section about centroidal axis perpendicular to plane of bending
$\bar{I}$	nondimensional impulse pressure loading
L	beam length
N	axial load, positive in compression
N_{cr}	axial compressive buckling load of beam
N_0	initial axial compressive load in beam
$\bar{N}$	nondimensional axial compressive load parameter $(\frac{A/L^2}{\pi^2 EI})$
$\bar{N}_0$	nondimensional initial compressive load parameter $(\frac{N_0 L}{\pi^2 EI})$
p	uniform tranverse pressure
$\bar{p}$	nondimensional transverse pressure parameter $(\frac{4}{\pi^5}\frac{pL^4}{EIr})$
$\bar{p}_0$	nondimensional time average of random pressure distribution
r	radius of gyration of beam cross-section $(\sqrt{I/A})$
S_0	power spectral density of white noise pressure history
$\bar{S}_0$	nondimensional power spectral density parameter $(\frac{32}{\pi^7}\frac{L^6}{E^2 I^2}\sqrt{\frac{EA}{\rho I}}\,S_0)$
$\bar{S}$	alternate power spectral density parameter $(\frac{4}{\pi^5}\frac{S_0}{EA\beta};\frac{\bar{S}_0}{8\bar{\mu}})$
t	time
T	nondimensional time parameter $(\frac{\pi^2}{L^2}\sqrt{\frac{EI}{\rho A}}\,t)$
w	beam deflection from buckled equilibrium position
w_m	amplitude of m^{th} term in Fourier series expansion of w
w_0	amplitude of initial buckled shape
w_s	static deflection of buckled beam from straight reference axis

$\bar{w}_0, \bar{w}_m$	nondimensional deflection amplitude parameters $(\frac{w_0}{r}, \frac{w_m}{r})$
x	distance along beam
β	viscous damping coefficient of beam material
ΔL	additional changes of horizontal length of the beam if the ends were unrestrained
ΔL_0	initial change of horizontal length of buckled beam
ΔN	change in axial load due to beam bending
δ_{mn}	Kronecker delta (=0 if $m \neq n$, =1 if $m = n$)
$\bar{\mu}$	nondimensional viscous damping parameter $\frac{\beta L^2}{\pi^2\sqrt{\rho A E I}}$)
ρ	density of beam material
$\bar{\sigma}_{av}^{\pm}$	the average stress in beam outer fibers
$\sigma_{max}^{\pm}$	maximum stress in beam outer fibers
σ_0	standard deviation of white noise pressure distribution
$\bar{\sigma}_{av}^{\pm}$	average stress parameter at outermost fibers of beam $(\frac{\sigma_{av}}{\pi^2 E}(\frac{L}{r})^2)$
$\bar{\sigma}_{max}^{\pm}$	maximum stress parameter at outermost fibers of beam $(\frac{\sigma_{max}}{\pi^2 E}(\frac{L}{r})^2)$
$\bar{\sigma}_0$	nondimensional standard deviation parameter $(\frac{4}{\pi^5}\frac{\sigma_0 L^4}{EI_r})$
$\bar{\sigma}_{static}$	static stress parameter for initially buckled beam

INTRODUCTION

Aircraft structural components such as engine air intake ducting and rear fuselage and empennage structures which are located in the vicinity of jet engine exhausts experience combined heating and random dynamic excitation which result from the acoustic or pseudoacoustic noise emitted by the jet efflux. In addition, in the VTOL and V/STOL operational modes of projected advanced aircraft, combined thermal and acoustic environments can be expected in areas of the wing and/or fuselage structure — the locations and magnitudes being highly dependent upon vehicle/engine configurations. The combined thermal-acoustic environment can also occur in different operational modes of re-entry vehicles such as the space shuttle.

A completely rigorous analytical method of obtaining the combined effects of thermal and acoustic loading is unavailable. Therefore, present design practices rely heavily on component testing in a simulated envirionment. Such tests, however, which are more in the nature of qualification tests, generally do not yield quantitative data. A program to obtain a better quantitative measure of the effects of the thermal-acoustic environment has been described in reference 1. Among the qualitative phenomena which have been revealed experimentally by that investigation is that there are limited ranges of temperature and acoustic environment which cause violent oil-canning vibrations of plate structures. If the sound pressure level of the random acoustic environment is kept constant and the

steady-state temperature is increased, the RMS strain response was observed to increase slowly until some "critical" temperature was reached beyond which oil-canning vibrations occurred and the RMS strain response increased rapidly at first. As the steady-state temperature was further increased, the RMS strain response reached a peak value and then decreased rapidly to some value lower than the pre-critical level. The large stress reversals that occur during oil-canning vibrations in sufficiently high intensity acoustic environments can lead to early fatigue failure.

The phenomenon is readily explained in a qualitative fashion as a consequence of buckling of the plate due to the thermal environment. As the steady-state temperature and the inplane compressive thermal stresses increase, the stiffness of the plate decreases until buckling occurs. If the temperature is somewhat higher, the plate would be in equilibrium in slightly deflected positions on either side of the flat reference position and the acoustic load causes oil-canning from one to the other. As the steady-state temperature and hence the amplitude of the static buckled configureation increases, however, the energy level of the acoustic loading becomes insufficient to produce oil-canning vibrations. A quantitative description of this phenomenon and of the regions of critical thermal-acoustic environment interaction is lacking, however.

Although the experimental data obtained in reference 1 were used to define a region of instability, the data are insufficient to inspire confidence in the accuracy or reasonableness of the semi-empirical criterion. The implication of this criterion is that oil-canning will occur only when the amplitude of the buckle is between 1.5 and 6 times the predicted

RMS deflection of the uncompressed plate under uniform random pressure, provided the RMS deflection is greater than 0.3 times the plate thickness. While the upper limit is possible, there does not appear to be any valid reason for the lower limit to exist. Since the RMS value of deflection is roughly related to the square root of the power spectral density of the laoding intensity, the criterion would appear to preclude snap-through for very high loading intensity.

A perusal of the literature indicates that the only analytical investigation of a similar problem is available in reference 2. Here the interest centers on the time required for the maximum deflection of a simply supported curved arch to *first* reach or exceed a certain critical value. The method used in reference 2 can be described as an "experimental" one since the equation of motion of the arch, represented by that for an equivalent single-degree-of-freedom system, is integrated numerically for loadings given by a random-number generator. Enough of these numerical experiments are conducted to yield a curve of the probability of first-passage snap-through at a given time as a function of time. The response of axially compressed initially buckled beams to deterministic transverse load has been discussed in a number of papers. The buckling and snap-through behavior of steep buckled simply supported beams under concentrated and uniform static transverse loading is investigated in reference 3. The snap-through of shallow buckled clamped beams due to harmonic support excitation was studied in reference 4. In references 5 to 8 results for the small large amplitude free vibrations of buckled beams are given. The response of such structures to random loading has not been studied however.

In view of the meager available literature on the problem, an investigation of the response of initially buckled beams was undertaken through AFOSR Grant No. 79-0013 with the University of Southern California. The present report describes the work done toward further understanding of the phenomenon. A number of investigations were carried out and are presented as separate sections. Included are investigations of the dynamic buckling of initially buckled simply supported beams under deterministic load, Monte Carlo determination of first snap-through probability, calculated RMS response under simulated random loading and comparison with the results of the method of equivalent linearization. Equivalent linearization and actual experimental results for clamped beams are also given.

Chapter 1

EQUATION OF MOTION

The equation of motion of an initially buckled beam is derived herein under the assumption of small strains, moderately large deflections, and negligible longitudinal inertia. A more rigorous derivation incorporating very large deflections and strains is given in reference 9 but is considered to be impractical for computational purposes.

Consider an initially straight beam whose ends are brought together a certain amount, d. If d is less than a critical value d_{cr}, the beam is compressed only and does not bend. The axial compressive load N_0 in the beam is less than the Euler buckling load and is given by

$$N_0 = EA\frac{d}{L} . \tag{1.1}$$

If, however, d is greater than d_{cr}, the beam buckles with a deflection $w_s(x)$. For relatively small buckle amplitudes the axial compressive load N_0 remains constant at the Euler buckling load N_{cr}.

For a simply supported beam the Euler buckling load is given by

$$N_{cr} = \frac{\pi^2 EI}{L^2} \tag{1.2}$$

The initial buckled shape is a half sine wave

$$w_s = w_0 \sin\frac{\pi x}{L} \tag{1.3a}$$

with an amplitude approximately given by

$$w_0 = \frac{2}{\pi}\sqrt{L(d-d_{cr})} \tag{1.3b}$$

and

$$d_{cr} = \frac{\pi^2 I}{AL^2} \tag{1.3c}$$

If the beam is clamped at both ends the Euler buckling load is now

$$N_{cr} = \frac{4\pi^2 EI}{L^2} \tag{1.4}$$

The initial buckled shape is given by

$$w_s = \frac{w_0}{2}\left(1-\cos\frac{2\pi x}{L}\right) \tag{1.5a}$$

with an initial amplitude given by Eq. (1.3b) where now

$$d_{cr} = \frac{4\pi^2 I}{AL^2} \tag{1.5b}$$

With the ends of the beam now fixed in the compressed position, the beam is next subjected to uniformly distributed time dependent loading (Fig. 1). The equation of motion of the beam, including viscous damping, is given by

$$EI\frac{\partial^4(w+w_s)}{\partial x^4} + N\frac{\partial^2(w+w_s)}{\partial x^2} + \rho A\frac{\partial^2 w}{\partial t^2} + \beta\frac{\partial w}{\partial t} + p = 0 \tag{1.6}$$

where w is the additional beam deflection and N is the axial compressive force exerted on the beam by the supports.

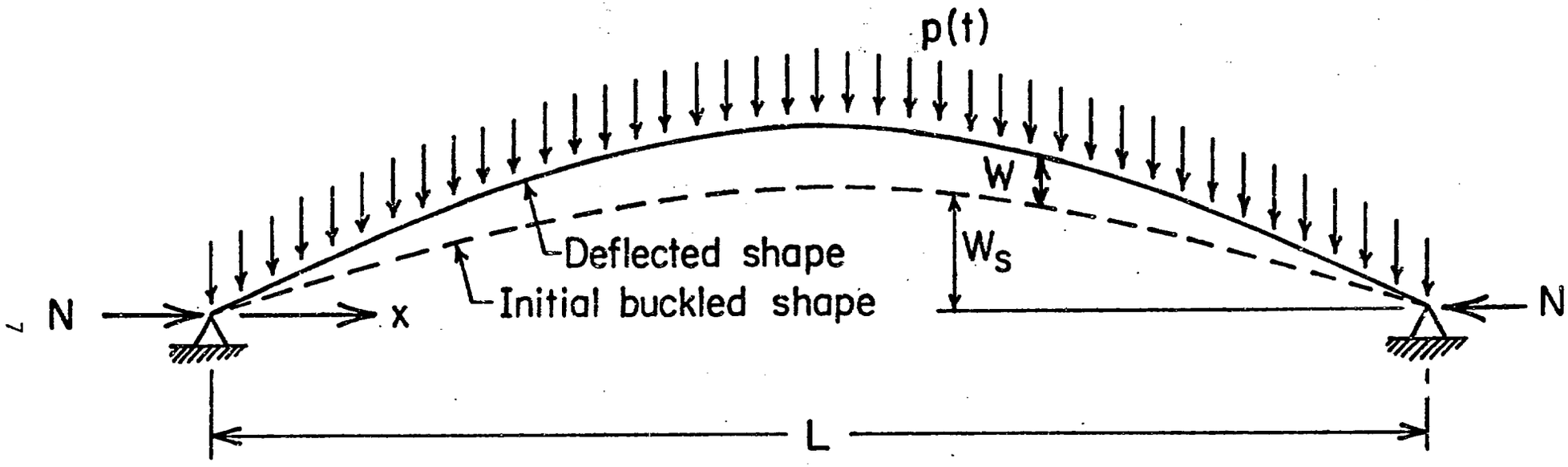

Fig. 1. Buckled Beam Subjected to Uniform Pressure

The change in the axial compressive force from its initial value N_0 is determined by the additional stretching or compression the beam undergoes during its motion. The amount by which the ends of the beam move together prior to motion is equal to the sum of the change of length due to the critical load and the amount by which the ends move together due to beam bending. Thus

$$\Delta L_0 = \frac{N_0 L}{EA} + \frac{1}{2}\int_0^L \left(\frac{dw_s}{dx}\right)^2 dx \tag{1.7}$$

where w_s vanishes if N_0 is less than N_{cr}. With w_s given by Eqs.(1.3a) or (1.5a), Eq.(1.7) yields the result of Eq.(1.3b). When the beam deflects from its static position, the beam ends would tend to move, were they not fixed in position, an additional amount equal to

$$\Delta L = \frac{1}{2}\int_0^L \left\{\left[\frac{\partial}{\partial x}(w+w_s)\right]^2 - \left(\frac{dw_s}{dx}\right)^2\right\} dx \tag{1.8}$$

This change of position must be negated by stretching the beam by an axial tensile force given by

$$\Delta N = \frac{EA\Delta L}{L} = \frac{EA}{2L}\int_0^L \frac{\partial w}{\partial x}\left(\frac{\partial w}{\partial x} + 2\frac{dw_s}{dx}\right) dx \tag{1.9a}$$

Thus

$$N = N_0 - \frac{EA}{2L}\int_0^L \frac{\partial w}{\partial x}\left(\frac{\partial w}{\partial x} + 2\frac{dw_s}{dx}\right) dx \tag{1.9b}$$

For a simply supported initially buckled beam, let the additional dynamic deformation be given by

$$w = \sum_{m=1}^{\infty} w_m \sin \frac{m\pi x}{L} \tag{1.10}$$

Then the equations for the time dependence of the coefficients w_m may be obtained by substitution in Eq.(1.6) to yield, in nondimensional form,

$$\frac{d^2\bar{w}_m}{d\bar{T}^2} + \bar{\mu}\frac{d\bar{w}_m}{d\bar{T}} + (m^2-\bar{N})m^2(\bar{w}_m+\bar{w}_0\delta_{m1}) = -\frac{\bar{p}}{m} \qquad m = 1,3,5... \tag{1.11a}$$

$$\frac{d^2\bar{w}_m}{d\bar{T}^2} + \bar{\mu}\frac{d\bar{w}_m}{d\bar{T}} + (m^2-\bar{N})m^2\bar{w}_m = 0 \qquad m = 2,4,6... \tag{1.11b}$$

with

$$\bar{N} = \bar{N}_0 + \frac{1}{4}\bar{w}_0^2 - \frac{1}{4}\sum_{n=1}^{\infty} n^2(\bar{w}_n+\bar{w}_0\delta_{n1})^2 \tag{1.11c}$$

The nature of the equations is best illustrated by considering only the term for m equal to unity. Then Eqs.(1.11) reduce to

$$\frac{d^2\bar{w}_1}{d\bar{T}^2} + \bar{\mu}\frac{d\bar{w}_1}{d\bar{T}} + \frac{1}{4}\bar{w}_1(\bar{w}_1+\bar{w}_0)(\bar{w}_1+2\bar{w}_0) = -\bar{p} \tag{1.12}$$

which is of the form of the equation of motion of a mass-spring system with a nonlinear spring stiffness. The restoring spring force is shown as a function of $\bar{w}_1/\bar{w}_0$ in Fig. 2. The spring resistance is of the softening type as $\bar{w}_1$ decreases from 0 and is actually destabilizing when

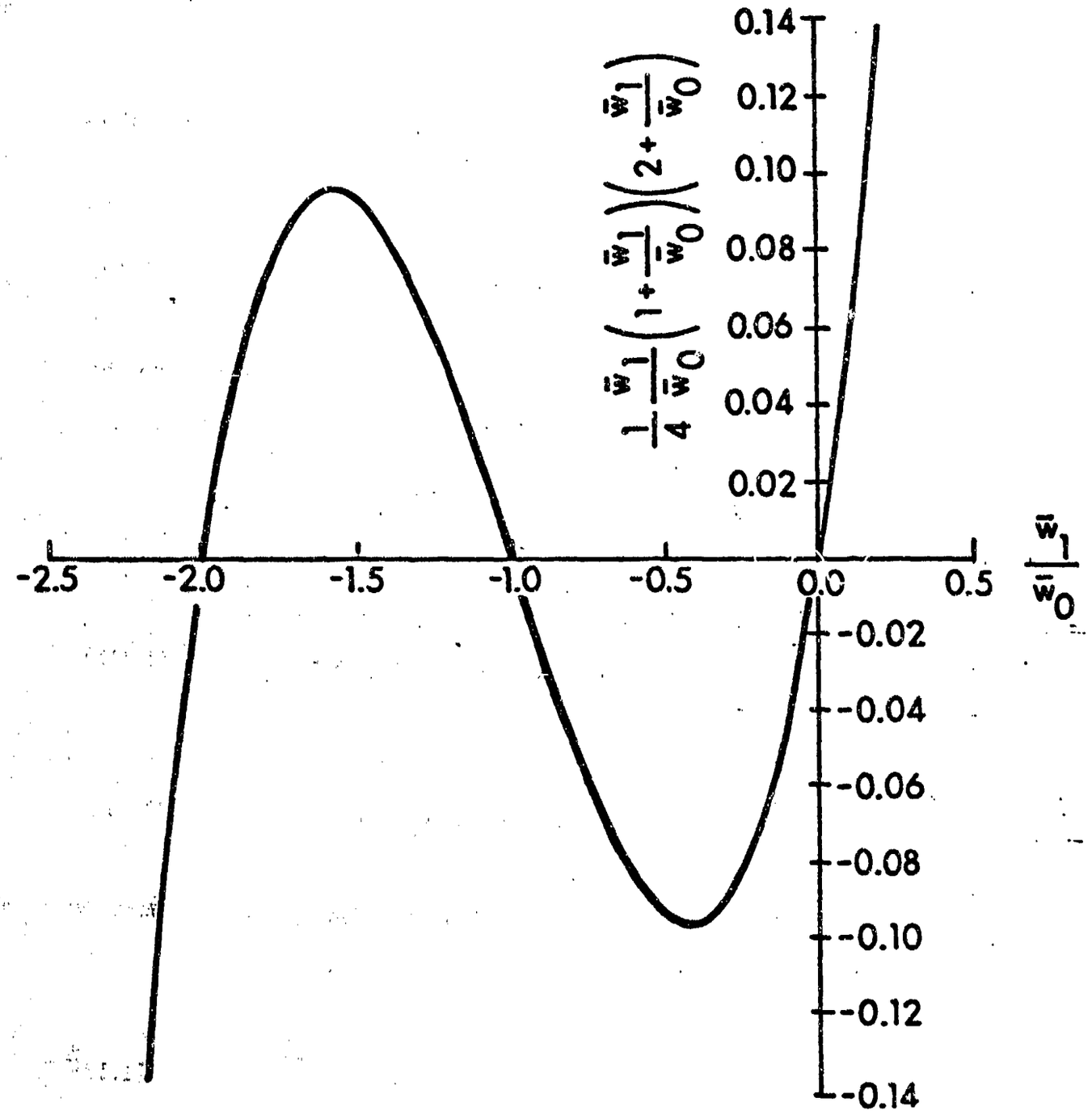

Fig. 2. One Mode Approximation to Beam Restoring Force

the beam becomes susceptible to snap-through from the buckled position on one side of the initially straight axis to the buckled position on the other side. Thus the beam would be expected to vibrate about the static buckled position for small excitations but to snap back and forth between the two equilibrium positions for larger excitations.

The succeeding chapters describe various investigations performed with the use of these equations.

Chapter 2

DYNAMIC STABILITY OF SIMPLY SUPPORTED INITIALLY BUCKLED BEAMS UNDER DETERMINISTIC LOADING

In order to get some idea of the order of magnitude of pressures to be considered, the dynamic stability of initially buckled beams under deterministic loading is investigated first. The analysis of snap-through under time-dependent loading is approximate and is similar to the investigation presented in reference 10 for shallow arches. The theory is limited to consideration of a single term in the series expansion of the deflection function for symmetric snap-through and to two terms for asymmetric snap-through. In the latter case the assumption is made that the minimum critical pressure is that for which the trajectory of motion passes through the saddle-point with zero velocity and is equivalent to an energy criterion for instability. The accuracy of the limitation of the deflection function and of the energy criterion has been investigated for shallow arches in references 11 and 12. It was concluded that while the accuracy of the results is limited, especially in the case of impulse type loading, the numbers obtained are reasonable "ball-park" estimates of critical pressure loadings and require, of course, considerably less computation than that involved in step-by-step integration of the coupled equations of motion for multiple series terms.

For the investigation of dynamic stability of initially buckled simply supported beams under deterministic loading, Eqs.(1.11) are used with the damping parameter taken as zero and only $\bar{w}_1$ and $\bar{w}_2$ retained in the infinite series of Eq.(1.10). Then the pertinent equations of motion reduce to

$$\frac{d^2\bar{w}_1}{dT^2} = -\bar{p} + \frac{1}{4}(\bar{w}_1+\bar{w}_0)[\bar{w}_0^2-(\bar{w}_1+\bar{w}_0)^2-4\bar{w}_2^2] \tag{2.1a}$$

$$\frac{d^2\bar{w}_2}{dT^2} = [\bar{w}_0^2-(\bar{w}_1+\bar{w}_0)^2-4\bar{w}_2^2-12]\bar{w}_2 \tag{2.1b}$$

With these equations, a number of approximate, but reasonably accurate, results may be obtained for some deterministic loadings of initially buckled beams.

2.1 Static Buckling

If dynamic effects are omitted, the symmetric load-deflection response of the beam is given by Eqs.(2-3a) as

$$\bar{p} = \frac{1}{4}(\bar{w}_1+\bar{w}_0)[\bar{w}_0^2-(\bar{w}_1+\bar{w}_0)^2] \tag{2.2}$$

yielding a center deflection which decreases from $\bar{w}_0$ as $\bar{p}$ increases from zero. The load reaches a maximum when

$$\frac{\partial\bar{p}}{\partial(\bar{w}_1+\bar{w}_0)} = 0 = \bar{w}_0^2-3(\bar{w}_1+\bar{w}_0)^2 \tag{2.3a}$$

from which

$$\bar{w}_1+\bar{w}_0 = \frac{\bar{w}_0}{\sqrt{3}} \tag{2.3b}$$

Then the critical value of $\bar{p}$ is given by Eqs.(2.2) and (2.3b) as

$$\bar{p} = \frac{\bar{w}_0^3}{6\sqrt{3}} \tag{2.4}$$

At this value of load the beam snaps through to an equilibrium position on the other side of the unbuckled beam axis.

A solution incorporating all of the symmetric terms of Eq.(1.10) can be obtained as well. Equations (1.11) for the static loading become

$$(\bar{N}-1)(\bar{w}_0+\bar{w}_1) = \bar{p} \tag{2.5a}$$

$$(\bar{N}-m^2)m^2\bar{w}_m = \frac{\bar{p}}{m} \qquad m = 3,5,\ldots \tag{2.5b}$$

Solution of Eqs.(2.5) and substitution in Eq.(1.11c) then yields a transcendental equation for $\bar{N}$ as

$$\bar{N} = 1 + \frac{1}{4}\bar{w}_0^2 - \frac{1}{4}\bar{p}^2 \sum_{m=1,3,5}^{\infty} \frac{1}{(\bar{N}-m^2)^2 m^4}$$

$$= 1 + \frac{1}{4}\bar{w}_0^2 - \frac{\pi^2}{64}\frac{\bar{p}^2}{\bar{N}^2}\left[\frac{\pi^2}{6} + \frac{1}{\bar{N}}\left(4-5\,\frac{\tan\frac{\pi}{2}\sqrt{\bar{N}}}{\frac{\pi}{2}\sqrt{\bar{N}}} + \sec^2\frac{\pi}{2}\sqrt{\bar{N}}\right)\right] \tag{2.6a}$$

or

$$\bar{p} = \frac{8\bar{N}}{\pi}\sqrt{\frac{1+\frac{1}{4}\bar{w}_0^2-\bar{N}}{\frac{\pi^2}{6} + \frac{1}{\bar{N}}\left(4-5\,\frac{\tan\frac{\pi}{2}\sqrt{\bar{N}}}{\frac{\pi}{2}\sqrt{\bar{N}}} + \sec^2\frac{\pi}{2}\sqrt{\bar{N}}\right)}} \tag{2.6b}$$

The maximum value of $\bar{p}$ occurs, for a given value of $\bar{w}_0$, when $d\bar{p}/d\bar{N}$ vanishes or when

$$1 + \frac{1}{4}\bar{w}_0^2 = \bar{N}\,\frac{\dfrac{\pi^2}{4} + \dfrac{1}{\bar{N}}\left(8 - \dfrac{45}{4}\,\dfrac{\tan\frac{\pi}{2}\sqrt{\bar{N}}}{\frac{\pi}{2}\sqrt{\bar{N}}} + \dfrac{13}{4}\sec^2\frac{\pi}{2}\sqrt{\bar{N}} - \dfrac{1}{2}\,\dfrac{\frac{\pi}{2}\sqrt{\bar{N}}\tan\frac{\pi}{2}\sqrt{\bar{N}}}{\cos^2\frac{\pi}{2}\sqrt{\bar{N}}}\right)}{\dfrac{\pi^2}{6} + \dfrac{1}{\bar{N}}\left(6 - \dfrac{35}{4}\,\dfrac{\tan\frac{\pi}{2}\sqrt{\bar{N}}}{\frac{\pi}{2}\sqrt{\bar{N}}} + \dfrac{11}{4}\sec^2\frac{\pi}{2}\sqrt{\bar{N}} - \dfrac{1}{2}\,\dfrac{\frac{\pi}{2}\sqrt{\bar{N}}\tan\frac{\pi}{2}\sqrt{\bar{N}}}{\cos^2\frac{\pi}{2}\sqrt{\bar{N}}}\right)} \tag{2.7}$$

Equations (2.6b) and (2.7) are thus parametric equations for the maximum value of $\bar{p}$ as a function of $\bar{w}_0$.

Rather than solve Eq.(2.7) for given values of $\bar{w}_0$, the error of the approximate solution given by Eq.(2.4) may be indicated by assuming values of $\bar{N}$ and calculating the corresponding value of $\bar{w}_0$ from Eq.(2.7). This value of $\bar{w}_0$ is then used in Eqs.(2.6) and (2.8b) to obtain approximate and "exact" values of $\bar{p}_{max}$. The range of values of $\bar{N}$ that may be considered in Eq.(2.7) is $1 \leq \bar{N} \leq 7.4981$. At the lower limit $\bar{w}_0$ is equal to zero, while at the upper limit the denominator of the right side of Eq.(2.7) vanishes so that $\bar{w}_0$ is infinite. The results of calculations made with Eqs.(2.4), 2.6b), and (2.7) are shown in Fig. 3. It is readily seen that the one term approximation and the exact solution yield almost identical results so long as $\bar{w}_0$ is less than about 6. For large values of $\bar{w}_0$ the exact solution is approximated by

$$\bar{p} = 5.856\,\bar{w}_0 \tag{2.8}$$

so that the exact and approximate solutions rapidly diverge.

As $\bar{w}_0$ increases it is possible that buckling may occur in an antisymmetric mode. The equation of motion for $\bar{w}_2$ is given by Eq.(1.11b) as

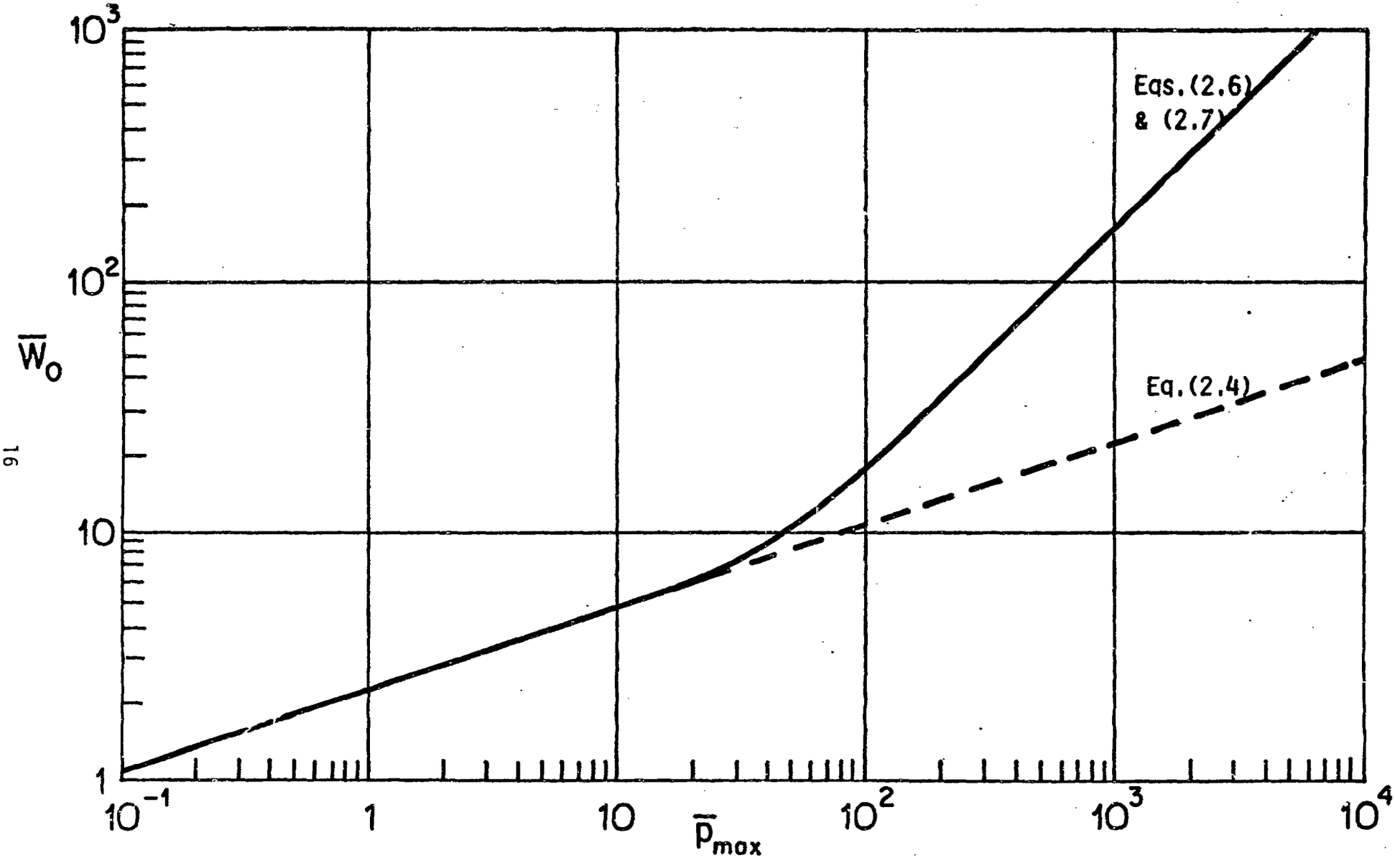

Fig. 3. Comparision of Exact and Approximate Static Snap-Through Pressures

$$\frac{d^2\bar{w}_2}{d\bar{T}^2} = 4(\bar{N}-4)\bar{w}_2 \tag{2.9}$$

So long as the coefficient of $\bar{w}_2$ or the right side of Eq.(2.9) is negative, a small antisymmetric disturbance remains small; when the coefficient becomes positive, however, the antisymmetric motion is unstable. Buckling in an antisymmetric mode thus can first occur if the coefficient of $\bar{w}_2$ in Eq.(2.9) vanishes, i.e., when

$$\bar{N} = 4 \tag{2.10}$$

for which the critical value of $\bar{p}$ is given by Eq.(2.6b) as

$$\bar{p} = \sqrt{\bar{w}_0^2-12}\ \frac{\frac{16}{\pi}}{\sqrt{\frac{\pi^2}{6}+\frac{5}{4}}} = 2.9933\sqrt{\bar{w}_0^2-12} \tag{2.11a}$$

Equation (2.11a) is valid if the value of $\bar{N}$ is less than the value at which snap-through occurs. Then Eq.(2.7) with $\bar{N}$ equal to 4 yields

$$\bar{w}_0 > 2\sqrt{5\,\frac{87+8\pi^2}{105+8\pi^2}} = 4.2477 \tag{2.11b}$$

The one term approximation yields the result

$$\bar{p} = 3\sqrt{\bar{w}_0^2-12} \tag{2.12a}$$

provided

$$\bar{w}_0 > \sqrt{18} = 4.2426 \qquad (2.12b)$$

which is in excellent agreement with the exact result.

It is interesting to compare the values obtained above with those of a shallow arch. which has a built-in initial shape identical to that of the buckled beam. The analysis of reference 10 yields the following critical pressures:

$$\bar{p} = \bar{w}_0 + \frac{1}{2}\left(\frac{\bar{w}_0^2-4}{3}\right)^{\frac{3}{2}} \qquad 2<\bar{w}_0<\sqrt{22} \qquad (2.13a)$$

$$\bar{p} = \bar{w}_0 + 3\sqrt{\bar{w}_0^2-16} \qquad \bar{w}_0>\sqrt{22} \qquad (2.13b)$$

For $\bar{w}_0$ less than 2, there is no snap-through and hence no critical pressure. The two sets of results are shown in Fig. 4 where it is seen that the buckled beam has a critical uniform pressure which is always less than that of the shallow arch. For values of $\bar{w}_0$ greater than about 4, the critical pressure of the buckled beam is about 25% less than that of the arch. If $\bar{w}_0$ is less than 4 the ratio of the critical load of the buckled beam to that of the shallow arch decreases. If $\bar{w}_0$ is 2, for example, the ratio is equal to 0.385.

2.2 Dynamic Buckling Due to Step Loading

Consider now the situation that occurs when the constant pressure is suddenly applied. If the deformation process is symmetric, with $\bar{p}$ constant a first integral of Eq.(2.1a) subject to the initial conditions of

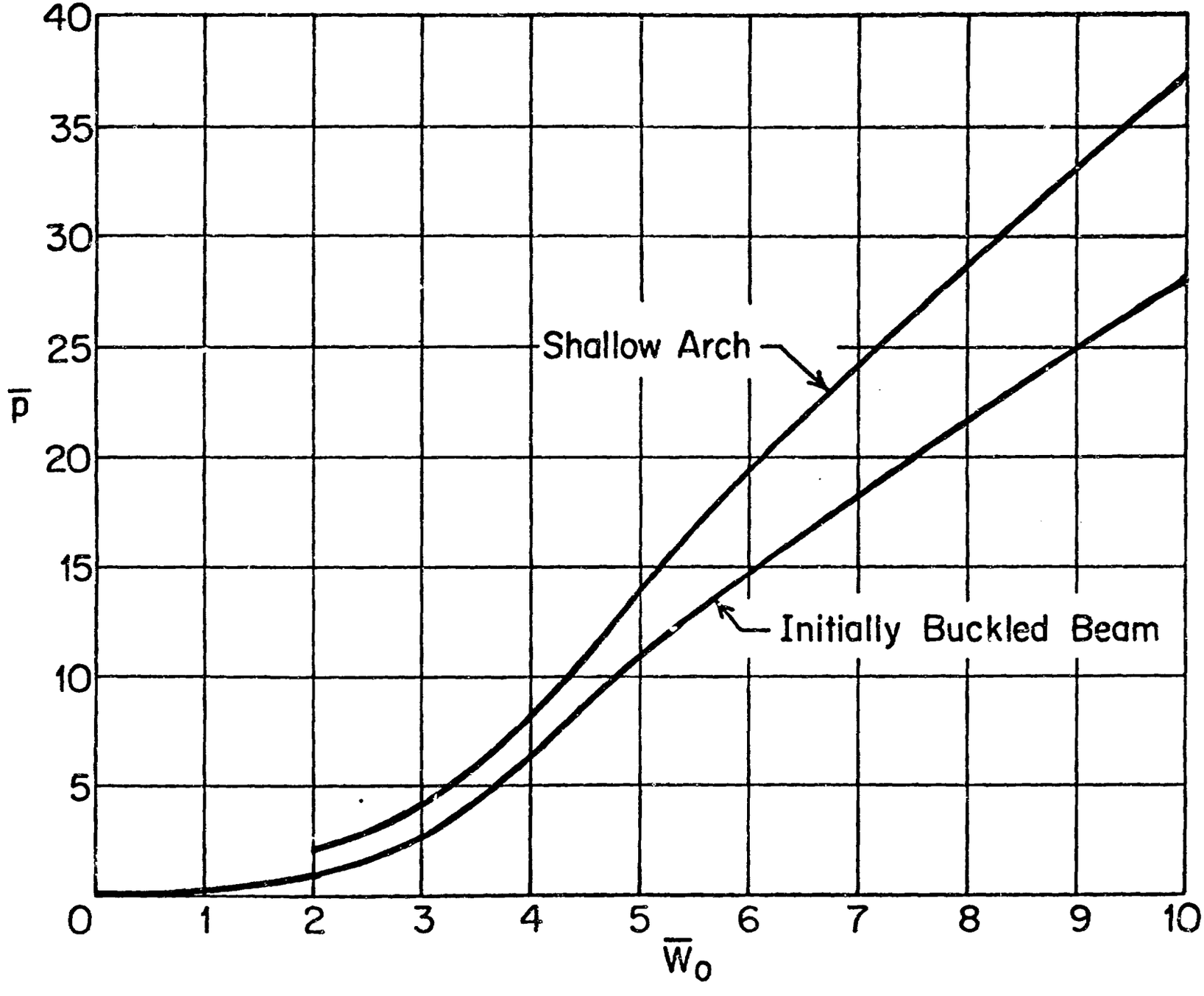

Fig. 4. Comparison of Static Critical Pressures for Buckled Beams and Shallow Arches

$$\bar{w}_1 = \frac{d\bar{w}_1}{d\bar{T}} = 0 \tag{2.14a}$$

is given by

$$\frac{1}{2}\left(\frac{d\bar{w}_1}{d\bar{T}}\right)^2 = -\bar{p}\bar{w}_1 - \frac{1}{16}\left[\bar{w}_0^2-(\bar{w}_1+\bar{w}_0)^2\right]^2 \tag{2.14b}$$

The minimum displacement is obtained when $d\bar{w}_1/d\bar{T}$ vanishes. Thus

$$\frac{16\bar{p}}{\bar{w}_0^3} = -\left[\left(\frac{\bar{w}_2}{\bar{w}_0}\right)^3 + 4\left(\frac{\bar{w}_1}{\bar{w}_0}\right)^2 + 4\left(\frac{\bar{w}_1}{\bar{w}_0}\right)\right] \tag{2.15}$$

The curve of $16\bar{p}/\bar{w}_0^3$ versus $\bar{w}_1/\bar{w}_0$ has a relative maximum at

$$\frac{\bar{w}_1}{\bar{w}_0} = -\frac{2}{3} \tag{2.16a}$$

at which

$$\bar{p} = \frac{2}{27}\,\bar{w}_0^3 \tag{2.16b}$$

For $\bar{p}$ less than that value, the beam vibrates with a minimum total displacement on the same side of the straight axis as the initial buckle. For $\bar{p}$ greater than that value, the beam has a minimum displacement which is beyond the buckled equilibrium position on the other side of the axis. Thus the critical value of $\bar{p}$ is given by Eq.(2.16b) which is 23% less than the value for static buckling given by Eq.(2.4).

It is possible, however, for dynamic buckling to occur by a combination of symmetric and antisymmetric motion. In this case the equations of

motion are given by Eqs.(2.1a) and (2.1b). A saddle point in the trajectories of constant potential energy occurs when the right sides of Eqs. (2.1) vanish, yielding

$$\bar{w}_0 + \bar{w}_1 = \frac{1}{3}\bar{p} \tag{2.17a}$$

$$\bar{w}_2^2 = \frac{1}{4}(\bar{w}_0^2 - \frac{1}{9}\bar{p}^2 - 12) \tag{2.17b}$$

If Eq.(2.17a) is multiplied by $d\bar{w}_1$, Eq.(2.17b) is multiplied by $d\bar{w}_2$ and the two are added, a first integral of the motion satisfying the initial conditions of zero velocity and displacement is

$$\frac{1}{2}\left[\left(\frac{d\bar{w}_1}{d\bar{\tau}}\right)^2 + \left(\frac{d\bar{w}_2}{d\bar{\tau}}\right)^2\right] = -\bar{p}\bar{w}_1 - \frac{1}{16}\left[\bar{w}_0^2 - (\bar{w}_0+\bar{w}_1)^2\right]^2 - \bar{w}_2^4 + \frac{1}{2}\bar{w}_2^2\left[\bar{w}_0^2 - (\bar{w}_0+\bar{w}_1)^2 - 12\right] \tag{2.18}$$

The minimum pressure for which snap-through will occur is that for which the trajectory of motion passes through the saddle point with zero velocity. The substitution of Eqs.(2.17) into the right side of Eq.(2.18) then yields

$$-\frac{\bar{p}^2}{6} + \bar{p}\bar{w}_0 + 9 - \frac{3}{2}\bar{w}_0^2 = 0 \tag{2.19a}$$

from which the critical pressure is obtained as

$$\bar{p} = 3(\bar{w}_0 - \sqrt{6}) \tag{2.19b}$$

The negative sign in Eq.(2.19b) is determined from the condition that the right side of Eq.(2.17b) must be positive, which also yields the result that Eq.(2.19b) is valid only if

$$\bar{w}_0 > \frac{3}{2}\sqrt{6} \tag{2.20}$$

At the value of $\bar{w}_0$ given by Eq.(2.20) the critical values of $\bar{p}$ given by Eqs.(2.16b) and (2.19b) are identical. It is interesting to note that as $\bar{w}_0$ increases, the critical step pressure approaches the critical static pressure. The ratio of the two varies from 0.77 for low values of $\bar{w}_0$ ($\bar{w}_0 < \frac{3}{2}\sqrt{6}$) to a minimum of 0.71 at $\bar{w}_0 = 2\sqrt{6}$ and thenceforth increases to unity. For $\bar{w}_0$ equal to 10, for example, the ratio is 0.80.

Equivalent critical pressures for the shallow arch may be obtained from reference 10 as

$$\bar{p} = \frac{1}{27}\left[\bar{w}_0^3 + 18\bar{w}_0 + (\bar{w}_0^2 - 6)^{\frac{3}{2}}\right] \qquad \frac{5}{3}\sqrt{6} > \bar{w}_0 > \sqrt{6} \tag{2.21a}$$

$$\bar{p} = 4(\bar{w}_0 - \sqrt{6}) \qquad \bar{w}_0 > \frac{5}{3}\sqrt{6} \tag{2.21b}$$

These are compared with the values given by Eqs. (2.16b) and (2.19b) in Fig. 5. It may be seen that the ratio of the critical pressure for the initially buckled beam and that of the shallow arch varies from 0.5 at $\bar{w}_0 = \sqrt{6}$ to 0.75 for $\bar{w}_0 > \frac{5}{3}\sqrt{6}$.

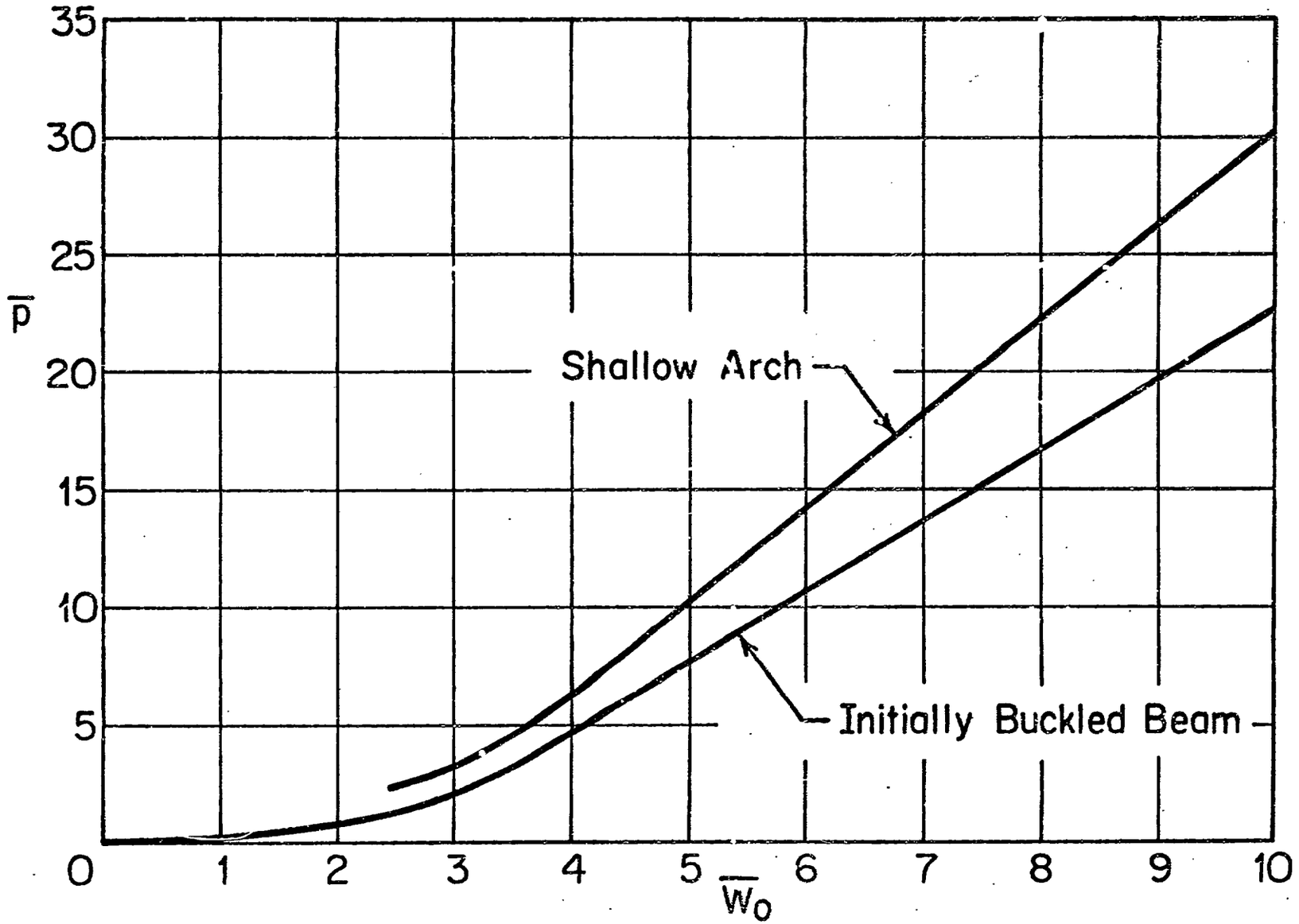

Fig. 5. Comparison of Critical Step-Loading Pressures for Buckled Beams and Shallow Arches

2.3 Dynamic Buckling Due to an Impulse Load

Consider now an impulse load given by

$$\bar{p} = \bar{I}\delta(T) \tag{2.22a}$$

where $\delta(T)$ is the Dirac delta function. From Eq.(2.1a) the initial velocity of the symmetric mode of deformation of the beam can be found to be

$$\frac{d\bar{w}_1}{dT} = -\bar{I} \tag{2.22b}$$

Integration of Eq.(2.1a) with $\bar{p}$ equal to zero and subject to the initial conditions

$$\frac{d\bar{w}_1}{dT} = -\bar{I}, \quad \bar{w}_1 = 0 \tag{2.23}$$

yields the velocity as

$$\left(\frac{d\bar{w}_1}{dT}\right)^2 = \bar{I}^2 - \frac{1}{8}\left[(\bar{w}_1+\bar{w}_0)^2-\bar{w}_0^2\right]^2 \tag{2.24}$$

The beam reaches its minimum position when $d\bar{w}_1/dT$ vanishes at

$$(\bar{w}_1+\bar{w}_0)^2 = \bar{w}_0^2 - 2\sqrt{2}\,\bar{I} \tag{2.25}$$

Snap-through will not occur so long as the minimum value of $\bar{w}_1+\bar{w}_0$ is greater than zero. Thus the critical value of $\bar{I}$ is

$$\bar{I}_{cr} = \frac{\bar{w}_0^2}{2\sqrt{2}} \tag{2.26}$$

If motion in an antisymmetric mode also occurs the equations of motion are given by Eqs.(2.1), with $\bar{p}$ given by Eq.(2.22a). A saddle point now occurs when

$$\bar{w}_0 + \bar{w}_1 = 0 \tag{2.27a}$$

$$\bar{w}_2^2 = \frac{1}{4}(\bar{w}_0^2 - 12) \tag{2.27b}$$

The first integral of the motion satisfying the initial conditions

$$\frac{d\bar{w}_1}{d\bar{T}} = -\bar{I}, \qquad \bar{w}_1 = \bar{w}_2 = \frac{d\bar{w}_2}{d\bar{T}} = 0 \tag{2.28}$$

is now

$$\frac{1}{2}\left[\left(\frac{d\bar{w}_1}{d\bar{T}}\right)^2 + \left(\frac{d\bar{w}_2}{d\bar{T}}\right)^2\right] = \frac{1}{2}\bar{I}^2 - \frac{1}{16}\left[\bar{w}_0^2 - (\bar{w}_0+\bar{w}_1)^2\right]^2 - \bar{w}_2^4$$

$$+ \frac{1}{2}\bar{w}_2^2\left[\bar{w}_0^2 - (\bar{w}_0+\bar{w}_1)^2 - 12\right] \tag{2.29}$$

Snap-through will occur if the trajectory passes through the saddle point. This will occur at a minimum impulse of

$$\bar{I} = \sqrt{3(\bar{w}_0^2 - 6)} \tag{2.30a}$$

Equation (2.27b) indicates that this solution is valid if

$$\bar{w}_0 > 2\sqrt{3} \tag{2.30b}$$

The corresponding expression for mixed mode buckling of a shallow arch can be obtained from reference 10 as

$$\bar{I} = \frac{1}{4}\sqrt{\bar{w}_0^4+40\bar{w}_0^2-32+\bar{w}_0(\bar{w}_0^2-16)^{3/2}} \qquad 3\sqrt{2} > \bar{w}_0 > 4 \qquad (2.31a)$$

$$\bar{I} = 4\sqrt{\frac{1}{3}(\bar{w}_0^2-6)} \qquad \bar{w}_0 > 3\sqrt{2} \qquad (2.31b)$$

The results given by Eqs.(2.26) and 2.30) for the initially buckled beam and by Eqs.(2.31) for the shallow arch are compared in Fig. 6. For sufficiently large values of the initial amplitude, the ratio of the critical impulses is given by

$$\frac{\bar{I}_{\text{initially buckled beam}}}{\bar{I}_{\text{shallow arch}}} = 0.75 \qquad (2.32)$$

2.4 Lowest Free Vibration Frequency

A final result that may be obtained is the lowest free vibration frequency of symmetric motion.

Let the beam be displaced and initially held at rest so that at time T equal to zero

$$\bar{w}_1(0) = \bar{w}_{10} > 0 \qquad (2.33a)$$

$$\frac{d\bar{w}_1(0)}{d\bar{T}} = 0 \qquad (2.33b)$$

Then the first integral of the equation of motion is given by

$$\left(\frac{d\bar{w}_1}{d\bar{T}}\right)^2 = \frac{1}{8}\left[(\bar{w}_{10}+\bar{w}_0)^2-(\bar{w}_1+\bar{w}_0)^2\right]\left[(\bar{w}_1+\bar{w}_0)^2+(\bar{w}_{10}+\bar{w}_0)^2-2\bar{w}_0^2\right] \qquad (2.34)$$

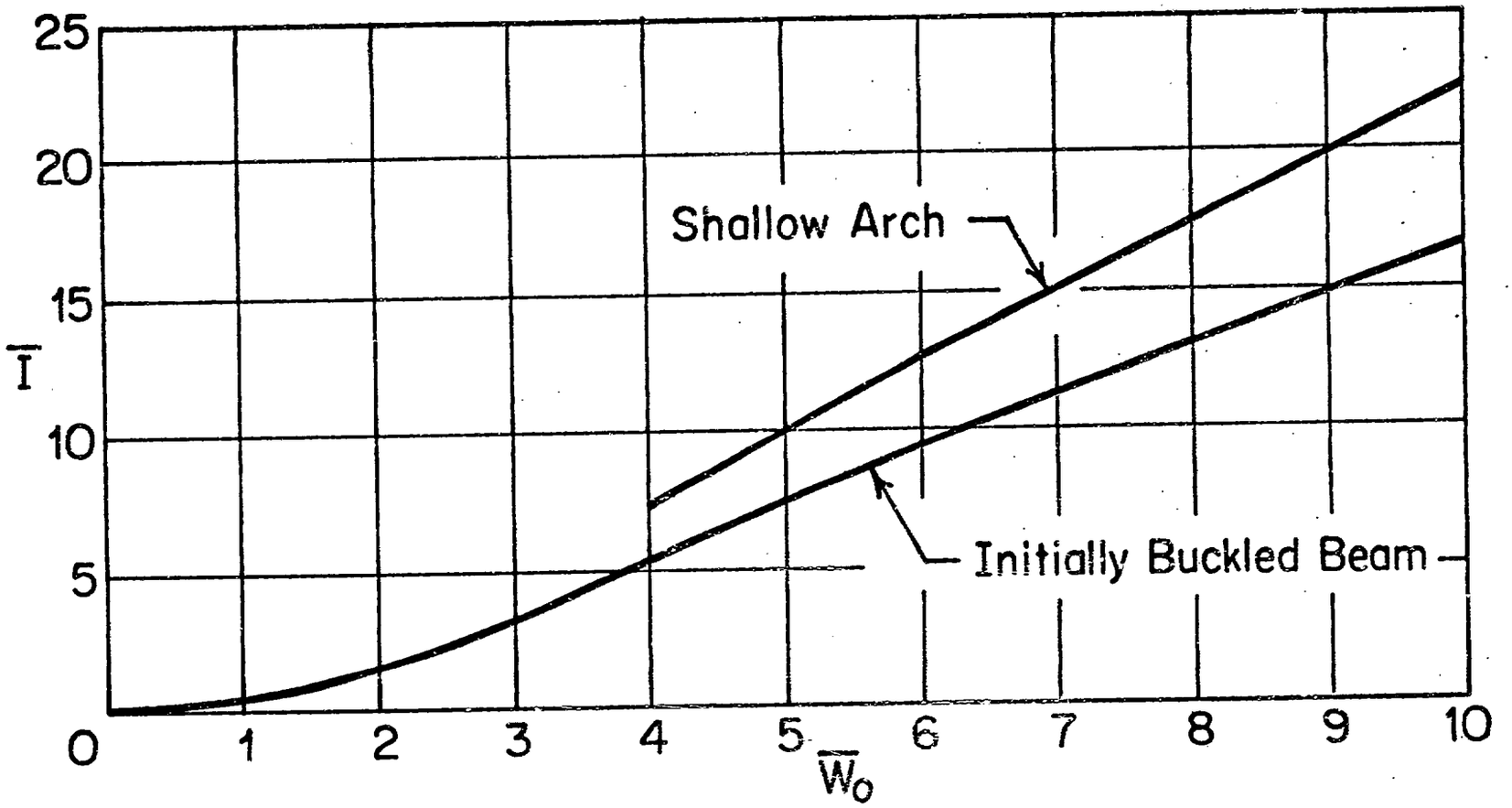

Fig. 6. Comparison of Critical Impulse Pressures for Buckled Beams and Shallow Arches

The solution of Eq.(2.34) is periodic and may be expressed as

$$T = \frac{\sqrt{2}}{\bar{w}_{10}+\bar{w}_0} F\left\{\sin^{-1}\sqrt{2\left[1-\left(\frac{\bar{w}_0}{\bar{w}_{10}+\bar{w}_0}\right)^2\right]},\ \sin^{-1}\sqrt{\frac{1-\left(\frac{\bar{w}_1+\bar{w}_0}{\bar{w}_{10}+\bar{w}_0}\right)^2}{\frac{1}{2}\left[1-\left(\frac{\bar{w}_0}{\bar{w}_{10}+\bar{w}_0}\right)^2\right]}}\right\} \tag{2.35a}$$

if $\bar{w}_{10} < (\sqrt{2}-1)\bar{w}_0$, and

$$T = \frac{1}{\sqrt{(\bar{w}_{10}+\bar{w}_0)^2-\bar{w}_0^2}} F\left\{\sin^{-1}\frac{1}{\sqrt{2\left[1-\left(\frac{\bar{w}_0}{\bar{w}_{10}+\bar{w}_0}\right)^2\right]}},\ \cos^{-1}\frac{\bar{w}_1+\bar{w}_0}{\bar{w}_{10}+\bar{w}_0}\right\} \tag{2.35b}$$

if $\bar{w}_{10} > (\sqrt{2}-1)\bar{w}_0$, where $F(\alpha,\phi)$ is an elliptic function of the first kind. The nondimensional period of vibration is then

$$\Delta T = \frac{2\sqrt{2}}{\bar{w}_{10}+\bar{w}_0} K\left\{\sin^{-1}\sqrt{2\left[1-\left(\frac{\bar{w}_0}{\bar{w}_{10}+\bar{w}_0}\right)^2\right]}\right\} \tag{2.36a}$$

if $\bar{w}_{10} \leq (\sqrt{2}-1)\bar{w}_0$ and

$$\Delta T = \frac{2}{\sqrt{(\bar{w}_{10}+\bar{w}_0)^2-\bar{w}_0^2}} K\left\{\sin^{-1}\frac{1}{\sqrt{2\left[1-\left(\frac{\bar{w}_0}{\bar{w}_{10}+\bar{w}_0}\right)^2\right]}}\right\} \tag{2.36b}$$

if $\bar{w}_{10} \geq (\sqrt{2}-1)\bar{w}_0$, with $K(\alpha)$ the complete elliptic function of the first kind. Since the nondimensional period ΔT is 2π for a straight unloaded simply supported beam, the frequency ratio may be written as

$$\frac{f}{f_0 \bar{w}_0} = \frac{\pi}{\sqrt{2}} \left(1 + \frac{\bar{w}_{10}}{\bar{w}_0}\right) \Bigg/ K\left\{\sin^{-1}\sqrt{2\left[1 - \frac{1}{\left(1 + \frac{\bar{w}_{10}}{\bar{w}_0}\right)^2}\right]}\right\} \tag{2.37a}$$

for $\bar{w}_{10}/\bar{w}_0 < \sqrt{2}-1$, and

$$\frac{f}{f_0 \bar{w}_0} = \pi \sqrt{\left(1 + \frac{\bar{w}_{10}}{\bar{w}_0}\right)^2 - 1} \Bigg/ K\left\{\sin^{-1}\frac{1}{\sqrt{2\left[1 - \frac{1}{\left(1 + \frac{\bar{w}_{10}}{\bar{w}_0}\right)^2}\right]}}\right\} \tag{2.37b}$$

for $\bar{w}_{10}/\bar{w}_0 > \sqrt{2}-1$. The results of these equations are shown graphically in Fig. 7. Note that the frequency vanishes when $\bar{w}_{10}/\bar{w}_0$ is equal to $\sqrt{2}-1$, but is extremely sensitive to amplitude of vibration. Identical results are implied by the analysis of reference 2 for clamped buckled beams.

If $\bar{w}_{10}/\bar{w}_0$ is less than $\sqrt{2}-1$, the beam oscillates about the buckled position with the minimum amplitude given by the value of $\bar{w}_1$ for which the argument of the elliptic integral in Eq.(2.35a) becomes equal to 90°. Then

$$\frac{\bar{w}_{1_{min}}}{\bar{w}_0} = \sqrt{2 - \left(1 + \frac{\bar{w}_{10}}{\bar{w}_0}\right)^2} - 1 \tag{3.38}$$

For $\bar{w}_{10}/\bar{w}_0 > \sqrt{2}-1$, the beam oscillates about the straight beam axis with its

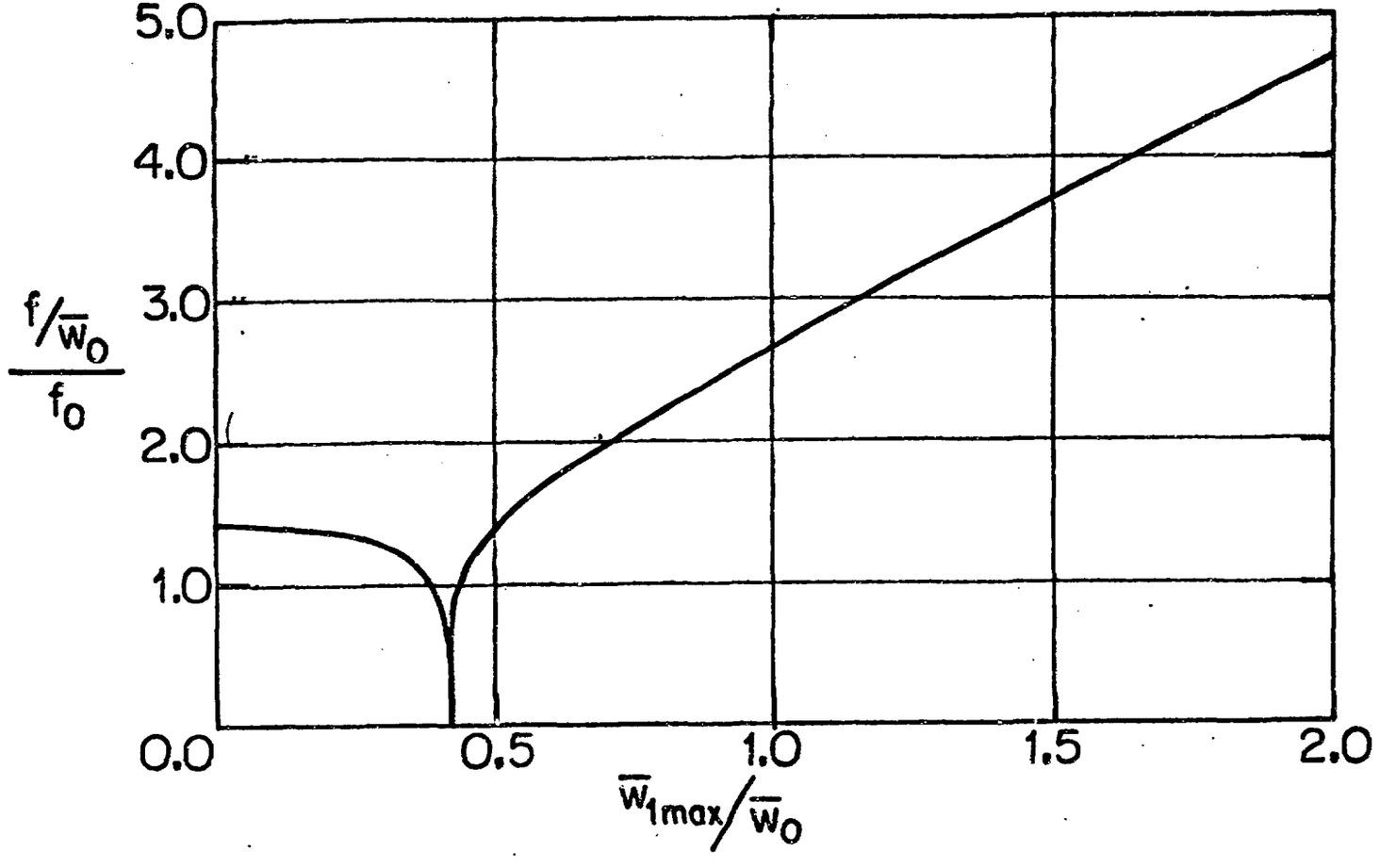

Fig. 7. Variation of Fundamental Frequency of Buckled Beam with Maximum Amplitude of Vibration

maximum negative deflection from the horizontal equal to the maximum positive deflection. These results have been derived in somewhat different form in references 5 to 8. The present form of the results is more compact, however.

Chapter 3

DYNAMIC STABILITY OF INITIALLY BUCKLED BEAMS UNDER UNIFORN RANDOM PRESSURE

An important consideration in the study of critical random loading of initially buckled beams is the definition of what constitutes instability and the method of calculation of that critical loading. If it is supposed that for low levels of spectral density of loading the beam vibrates about its buckled equilibrium position while at high levels of spectral density the beam snaps-through repeatedly and vibrates about its straight zero-deflection position, then presumably there is a critical value or range of spectral density value for which snap-through is first initiated.

In reference 2 the similar problem of snap-through of a shallow circle under random loading was studied by means of a one term approximation to the deflection function. With such an approximation it is possible to draw curves of constant energy and to define a critical value of energy which divides stable and unstable regions. The structure is then said to become unstable when the energy content, the sum of kinetic energy and strain energy of the structure, becomes equal to or exceeds this critical value. When many terms are considered an energy criterion is not readily discernible. Thus an alternate definition of instability is taken herein as the center deflection of the beam becoming less than zero. Such a criterion is implicit in the derivation of critical pressures for beams subjected to step-loading and impulse loading.

With this definition of instability it becomes necessary to integrate the equations of motion of the beam. The equations of motion for symmetric motion of a simple supported beam are given by Eqs.(1.11) as

$$\frac{d^2\bar{w}_m}{d\bar{T}^2} + \bar{\mu}\frac{d\bar{w}_m}{d\bar{T}} + [(2m-1)^2 - \bar{N}](2m-1)^2(\bar{w}_m + \bar{w}_0\delta_{m1})$$

$$= -\frac{\bar{p}}{2m-1} \qquad m = 1,2,3,... \tag{3.1a}$$

$$\bar{N} = \bar{N}_0 + \frac{1}{4}\bar{w}^2 - \frac{1}{4}\sum_{n=1}^{\infty}(2n-1)^2(\bar{w}_n + \bar{w}_0\delta_{n1})^2 \tag{3.1b}$$

To integrate these nonlinear equations of motion, a fourth-order Runge-Kutta method of numerical integration (reference 13) was used. A random loading function having a Gaussian distribution with a mean of zero and a specified deviation $\bar{\sigma}_0$ was generated. The loading function consists of steps which are constant over a given constant increment of time ΔT. A typical generated time history of loading is shown in Fig. 8. The statistics of the distribution have been studied in references 2 and 14 from which the value of the power spectral density parameter can be determined as

$$\bar{S}_0 = \bar{\sigma}_0^2\Delta T \tag{3.2}$$

In the numerical integration process, the constant integration time step was taken as some integral division of ΔT, generally $\Delta T/5$. The number of terms in the Fourier series expansion of the deflection function was taken as three in all cases.

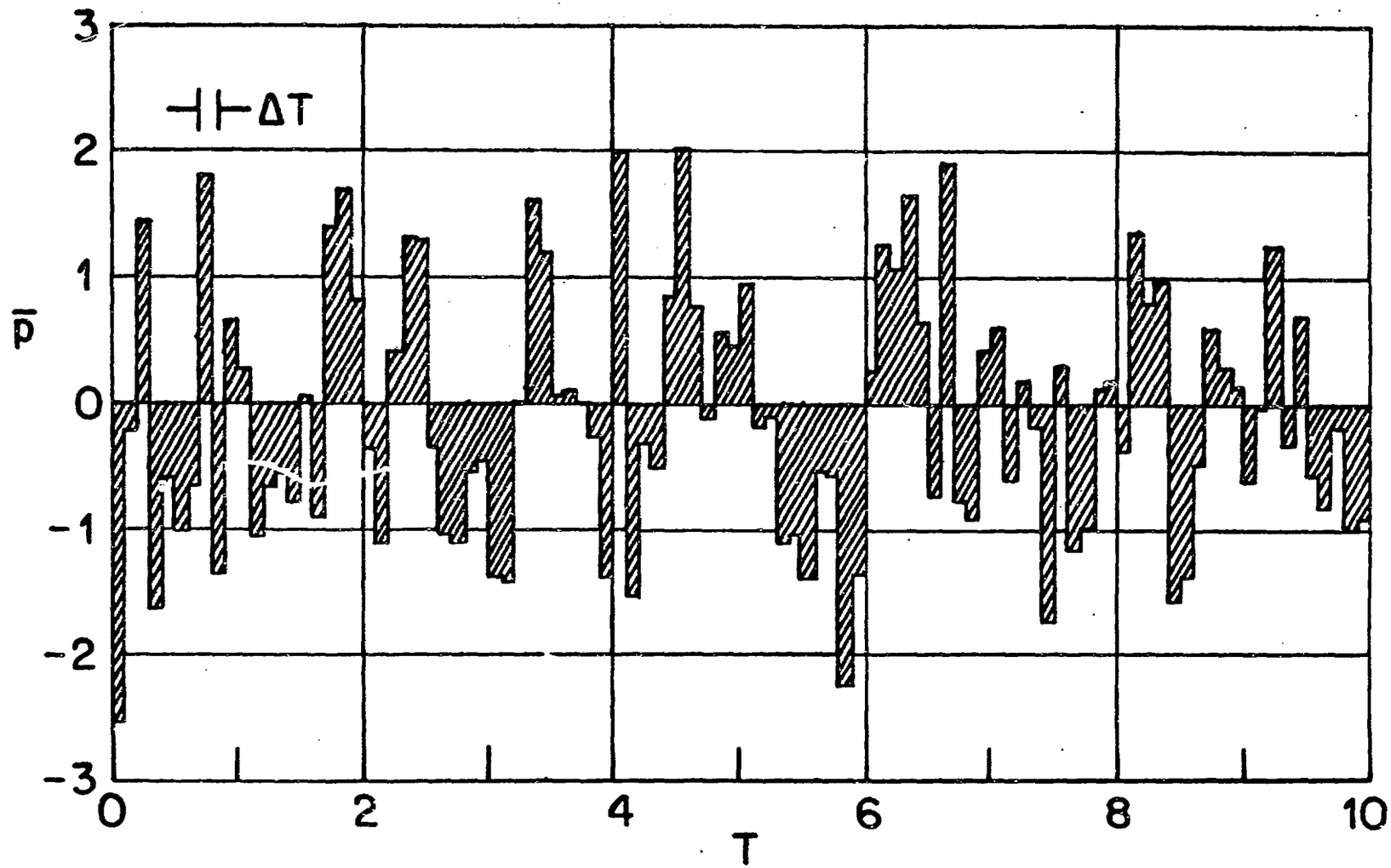

Fig. 8. Typical Generated Random Pressure Variation with Time

In the analysis of the response of a structure to random loading, the results obtained can only be presented in the form of probability distributions of certain events or as averages of certain quantities. A specific response case is of interest only for its contribution to the probability distribution or average rather than for the details. This is illustrated in Fig. 9 where three different response-time histories are shown for different loadings having the same power spectral density. One case snaps from one buckled position to the other repeatedly within three periods of lowest unstressed beam frequency, another meanders and snaps through only at the end of the third period, while the third exhibits an intermediate behavior. A first attempt at obtaining crucial data was to calculate probability curves for first snap-through of initially buckled beams, the so-called "first passage" problem.

3.1 Monte-Carlo Determination of First Snap-Through Probability

The technique used to obtain probability curves for the time required for snap-through to occur was to assign a value of the buckle amplitude $\bar{w}_0$, the time step ΔT, the damping coefficient $\bar{\mu}$, the mean load value $\bar{p}_0$, taken as 0.0 in all calculations, the standard deviation of the load history $\bar{\sigma}_0$, and an arbitrary "seed" value IX, an integer having ten or fewer digits. The equations of motion were integrated until the total center deflection changed sign or until the maximum value of time that was chosen to be considered was reached. The time interval in which this occurred was recorded. The random number generated "seed" value at this time was then used as the starting point for the next run. This procedure was repeated 6000 times

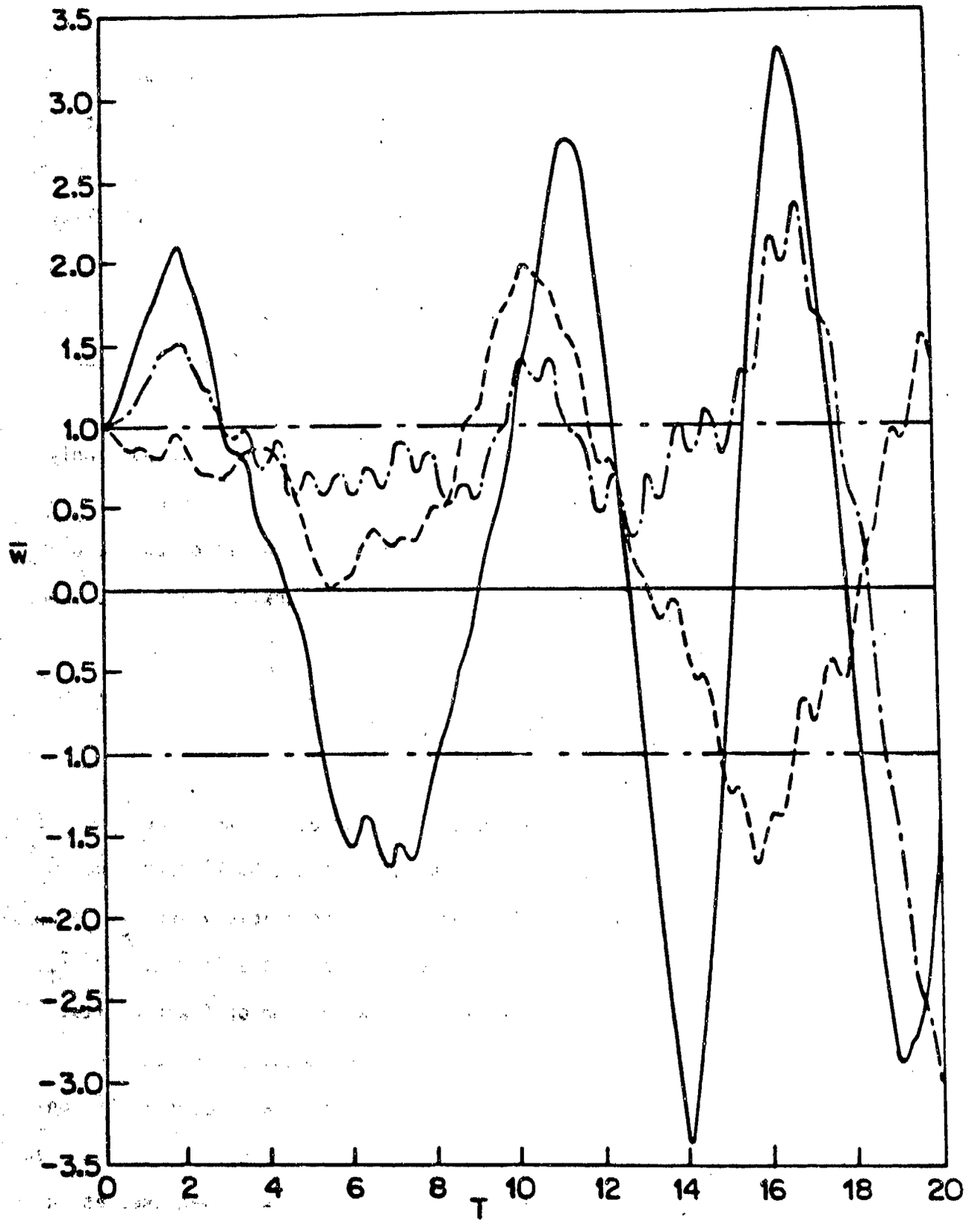

Fig. 9. Typical Response-Time Histories for a Beam Subjected to Different Loadings having the same Power Spectral Density

for each set of values of the parameters. In all cases, the initial values of the Fourier sereis terms and their first time derivative were taken as zero. The end result of these runs was a probability versus time curve for "snap-through" occurring in less than the stated time for a particular set of parameters. The self-contained computer program for this process is given in Appendix A.

In Fig. 10 and Table 1 are shown the results obtained for zero damping and various values of the initial buckle amplitude ratio $\bar{w}_0$ and power spectral density parameter $\bar{S}_0$. Although the curves were obtained for ΔT equal to 0.10 in all cases, the probability curves for other values of ΔT and $\bar{\sigma}$ yielding the same value of $\bar{S}_0$ should be similar as indicated by the results shown in Table 2. The variation of the probability of snap-through occurring in less than a given time for a beam with a given buckle amplitude increases, of course, as the power spectral density increases.

The results of Fig. 10 do not readily indicate any relationships between the sets of curves for various values of initial buckle amplitude $\bar{w}_0$. These relationships, however, may be deduced from consideration of Eqs.(2.1) when only one term is retained in the infinite series, i.e.,

$$\frac{d^2\bar{w}_1}{dT^2} + \mu\frac{d\bar{w}_1}{dT} + \frac{1}{4}\bar{w}_1(\bar{w}_1+\bar{w}_0)(\bar{w}_1+2\bar{w}_0) = -\bar{p} \qquad (3.3a)$$

If Eq.(3.3a) is divided by $\bar{w}_0^3$ the following is obtained

$$\frac{d^2\frac{\bar{w}_1}{\bar{w}_0}}{d(w_0T)^2} + \frac{\mu}{w_0}\frac{d\frac{\bar{w}_1}{\bar{w}_0}}{d(w_0T)} + \frac{1}{4}\frac{\bar{w}_1}{\bar{w}_0}\left(\frac{\bar{w}_1}{\bar{w}_0}+1\right)\left(\frac{\bar{w}_1}{\bar{w}_0}+2\right) = -\frac{\bar{p}}{\bar{w}_0^3} \qquad (3.3b)$$

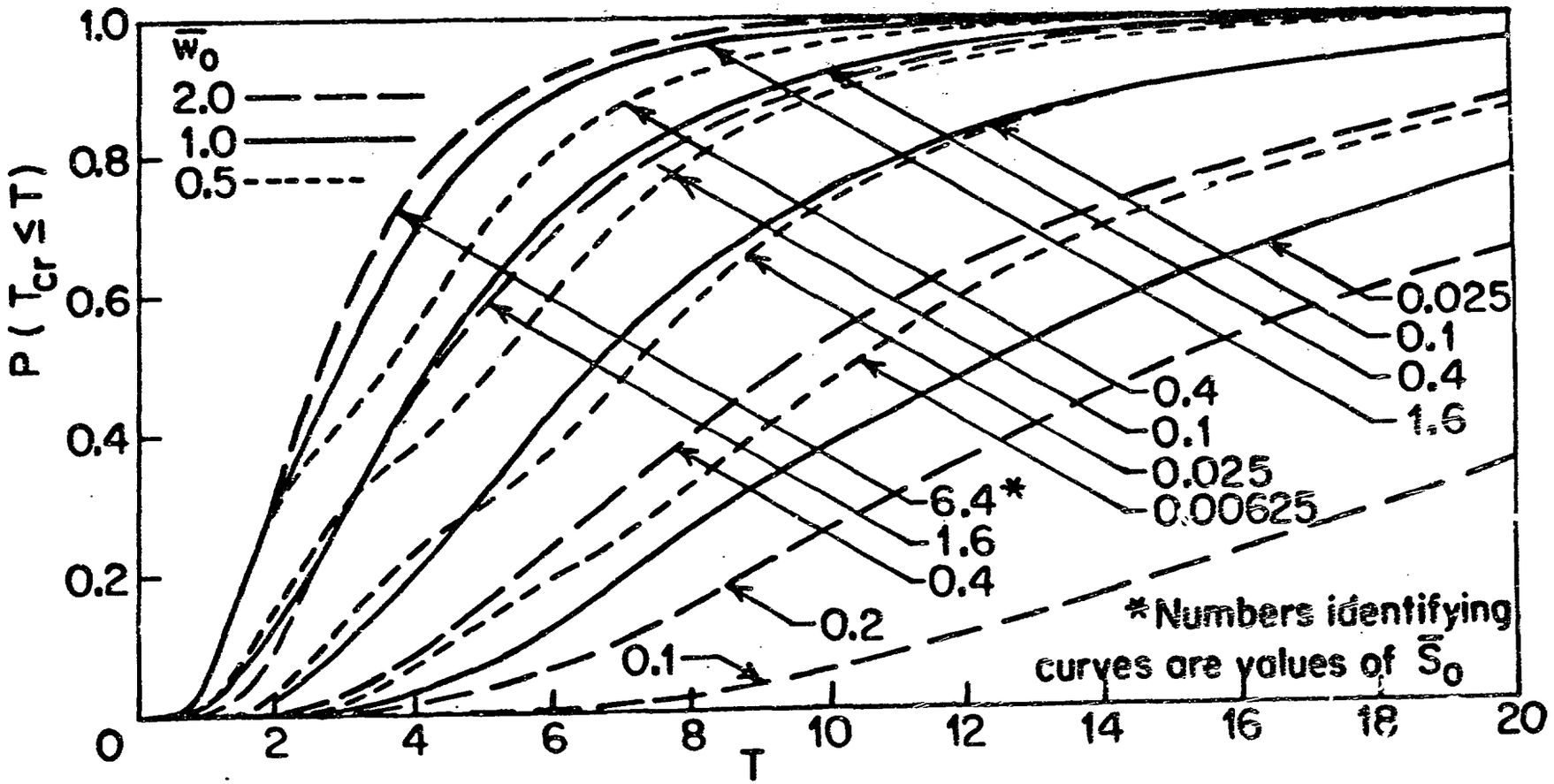

Fig. 10. Uncorrelated Snap-Through Probability Curves

Table 1. Monte-Carlo Results for Probability Curves of Figure 9 ($\Delta T = 0.1$, $\bar{\mu} = 0.0$)

(a) $\bar{w}_0 = 0.5$

$T_{cr}>$	$T_{cr}<$	$\bar{\sigma}$							
		2.0		1.0		0.5		0.25	
		N*	$P(T_{cr}<T)$	N*	$P(T_{cr}<T)$	N*	$P(T_{cr}<T)$	N*	$P(T_{cr}<T)$
0.0	1.0	296	0.049	1	0.000	0	0.000	0	0.000
1.0	2.0	1613	0.318	963	0.161	170	0.018	1	0.000
2.0	3.0	668	0.430	846	0.302	649	0.137	79	0.013
3.0	4.0	782	0.560	539	0.392	597	0.236	357	0.073
4.0	5.0	847	0.701	540	0.482	400	0.302	394	0.134
5.0	6.0	618	0.804	743	0.605	487	0.384	351	0.197
6.0	7.0	420	0.874	658	0.715	606	0.485	341	0.254
7.0	8.0	272	0.919	484	0.796	608	0.586	420	0.324
8.0	9.0	164	0.947	308	0.847	497	0.669	435	0.396
9.0	10.0	86	0.961	229	0.885	381	0.733	484	0.477
10.0	11.0	79	0.974	177	0.915	304	0.783	416	0.546
11.0	12.0	51	0.983	137	0.938	255	0.826	321	0.600
12.0	13.0	29	0.988	89	0.952	193	0.858	308	0.651
13.0	14.0	26	0.992	72	0.964	170	0.886	252	0.693
14.0	15.0	11	0.994	54	0.973	112	0.905	219	0.730
15.0	16.0	16	0.996	35	0.979	96	0.921	203	0.764
16.0	17.0	9	0.998	37	0.985	94	0.937	178	0.793
17.0	18.0	3	0.998	24	0.989	70	0.948	141	0.817
18.0	19.0	4	0.999	13	0.992	63	0.959	162	0.844
19.0	20.0	1	0.999	19	0.995	56	0.968	112	0.862

*Total number of cases = 6000

Table 1: Continued

(b) $\bar{w}_0 = 1.0$

$T_{cr}>$	$T_{cr}<$	$\bar{\sigma}$							
		4.0		2.0		1.0		0.5	
		N	$P(T_{cr}<T)$	N	$P(T_{cr}<T)$	N	$P(T_{cr}<T)$	N	$P(T_{cr}<T)$
0.0	1.0	296	0.049	3	0.001	0	0.000	0	0.000
1.0	2.0	1586	0.314	875	0.146	98	0.016	0	0.000
2.0	3.0	1080	0.494	858	0.289	538	0.106	33	0.006
3.0	4.0	1268	0.705	1040	0.463	589	0.204	156	0.032
4.0	5.0	662	0.815	837	0.602	675	0.317	191	0.063
5.0	6.0	461	0.892	696	0.718	752	0.442	326	0.118
6.0	7.0	235	0.931	471	0.797	615	0.545	437	0.191
7.0	8.0	139	0.955	350	0.855	484	0.625	436	0.263
8.0	9.0	121	0.975	237	0.895	415	0.694	376	0.326
9.0	10.0	55	0.984	174	0.924	321	0.748	315	0.378
10.0	11.0	45	0.991	129	0.945	273	0.793	331	0.434
11.0	12.0	19	0.995	101	0.961	219	0.830	293	0.482
12.0	13.0	14	0.997	61	0.972	187	0.861	282	0.529
13.0	14.0	5	0.998	50	0.980	158	0.887	274	0.575
14.0	15.0	10	0.999	41	0.987	106	0.905	268	0.620
15.0	16.0	1	1.000	27	0.992	105	0.923	232	0.658
16.0	17.0	0	1.000	19	0.995	90	0.938	190	0.690
17.0	18.0	1	1.000	5	0.997	67	0.949	171	0.719
18.0	19.0	1	1.000	10	0.997	60	0.959	197	0.751
19.0	20.0	0	1.000	4	0.998	42	0.966	157	0.778

Table 1: Continued

(c) $\bar{w}_0 = 2.0$

$T_{cr}>$	$T_{cr}<$	$\bar{\sigma}$									
		8.0		4.0		2.0		$\sqrt{2}$		1.0	
		N	$P(T_{cr}<T)$	N	$P(T_{cr}<T)$	N	$P(T_{cr}<T)$	N	$P(T_{cr}<T)$	N	$P(T_{cr}<T)$
0.0	1.0	277	0.046	2	0.000	0	0.000	0	0.000	0	0.000
1.0	2.0	1665	0.324	610	0.102	26	0.004	0	0.000	0	0.000
2.0	3.0	1682	0.604	1083	0.283	147	0.029	13	0.002	0	0.000
3.0	4.0	1021	0.774	1093	0.465	431	0.101	68	0.014	4	0.001
4.0	5.0	518	0.774	1093	0.456	431	0.101	68	0.014	4	0.001
5.0	6.0	343	0.918	637	0.682	454	0.237	170	0.064	16	0.004
6.0	7.0	231	0.956	511	0.768	510	0.322	238	0.104	40	0.011
7.0	8.0	110	0.975	354	0.827	481	0.402	272	0.149	63	0.022
8.0	9.0	66	0.986	261	0.870	427	0.473	344	0.207	102	0.039
9.0	10.0	41	0.992	200	0.903	384	0.537	317	0.259	122	0.059
10.0	11.0	19	0.996	175	0.933	328	0.592	297	0.309	131	0.081
11.0	12.0	12	0.998	101	0.949	290	0.640	275	0.355	130	0.102
12.0	13.0	6	0.999	92	0.965	252	0.682	298	0.404	182	0.133
13.0	14.0	3	0.999	59	0.975	234	0.721	276	0.450	168	0.161
14.0	15.0	1	0.999	41	0.981	217	0.758	259	0.494	190	0.192
15.0	16.0	2	1.000	22	0.985	178	0.787	234	0.533	200	0.226
16.0	17.0	2	1.000	25	0.989	170	0.816	221	0.569	185	0.257
17.0	18.0	0	1.000	19	0.992	142	0.839	199	0.603	187	0.288
18.0	19.0	1	1.000	13	0.995	134	0.862	181	0.633	186	0.319
19.0	20.0	0	1.000	5	0.995	108	0.880	184	0.663	188	0.350

Table 2: Comparison of Probability Values Obtained using Different Time Steps

$\bar{w}_0 = 1.0$, $\bar{\mu} = 0.0$

$\bar{S}_0$		0.4				0.1			
$\bar{\sigma}$		2.0		$2\sqrt{2}$		1.0		$\sqrt{2}$	
ΔT		0.10		0.05		0.10		0.05	
		N	$P(T_{cr}<T)$	N	$P(T_{cr}<T)$	N	$P(T_{cr}<T)$	N	$P(T_{cr}<T)$
0.0	1.0	3	0.001	17	0.003	0	0.000	0	0.000
1.0	2.0	875	0.146	863	0.147	98	0.016	102	0.017
2.0	3.0	858	0.289	821	0.284	538	0.106	523	0.104
3.0	4.0	1040	0.463	978	0.447	589	0.204	598	0.204
4.0	5.0	837	0.602	993	0.612	675	0.317	709	0.322
5.0	6.0	696	0.718	692	0.727	752	0.442	771	0.451
6.0	7.0	471	0.797	450	0.802	615	0.545	632	0.556
7.0	8.0	350	0.855	350	0.861	484	0.625	481	0.636
8.0	9.0	237	0.895	212	0.896	415	0.694	384	0.700
9.0	10.0	174	0.924	214	0.932	321	0.748	365	0.761
10.0	11.0	129	0.945	129	0.953	273	0.793	292	0.810
11.0	12.0	101	0.961	84	0.967	219	0.830	227	0.847
12.0	13.0	61	0.972	55	0.976	187	0.861	175	0.877
13.0	14.0	50	0.980	50	0.985	158	0.887	124	0.897
14.0	15.0	41	0.987	27	0.989	106	0.905	129	0.919
15.0	16.0	27	0.992	21	0.993	105	0.923	87	0.933
16.0	17.0	19	0.995	12	0.995	90	0.938	65	0.944
17.0	18.0	5	0.996	7	0.996	67	0.949	65	0.955
18.0	19.0	10	0.997	7	0.997	60	0.959	50	0.964
19.0	20.0	4	0.998	4	0.998	42	0.966	43	0.970

Since the first term predominates in the series, the above equation indicates that initially buckled beams having the same modified loading function $\bar{p}/\bar{w}_0^3$ as a function of modified time $\bar{w}_0 T$ will have nearly identical deflection ratios $\bar{w}_1/\bar{w}_0$ as a function of $\bar{w}_0 T$. Since the deviation $\bar{\sigma}_0$ of the random loading is a measure of the load intensity, these results suggest that random loadings having the same spectral density value of

$$\frac{\bar{\sigma}_0}{\bar{w}_0^3}^2 \bar{w}_0 \Delta T = \frac{\bar{\sigma}_0^2 \Delta T}{\bar{w}_0^5} = \frac{\bar{S}_0}{\bar{w}_0^5} \tag{3.4}$$

should yield nearly identical probability curves as a function of $w_0 T$.

That this conclusion is reasonably correct is indicated by the curves of Fig. 10 replotted in Fig. 11. The various curves show a monotonic increase of probability fucntion as the parameter $\bar{\sigma}_0^2 \Delta T/\bar{w}_0^5$ increases. Only two of the sets of values for different values of $\bar{w}_0$ yield the same value of the modified spectral density parameter, (a) $\bar{w}_0 = 0.5, \bar{\sigma}_0 = 0.25$, $\Delta T = 0.1$ and (b) $\bar{w}_0 = 2, \bar{\sigma}_0 = 8$, $\Delta T = 0.1$. Where the data for the two sets of values overlap, the values are virtually identical. A comparison of the results is given in Table 3.

The effect of damping on the probability curves is indicated by the results given in Table 4 and Fig. 12 where probability values for a beam with an initial buckle amplitude ratio of 1.0 subjected to loadings having the same power spectral density parameter are shown by the solid curves. The results indicate that small damping has little effect on the probability of first snap-through although increasing damping significantly reduces the probability of snap-through. The one term equation of motion,

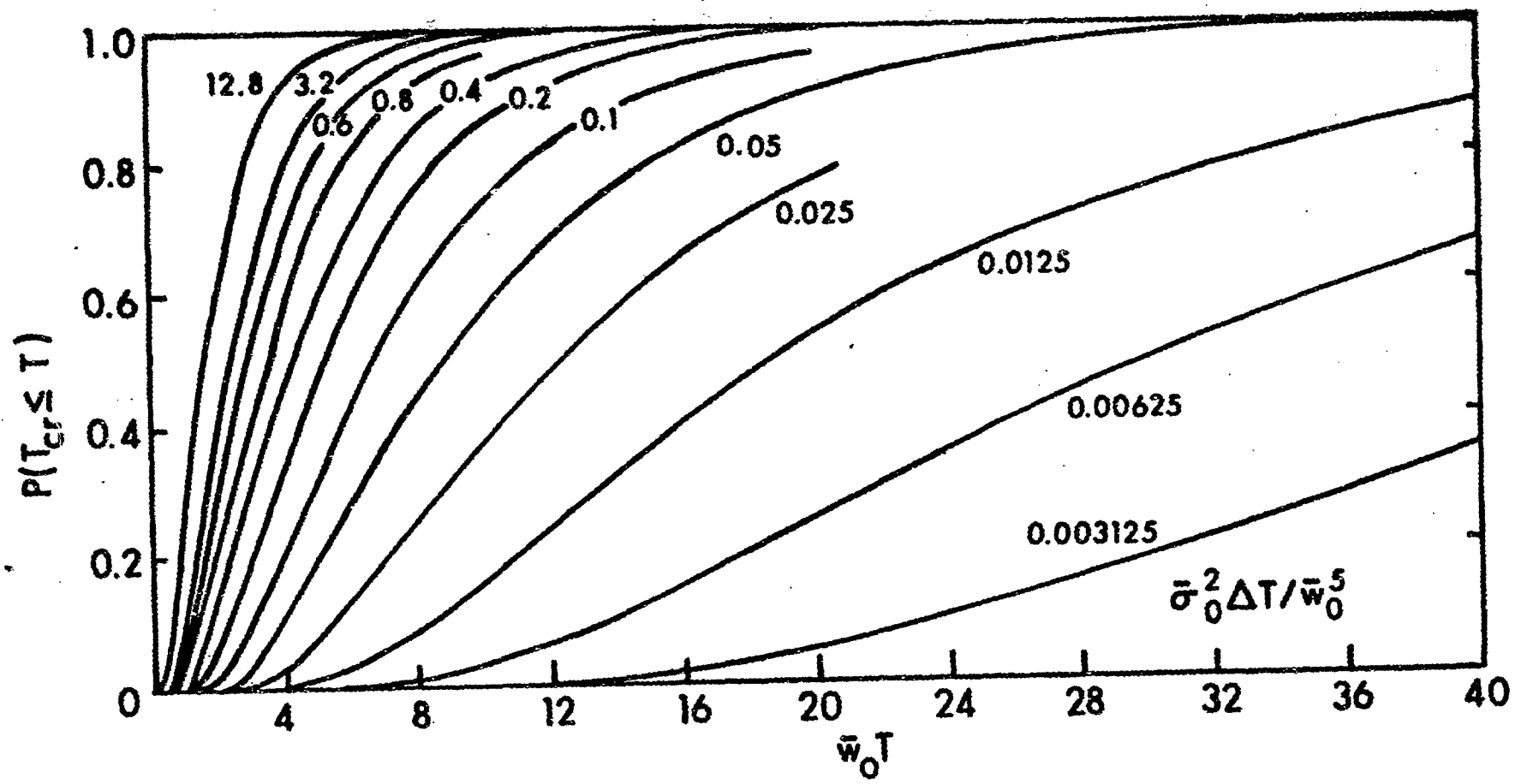

Fig. 11. Correlated Probability Curves

Table 3: Comparison of Correlated Probability Data
$\bar{\mu} = 0.0$, $\Delta T = 0.1$

	$\bar{w}_0 = 0.5$ $\bar{\sigma}_0 = 0.25$	$w_0 = 2$ $\bar{\sigma}_0 = 8$
$\bar{w}_0 T$	$P(T_{cr} < T)$	$P(T_{cr} < T)$
2.0	0.073	0.046
4.0	0.324	0.324
6.0	0.600	0.604
8.0	0.764	0.774
10.0	0.862	0.861

Table 4. Monte-Carlo Results for Probability Curves of Figure 1

$\bar{w}_0 = 1.0$, $\bar{\sigma}_0 = 1.0$, $\Delta T = 0.1$

$T_{cr}>$	$T_{cr}<$	$\bar{\mu}$									
		0.00		0.01		0.10		0.50		1.00	
		N*	$P(T_{cr}<T)$	N*	$P(T_{cr}<T)$	N*	$P(T_{cr}<T)$	N*	$P(T_{cr}<T)$	N*	$P(T_{cr}<T)$
0.0	1.0	0	0.000	0	0.000	0	0.000	0	0.000	0	0.000
1.0	2.0	98	0.016	103	0.017	73	0.012	9	0.002	0	0.000
2.0	3.0	538	0.106	545	0.108	446	0.087	143	0.025	16	0.003
3.0	4.0	589	0.204	566	0.202	471	0.165	214	0.061	61	0.013
4.0	5.0	675	0.317	635	0.308	549	0.257	245	0.102	62	0.023
5.0	6.0	752	0.442	776	0.438	684	0.371	277	0.148	88	0.038
6.0	7.0	615	0.545	635	0.543	589	0.469	297	0.198	89	0.053
7.0	8.0	484	0.625	488	0.625	461	0.546	313	0.250	103	0.070
8.0	9.0	415	0.694	415	0.694	404	0.613	279	0.296	117	0.089
9.0	10.0	321	0.748	304	0.745	356	0.672	262	0.340	117	0.109
10.0	11.0	273	0.793	262	0.788	277	0.718	242	0.380	110	0.127
11.0	12.0	219	0.830	226	0.826	242	0.759	222	0.417	115	0.146
12.0	13.0	187	0.861	185	0.857	197	0.792	177	0.447	105	0.164
13.0	14.0	158	0.887	149	0.882	193	0.824	218	0.483	83	0.178
14.0	15.0	106	0.905	117	0.901	155	0.850	159	0.510	89	0.193
15.0	16.0	105	0.923	110	0.919	134	0.872	143	0.533	108	0.211
16.0	17.0	90	0.938	91	0.935	126	0.893	163	0.561	82	0.224
17.0	18.0	67	0.949	62	0.945	92	0.908	166	0.588	100	0.241
18.0	19.0	60	0.959	71	0.957	93	0.924	157	0.614	92	0.256
19.0	20.0	42	0.966	54	0.966	73	0.936	130	0.636	79	0.269

*Total number of cases = 5000

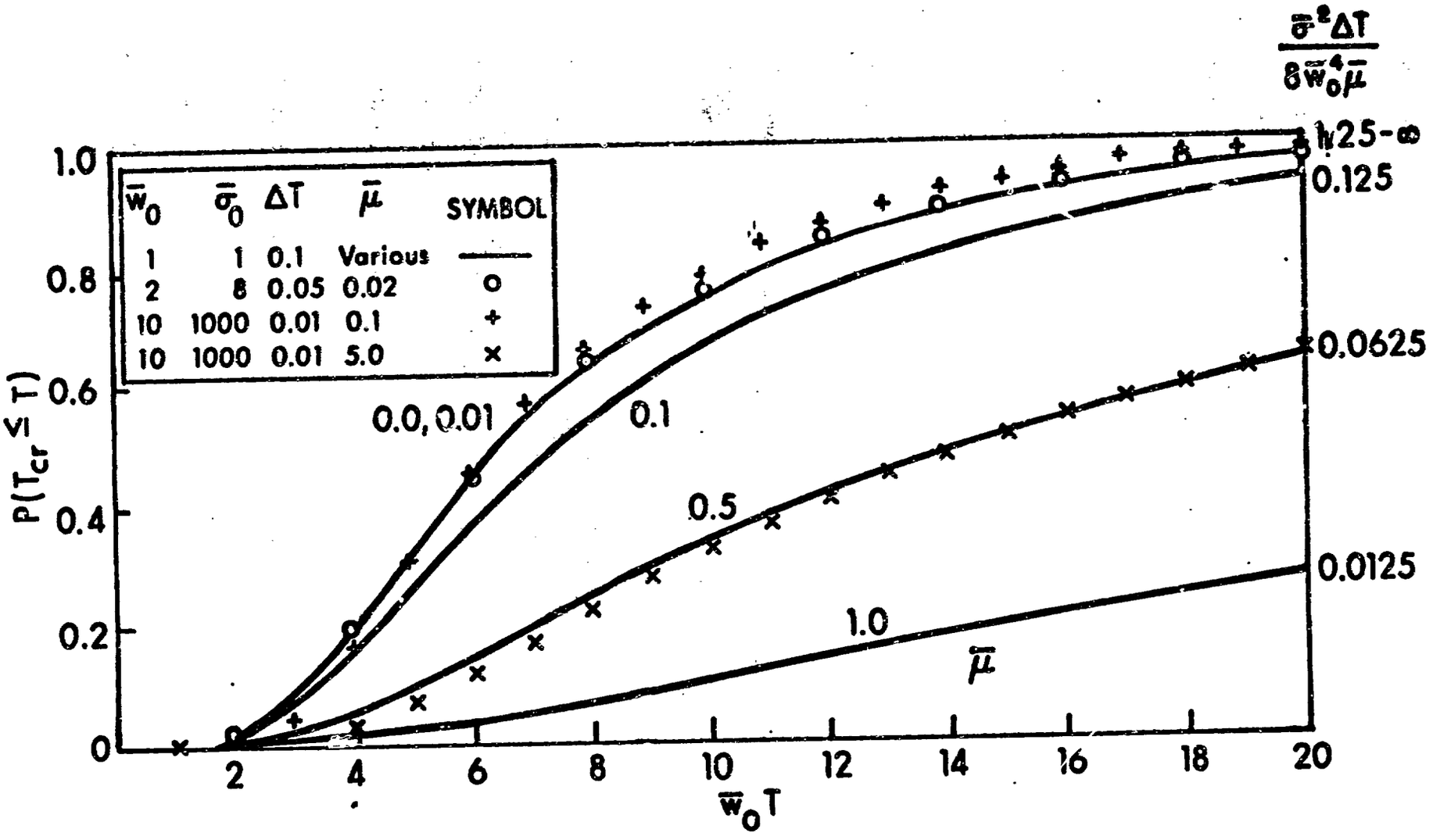

Fig. 12. Effect of Damping in Probability Curves

Eq.(3.3b), indicate that these curves should be nearly identical for beams of different initial buckle amplitudes $\bar{w}_0$ having the same value of $\bar{\sigma}_0/\bar{w}_0^3$ $\bar{w}_0\Delta T$, and $\bar{\mu}/\bar{w}_0$. Results calculated for beams with values of $\bar{w}_0$ equal to 2 and 10 and with appropriate values of σ_0 and $\bar{\mu}$ are given in Table 5 and are shown in Fig. 13. The agreement between the various results is quite satisfactory.

A further correlating parameter for these results is suggested by the investigation of reference 15 where the primary white noise spectral density parameter $\bar{S}$ can be shown to be related to the simulation parameters by

$$\bar{S} = \frac{\bar{\sigma}_0^2\Delta T}{8\bar{\mu}}$$

In reference 15 the results were found to be insensitive to the additional parameter $\bar{\mu}$. It is possible then that beams of different initial amplitudes having the same value of

$$\frac{1}{8}\left(\frac{\bar{\sigma}_0}{\bar{w}_0^3}\right)^2 \frac{\bar{w}_0\Delta T}{\bar{\mu}/\bar{w}_0} = \frac{\bar{\sigma}_0^2\Delta T}{8\bar{w}_0^4\bar{\mu}} = \frac{\bar{S}}{\bar{w}_0^4}$$

would have similar probability curves as a function of $\bar{w}_0 T$. Additional results given in Table 5 and shown in Fig. 13 indicate that this correparameter is not valid, however, since the curves of Fig. 13 although coinciding quite well with the corresponding curve of Fig. 12. In Fig. 12 the results indicate that beams with values of $\bar{S}/\bar{w}_0^4$ from 1.25 to ∞ should have identical probability curves. This same result is apparent in Fig. 13. In Fig. 12, however, the value of $\bar{\sigma}_0^2\Delta T/\bar{w}_0^5$ is equal to 0.1 whereas in Fig. 13 the value of $\bar{\sigma}_0^2\Delta T/\bar{w}_0^5$ is equal to 1. Thus $\bar{\sigma}_0^2\Delta T/8\bar{w}_0^4\bar{\mu}$

Table 5: Additional Monte-Carlo Results Illustrating Correlation Parameters

$w_0 T_{cr}>$	$w_0 T_{cr}<$	$\bar{w}_0 = 10$								$\bar{w}_0 = 1$	
		$\bar{\sigma}_0 = 1000$ $\bar{\mu} = 5.0$	$\Delta T = 0.1$	$\bar{\sigma}_0 = 1000$ $\bar{\mu} = 0.1$	$\Delta T = 0.1$	$\bar{\sigma}_0 = 10$ $\bar{\mu} = 1.0$	$\Delta T = 0.1$	$\bar{\sigma}_0 = 1000$ $\bar{\mu} = 0.1$	$\Delta T = 0.01$	$\bar{\sigma} = 1$ $\bar{\mu} = 0.01$	$\Delta T = 1$
0.0	1.0	0	0.000	35	0.006	27	0.005	0	0.000	29	0.005
1.0	2.0	0	0.000	1039	0.179	954	0.164	10	0.002	1478	0.251
2.0	3.0	34	0.006	1037	0.352	969	0.325	288	0.050	830	0.390
3.0	4.0	173	0.035	1135	0.541	1045	0.499	667	0.161	1186	0.581
4.0	5.0	245	0.075	1081	0.721	1074	0.678	878	0.307	822	0.724
5.0	6.0	272	0.121	710	0.840	729	0.800	872	0.453	563	0.818
6.0	7.0	305	0.172	353	0.898	394	0.865	728	0.574	355	0.877
7.0	8.0	318	0.225	220	0.935	281	0.912	518	0.660	238	0.917
8.0	9.0	308	0.276	162	0.962	189	0.944	422	0.731	184	0.948
9.0	10.0	264	0.320	81	0.976	120	0.964	328	0.785	107	0.965
10.0	11.0	263	0.364	71	0.987	87	0.978	285	0.833	81	0.979
11.0	12.0	214	0.399	34	0.993	51	0.987	219	0.869	42	0.986
12.0	13.0	239	0.439	18	0.996	21	0.990	148	0.894	26	0.990
13.0	14.0	203	0.473	9	0.998	26	0.995	123	0.914	22	0.994
14.0	15.0	188	0.504	7	0.999	10	0.996	119	0.934	14	0.996
15.0	16.0	176	0.534	5	1.000	8	0.998	94	0.950	7	0.997
16.0	17.0	190	0.565	2	1.000	8	0.998	73	0.962	6	0.998
17.0	18.0	144	0.589	0	1.000	2	0.999	54	0.971	0	0.998
18.0	19.0	159	0.616	0	1.000	1	0.999	44	0.978	3	0.999
19.0	20.0	154	0.642	0	1.000	1	1.000	39	0.985	3	0.999

Table 5: Continued

$\bar{w}_0 T_{cr}>$	$\bar{w}_0 T_{cr}<$	$\bar{w}_0 = 2$ $\bar{\mu} = 0.02$ $\Delta T = 0.05$ $\bar{\sigma}_0 = 8$	
		N	$P(T_{cr} < T)$
0.0	2.0	80	0.013
2.0	4.0	1087	0.195
4.0	6.0	1477	0.441
6.0	8.0	1154	0.633
8.0	10.0	721	0.753
10.0	12.0	482	0.834
12.0	14.0	332	0.889
14.0	16.0	213	0.924
16.0	18.0	140	0.948
18.0	20.0	121	0.968

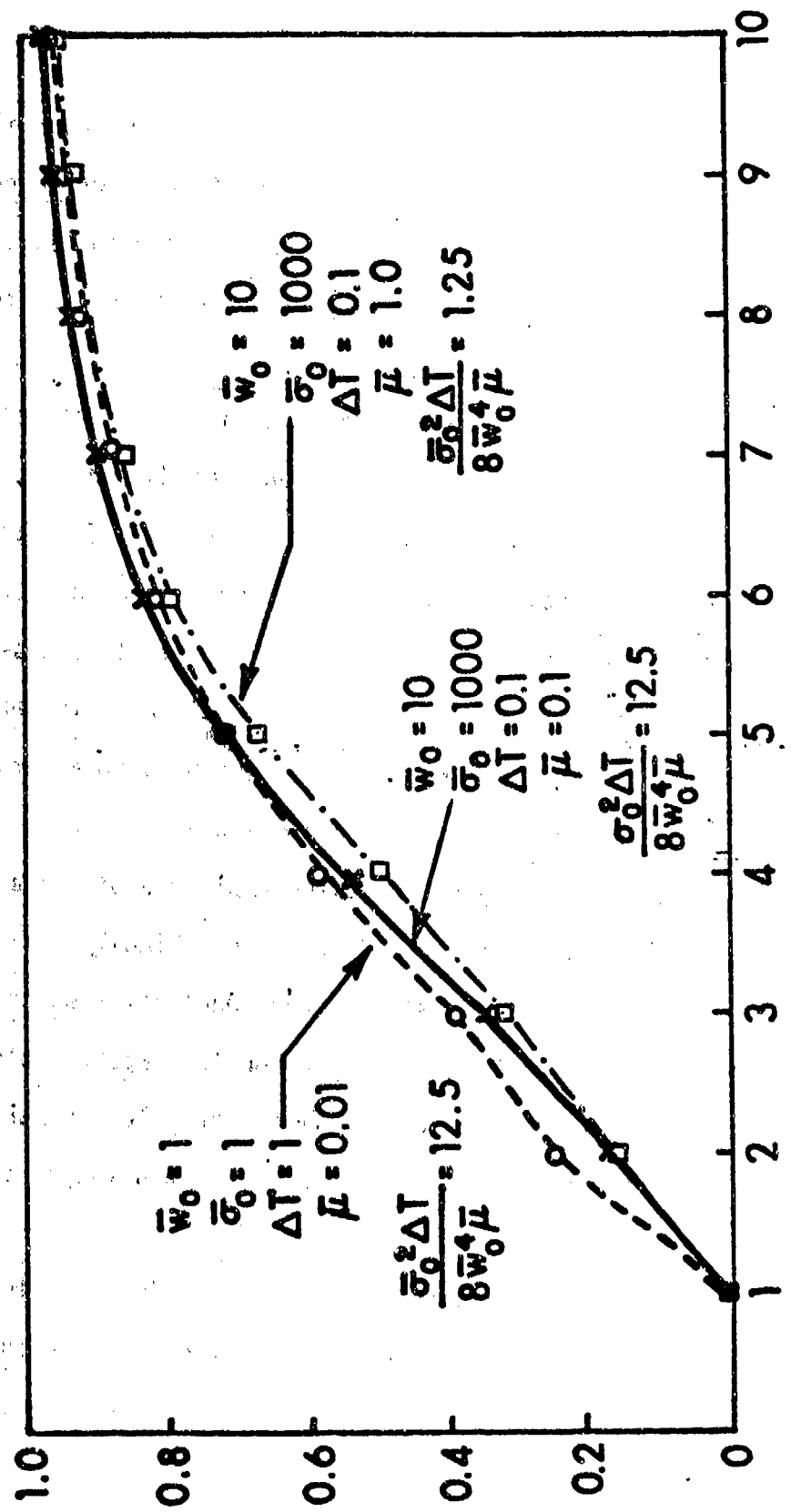

Fig. 13. Effect of Various Parameter Values on Probability Distributions

and $\bar{\sigma}_0^{-2}\Delta T/\bar{w}_0^{-5}$ are apparently separate parameters which define the probability curves. The curves of Fig. 11 for $\bar{\mu}$ equal to 0 are thus upper bounds to the probability curves for beams with other values of $\bar{\mu}$ and should be valid for values of the modified spectral density parameter $\bar{S}_0/\bar{w}_0^{-4}$ greater than about 1.

Although the results indicate that small damping has little effect on the probability of first snap-through, small amounts of damping do, however, have a significant effect on the response history. In Fig. 14 the response of beams having a buckle amplitude ratio of 1.0 but different values of the damping parameter and subjected to the same load history is shown . For no damping the beam vibrates violently with increasing amplitude and increasing frequency, a phenomenon which is in accord with the approximate variation of frequency with amplitude derived in Section 2.4. Small amounts of damping decrease the amplitude of vibration although the beam continues to snap back and forth. Finally sufficiently large damping causes the beam to snap-through once after which it vibrates about the buckled equilibrium positions on the opposite side of the straight axis. If the load were to be applied for a longer period the beam would undoubtedly snap back and forth but with a longer time interval between the event.

The axial load in the beam while this response occurs is shown in Fig. 15. With no damping the axial load eventually changes very rapidly from compression to tension and back. Increasing amounts of damping tend to smooth out the axial load variation.

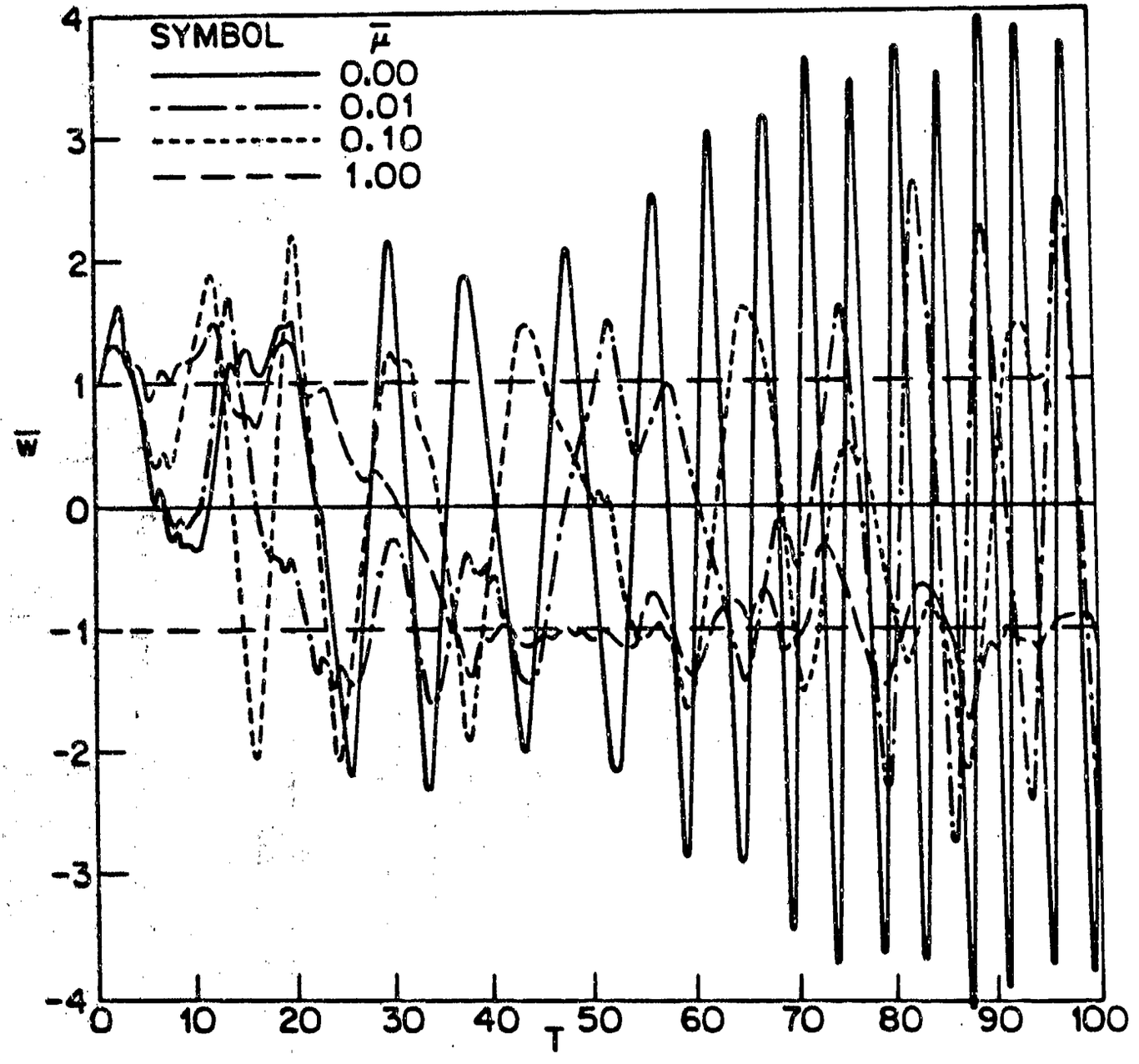

Fig. 14. Effect of Damping in Response-Time History

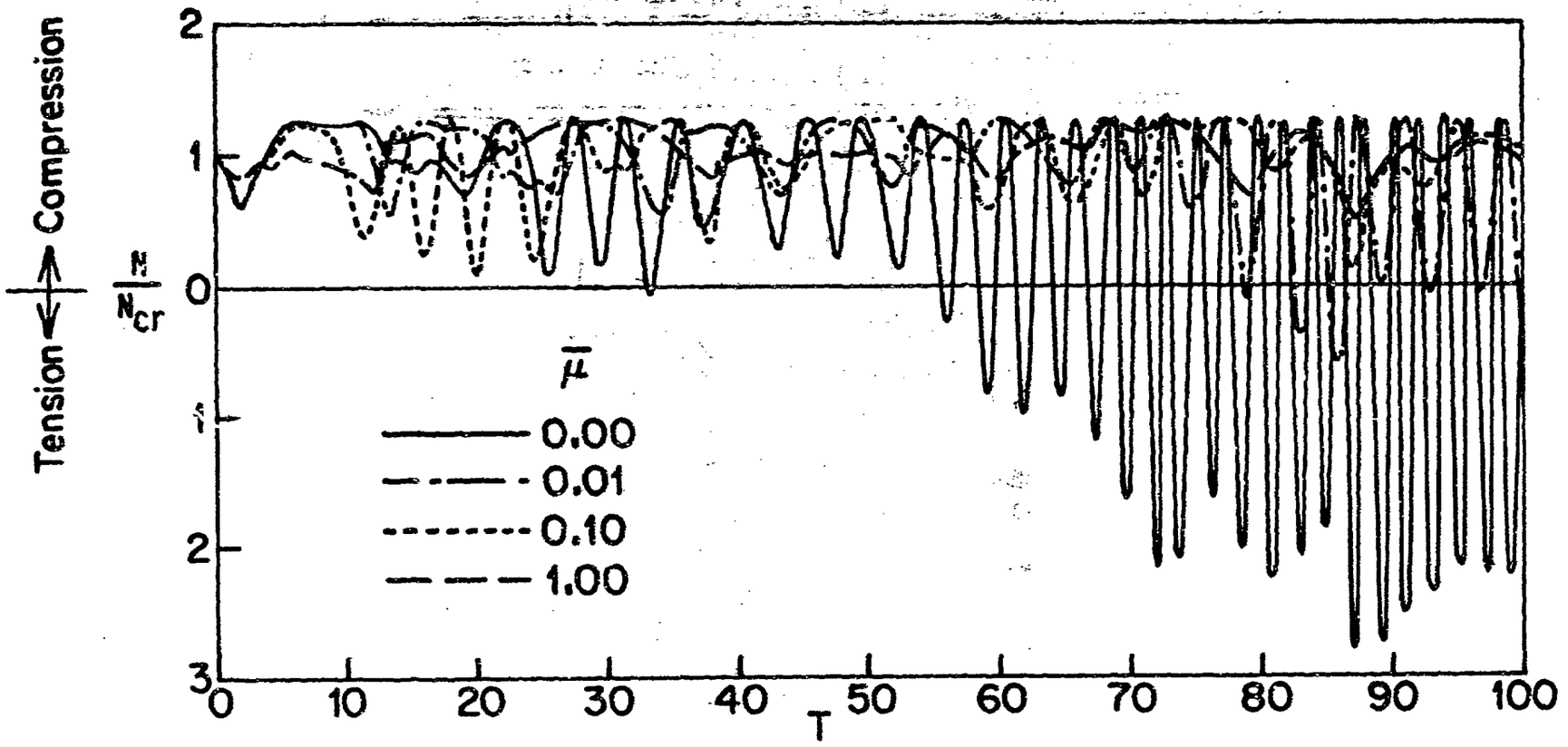

Fig. 15. Effect of Damping in Axial Load-Time History

The foregoing results suggest that while probability curves of first snap-through may be of interest they are of little use in determining critical ranges of spectral density parameter since these are presumably defined by zero or small probability of first snap-through over an infinite or sufficiently large time range. The calculations needed to produce this information are quite costly since numerical integration of a large number of cases over a very long time period would be required. In addition, probability curves do not indicate any qualitative information about the intensity of the snap-through motion. The results of snap-through events separated by long intervals of time during which relatively small oscillations about one of the two buckled equilibrium positions occurs will, of course, be of much less importance from the point of view of fatigue life than frequent and large oscillations from one buckled position to the other. An alternate calculation procedure yielding averages was therefore considered next as offering the possibility of more useful information.

3.2 Calculation of Average Snap-Through Frequency

In the previous section an attempt was made to determine a critical snap-through spectral density parameter based on a calculation of the spectral density parameter for which the probability of snap-through was nearly zero for all time. A description of the behavior of the initially buckled beam can be based on time averages rather than ensemble averages, however. The computer program developed for the Monte-Carlo calculation of probability values was modified, as shown in Appendix B, to calculate the response of a compressed beam, buckled or unbuckled, over any desired

length of time and to obtain time averages of various quantities at stated intervals. The primary object of investigation is the average frequency of snap-through, defined as the number of zero crossings N(T) of the maximum deflection divided by the time T, i.e.,

$$f = \lim_{T \to \infty} \frac{N(T)}{T}$$

The procedure used was to generate the simulated random pressure distribution described in the previous section and to calculate the response by means of a forth-order Runge-Kutta integration of the equations of motion, Eqs.(3.1), using three modes. The number of crossings of the zero axis of the maximum deflection function, both from above and from below, was counted during the calculation procedure. At stated intervals, a time average of the crossing rate was calculated. It was observed that this calculated rate was reasonably constant when the time was sufficiently long, and that different loading sequences led to essentially the same result. Some of the results are shown in Table 6. The time averages shown for $\bar{w}_0$ equal to 10.0 suggest the calculation of a critical spectral density parameter based on the average frequency vanishing is becoming very small since for $\bar{\sigma}_0$ equal to 10 the average frequency is zero whereas for $\bar{\sigma}_0$ equal to 100 the average frequency of snap-through is 1.56. Additional calculations were made to define curves of average frequency as a function of the spectral density parameter $\bar{S}$. These are given in Table 7 where the average zero-crossing frequency at the end of the integrated response is shown for beams of varying initial buckle amplitudes. The maximum final parameter

Table 6: Effect of Seed Value and Maximum Integration Time on Average Zero-Crossing Frequency
$\bar{\mu} = \Delta T = 0.1$

$\bar{w}_0$	1.0		10.0			
$\bar{\sigma}_0$	100		100		10	
Seed Value	999999999	123456789	999999999	369121518	999999999	369121518
T	N(T)/T	N(T)/T	N(T)/T	N(T)/T	N(T)/T	N(T)/T
3141.6	1.980	1.909	1.548	——	——	——
6283.2	1.945	1.916	1.579	1.55	0.000	0.000
9424.8	1.947	1.926	1.551	——	——	——
12566.4	1.948	1.935	1.555	1.55	0.000	0.000
15708.0	1.953	1.935	1.556	——	——	——
18849.6	1.957	——	1.552	1.54	0.000	0.000
21991.2	1.961	——	1.555	——	——	——
25132.8	1.969	——	1.547	1.55	0.000	0.000
28274.4	1.957	——	1.550	——	——	——
31416.0	1.595	——	1.550	1.56	0.000	0.000

Table 7: Variation of Average Crossing Frequency of Response with Various Parameters

$\bar{W}_0$	$\bar{\mu}$	ΔT	$\bar{\sigma}_0$	f
0.0	0.10	0.10	0.01	0.34
			0.10	2.34
($\bar{N}_0 = 0.0$)			1.00	0.36
			10.00	0.68
			31.62	1.14
			100.00	1.96
			316.23	3.24
			1000.00	5.25
1.0	0.10	0.10	0.10	0.000
			0.32	0.033
			1.00	0.14
			3.16	0.30
			10.00	0.61
			31.62	1.10
			100.00	1.96
			316.23	3.27
			1000.00	5.28
	1.00	0.10	316.23	1.93
2.0	0.10	0.10	1000.00	5.26
10.0	0.10	0.10	10.00	0.000
			13.00	0.005
			15.00	0.018
			18.00	0.062
			25.00	0.25
			131.62	0.43
			100.00	1.55
			316.23	12.97
			1000.00	5.12
	0.05	0.10	15.00	0.10
			18.00	0.21
	0.20	0.10	10.00	0.000
	1.00	0.10	100.00	0.42
10.0	0.10	0.20	7.07	0.000
			9.19	0.001
			12.73	0.035
			17.68	0.22
			22.36	0.32
			70.71	1.31
	.059	0.10	10.00	0.001
	.044			0.018
	.031			0.068
	.016			0.21
	.010			0.34
	.001			0.68
	.0001			0.77
	.00001			0.96
20.0	0.10	0.10	40.00	0.012
			52.00	0.060
			60.00	0.14
			100.00	0.63
			316.23	2.04
			1000.00	3.87
	0.20	0.05	80.00	0.033
			104.00	0.17
			144.00	0.47
			200.00	0.87
			252.98	1.21
			800.00	3.16
			2529.82	5.83
			8000.00	9.29
	0.10	0.05	100.00	0.42
			316.23	2.07
			1000.00	4.26

used to calcualte the time averages was first taken as 31416.0 (about 5000 uncompressed beam fundamental mode periods. In later calculations T_{max} was reduced to one-half and later to one-quarter of this value since the final result did not change significantly. The first set of results in Table 7 are for an uncompressed beam ($\bar{w}_0 = \bar{N}_0 = 0$). In this case the average zero-crossing frequency does not vanish as the standard deviation of the loading function becomes small but appears to approach a constant value of about 0.34. It is shown in reference 16 that a nonlinear single-degree-of-freedom system of the Duffing type has an expected zero-crossing frequency equal to the undamped natural frequency of the system. In the present case the beam would have 2 crossings in a value of T equal to 2π so that the expected value of f would be $1/\pi$ or about 0.32 which is very close to the calculated value.

For other values of initial buckle amplitude the results obtained by varying the spectral density parameter of the loading indicate the existence of a critical value below which snap-through does not occur or rarely occurs. THe results obtained are plotted as a function of the parameter $\bar{S}$ of reference 15 in Fig. 16.

The results indicate as in the previous section, that the parameter $\bar{S}$ is not the sole parameter that affects the results. Many of the calculations were made for $\bar{\mu}$ at ΔT both equal to 0.1 and varying $\bar{\sigma}_0$, which yield single curves for average frequency as a function of $\bar{S}$. Additional calculations for $\bar{w}_0$ equal to 10 and 20, with different values of $\bar{\mu}$ and ΔT yielded curves or points which do not coincide. The curves indicate however, that the critical value of $\bar{S}$ for a beam having a given initial buckle

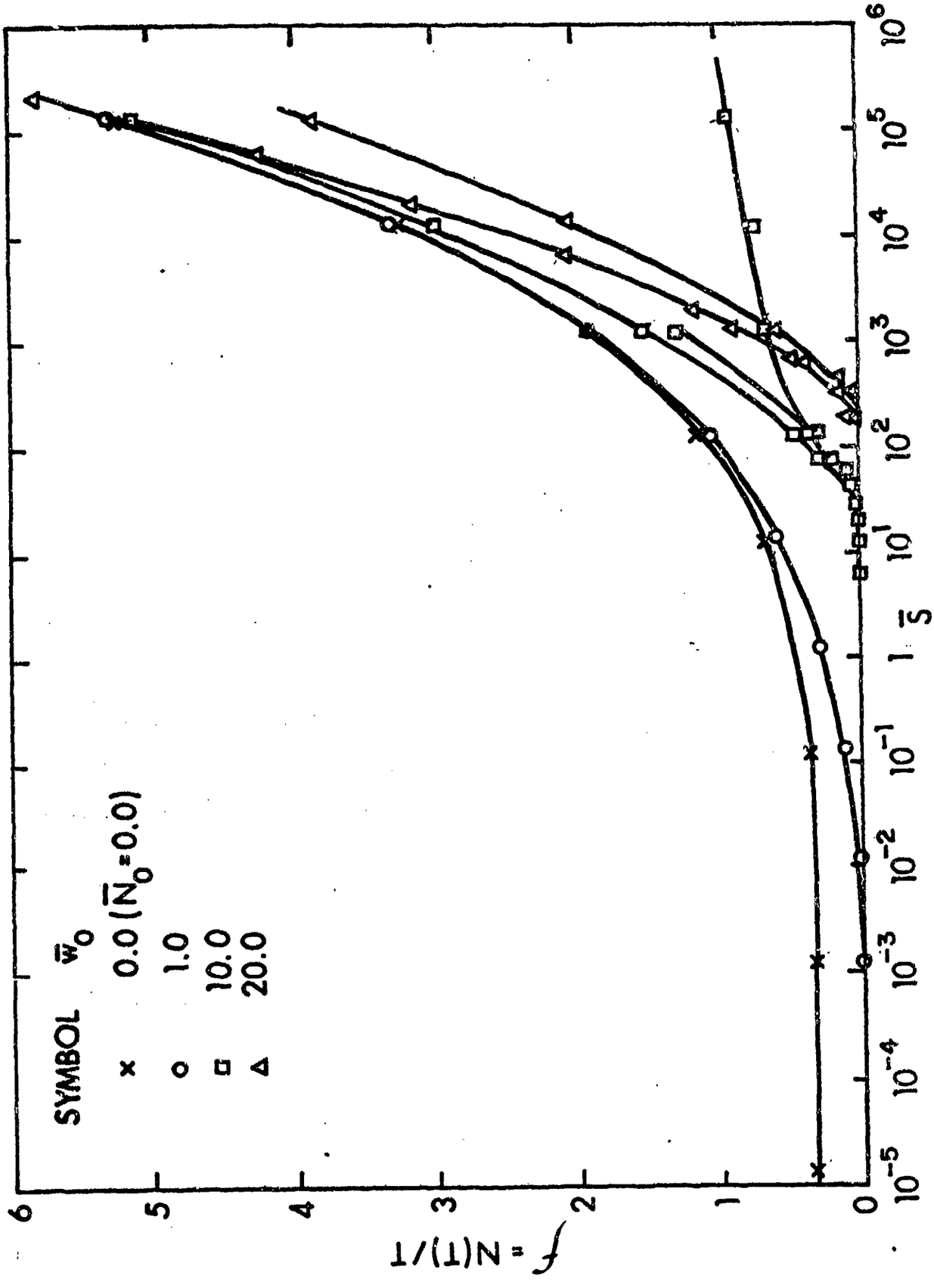

Fig. 16. Variation of Average Zero-Crossing Frequency with Spectral Density Parameter

amplitude $\bar{w}_0$ may be relatively insensitive to the variation of the various parameters.

For $\bar{w}_0$ equal to unity the critical value of $\bar{S}$, the spectral density parameter, appears to be very small on the order of 10^{-3}, whereas for $\bar{w}_0$ of 10 the value of $\bar{S}$ increased to about 10 and to about 100 for $\bar{w}_0$ of 20. These values are roughly in accord with the predictions of the correlating parameter $\bar{S}/\bar{w}_0^4$ which, if the value of $\bar{S}$ is 10^{-3} for $\bar{w}_0$ equal to unity, would yield values of 10 for $\bar{w}_0$ of 10 and 160 for $\bar{w}_0$ of 20. This conjecture is tested in Fig. 17 where the results for initially buckled beams are replotted. The frequency has been modified by division by $\bar{w}_0$, since the results should depend on $\bar{w}_0 T$, while the spectral density parameter has been divided by $\bar{w}_0^4$. It will be seen that the results for the beams of different initial buckle amplitudes appear to nearly coincide in the vicinity of the critical value of $\bar{S}/\bar{w}_0^4$. Thus an estimate of the critical spectral density parameter for snap-through and subsequent oscillation between buckled equilibrium positions is given by

$$\bar{S} = 0.001\,\bar{w}_0^4 \tag{3.5}$$

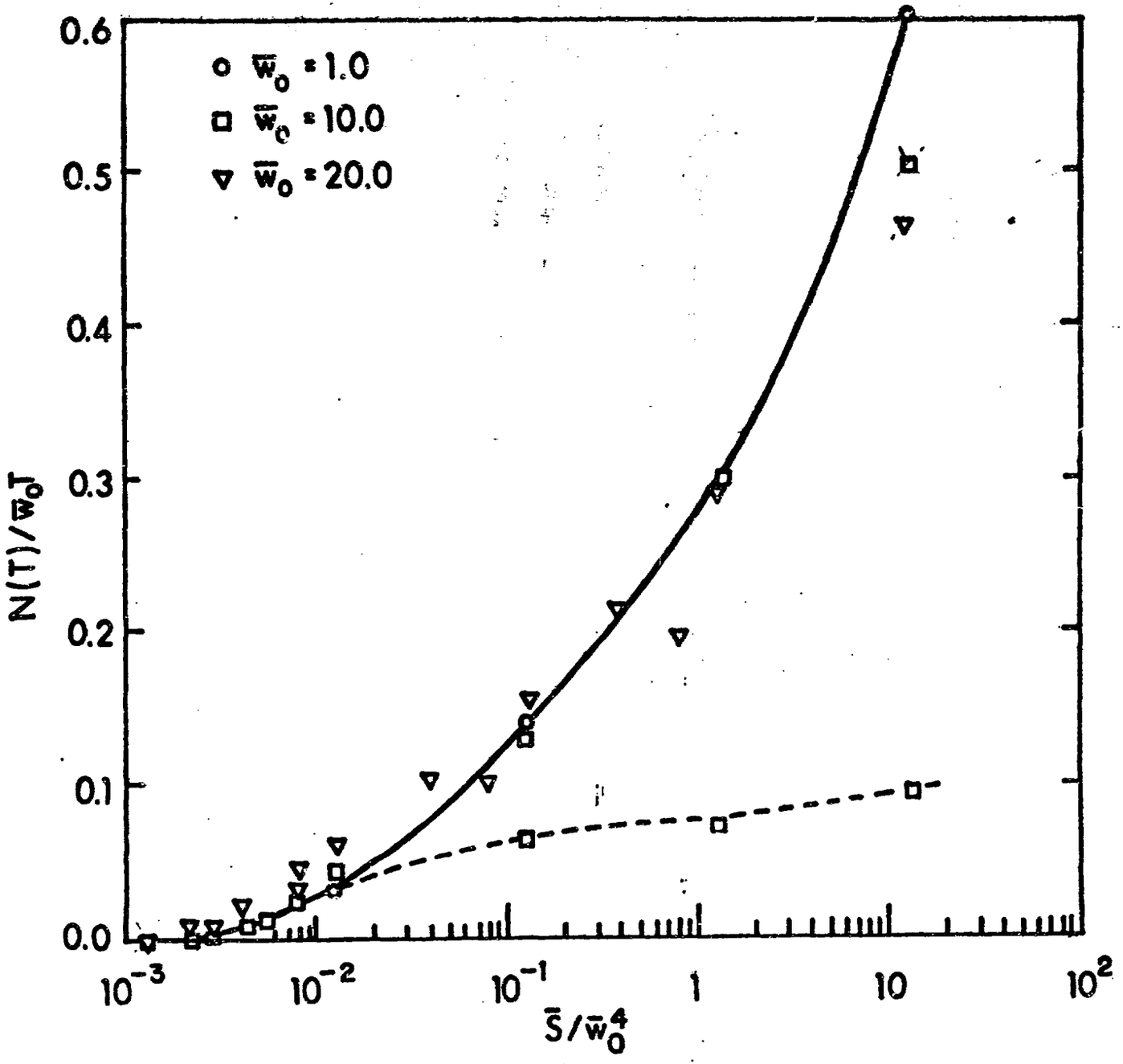

Fig. 17. Variation of Modified Zero-Crossing Frequency with Modified Spectral-Density Parameter

Chapter 4

RMS RESPONSE OF INITIALLY BUCKLED BEAMS UNDER UNIFORM RANDOM PRESSURE

4.1 Numerical Integration Results

Although knowledge of thie critical spectral density of loading is useful, it is also of interest to determine the expected average and root-mean-square (RMS) deflections and stresses of the beam since these affect the fatigue life of the structure. During the integration process which led to the result of the maximum preceding chapter, a record was kept of the RMS deflections and stresses at the beam center. The integrated deflections and stresses and their squares over the time period were calculated using the Simpson's Rule formula (reference 17).

$$\int_{x_0}^{x_{2n}} f(x)dx = \frac{h}{3}[f_0+4(f_1+f_3+\cdots+f_{2n-1})+2(f_2+f_4+\cdots+f_{2n-2})+f_{2n}] \quad (4.1)$$

At stated times the average and RMS deflection and stresses were obtained as

$$\langle \bar{w}^2_{max} \rangle^{\frac{1}{2}} = \left[\frac{1}{T} \int_0^T \bar{w}^2_{max}(\xi)d\xi \right]^{\frac{1}{2}} \quad (4.2a)$$

$$\langle (\bar{\sigma}^{\pm}_{max} \rangle^{\frac{1}{2}} = \left\{ \frac{1}{T} \int_0^T [\bar{\sigma}^{\pm}_{max}(\xi)]^2 d\xi \right\}^{\frac{1}{2}} \quad (4.2b)$$

where

$$\bar{w}_{max} = \sum_{n=1,3,5,\ldots}^{\infty} (-1)^{\frac{n-1}{2}} (\bar{w}_n + \bar{w}_0 \delta_{n1}) \tag{4.3a}$$

and the stresses at the top and bottom of the beam, considered positive if compression, are given by

$$\bar{\sigma}^{\pm}_{max} = \bar{N}_0 + \frac{1}{4}\bar{w}_0^2 - \frac{1}{4} \sum_{n=1,3,5,\ldots}^{\infty} n^2 (\bar{w}_n + \bar{w}_0 \delta_{n1})^2$$

$$\mp \frac{h}{r} \sum_{n=1,3,5}^{\infty} (-1)^{\frac{n-1}{2}} n^2 (\bar{w}_n + \bar{w}_0 \delta_{n1}) \tag{4.3b}$$

It was observed that after a sufficiently long time period the averaged values became reasonably constant. The mean values calculated at the end of the maximum time period considered in each case are tabulated in Table 8. Only the RMS stress having the greatest magnitude is given. For sufficiently large values of the parameter $\bar{S}$ the two values of stress were essentially the same.

The tabulated values are shown by the indiviaual points in Figure 18 and 19 together with some theoretical results. which will be discussed later. The results exhibit remarkably little scatter and thus indicate the very primary importance of the spectral density parameter $\bar{S}$ and the lesser importance of the damping parameter $\bar{\mu}$.

The results also indicate, as would be expected, that the effect of initial buckling becomes less important as the spectral density parameter $\bar{S}$ increases. The deflections and stresses are then large enough for the beam behavior to be similar to that of an unbuckled beam under large loading. The RMS deflections appear to first decrease as the spectral density

Table 8: Simulated RMS Values

$\bar{w}_0$	$\bar{\sigma}_0$	ΔT	$\bar{\mu}$	$\bar{S}$	$\langle \bar{w}^2_{max} \rangle^{1/2}$	$\langle \bar{\sigma}^2_{max} \rangle^{1/2}$
0	0.01	0.1	0.1	1.25×10^{-3}	0.07	0.13
	1.00	↓	↓	1.25×10^{-1}	0.60	1.14
	10.00			1.25×10	2.91	7.14
	31.62			1.25×10^{2}	5.27	17.40
	100.00			1.25×10^{3}	9.32	43.07
	316.22			1.25×10^{4}	16.05	106.8
	1000.00			1.25×10^{5}	25.96	267.1
1	0.01	0.1	0.1	1.25×10^{-3}	0.99	2.71
	0.32	↓	↓	1.25×10^{-2}	0.91	1.98
	1.00			1.25×10^{-1}	1.11	2.23
	10.00			1.25×10	3.11	7.36
	31.62			1.25×10^{2}	5.38	17.55
	100.00			1.25×10^{3}	9.39	44.43
	100.00		↓	1.25×10^{3}	9.38	42.94
	316.22		1.0	1.25×10^{3}	9.52	44.18
	316.22		0.1	1.25×10^{4}	16.24	108.2
	1000.00	↓	0.1	1.25×10^{5}	26.19	270.6
2	1000.00	0.1	0.1	1.25×10^{5}	26.21	270.5
10	10.00	0.1	0.2	6.25	9.93	6.29
	10.00	0.1	0.1	1.25×10	9.80	20.68
	10.00	0.1	0.1	1.25×10	9.82	20.52
	7.07	0.2	0.1	1.25×10	9.85	20.15
	10.00	0.1	0.059	2.12×10	9.63	21.91
	9.19	0.2	0.1	2.11×10	9.69	21.37
	13.00	0.1	0.1	2.11×10	9.61	22.23
	15.00	0.1	0.1	2.81×10	9.43	23.42
	10.00	0.1	0.144	2.84×10	9.41	23.57
	10.00	0.1	0.031	4.03×10	9.07	26.23
	12.73	0.2	0.1	4.05×10	9.29	24.41

Table 8: Continued

$\bar{w}_0$	$\bar{\sigma}_0$	ΔT	$\bar{\mu}$	$\bar{S}$	$\langle \bar{w}^2_{max} \rangle^{1/2}$	$\langle \bar{\sigma}^2_{max} \rangle^{1/2}$
10	10.00	0.2	0.1	4.05×10	9.29	24.41
	17.68	0.2	0.1	7.81×10	8.64	29.20
	31.62	0.1	0.1	1.25×10^2	8.40	33.00
	100.00	0.1	1.0	1.25×10^2	8.60	32.35
	10.00	0.1	0.01	1.25×10^2	8.27	32.52
	22.36	0.2	0.1	1.25×10^2	8.46	30.86
	100.00	0.1	0.1	1.25×10^3	10.56	50.77
	100.00	0.1	0.1	1.25×10^3	10.57	52.89
	100.00	0.1	0.1	1.25×10^3	10.52	50.49
	10.00	0.1	0.001	1.25×10^3	8.40	37.52
	70.71	0.2	0.1	1.25×10^3	10.18	42.34
	316.22	0.1	0.1	1.25×10^4	16.58	102.4
	10	0.1	0.0001	1.25×10^4	8.26	38.72
	1000	0.1	0.1	1.25×10^5	26.44	263.2
20	80.00	0.05	0.2	2.00×10^2	18.58	63.75
	40.00	0.1	0.1	2.00×10^2	18.82	54.47
	52.00	0.1	0.1	3.38×10^2	18.08	63.38
	104.00	0.05	0.2	3.38×10^2	17.33	70.82
	60.00	0.1	0.1	4.50×10^2	17.39	69.41
	100.00	0.05	0.1	6.25×10^2	16.14	82.15
	144.00	0.05	0.2	6.48×10^2	15.94	83.16
	100.00	0.1	0.1	1.25×10^3	15.81	84.93
	200.00	0.05	0.2	1.25×10^3	15.41	92.45
	252.98	0.05	0.2	2.00×10^3	15.50	98.72
	316.22	0.05	0.1	6.25×10^3	16.73	118.7
	316.22	0.1	0.1	1.25×10^4	17.98	110.3
	800.00	0.05	0.2	2.00×10^4	20.41	153.7
	1000.00	0.05	0.1	6.25×10^4	24.72	211.8
	1000.00	0.1	0.1	1.25×10^5	24.51	184.3
	2529.82	0.05	0.2	2.00×10^5	31.90	352.5
	8000.00	0.05	0.2	2.00×10^6	49.34	829.2
50	31.62	0.1	0.1	1.25×10^2	49.91	89.32
	100.00	0.1	0.1	1.25×10^3	48.97	106.2

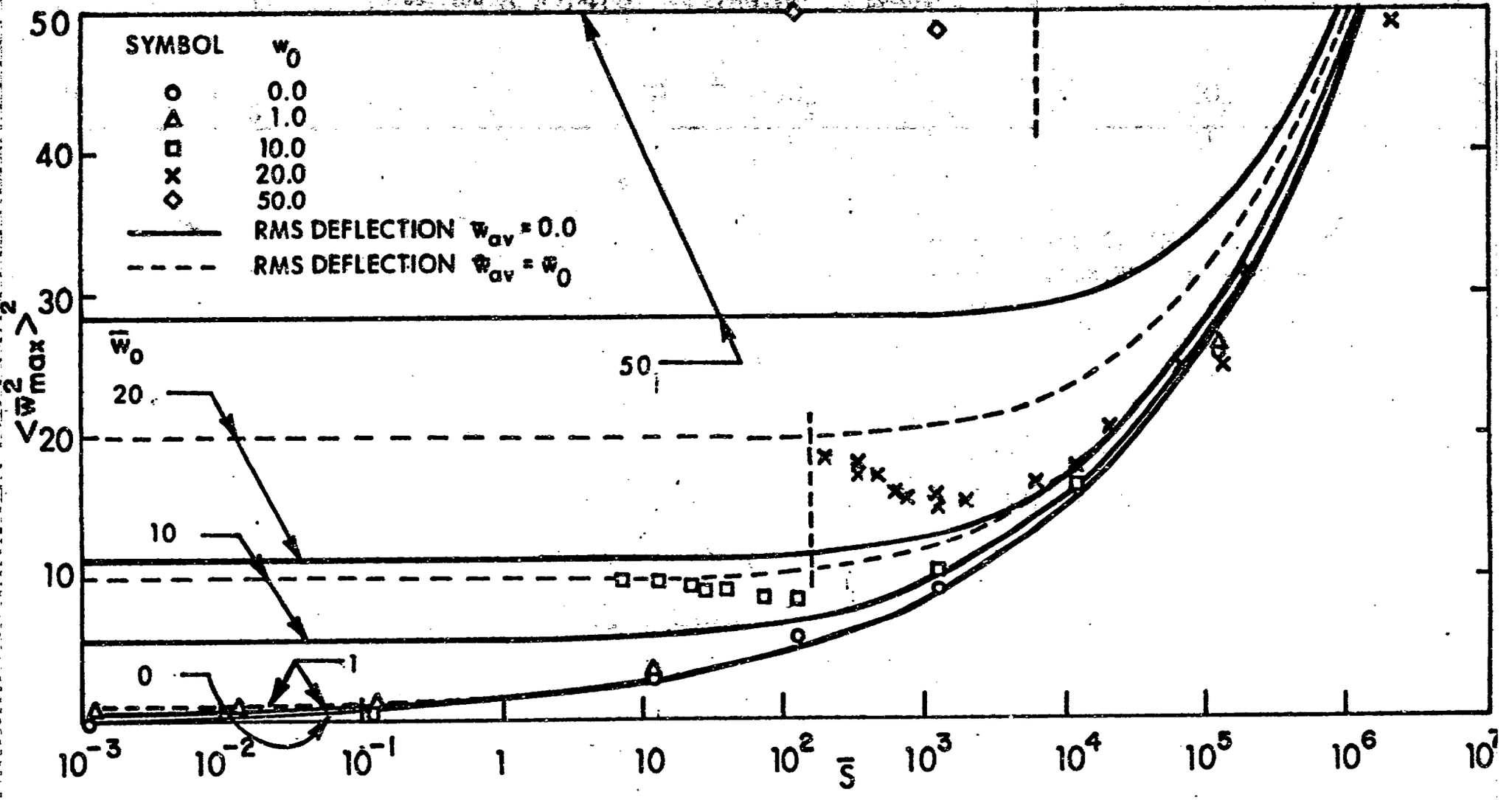

Fig. 18. Comparison of Analytical and Simulated RMS Deflections

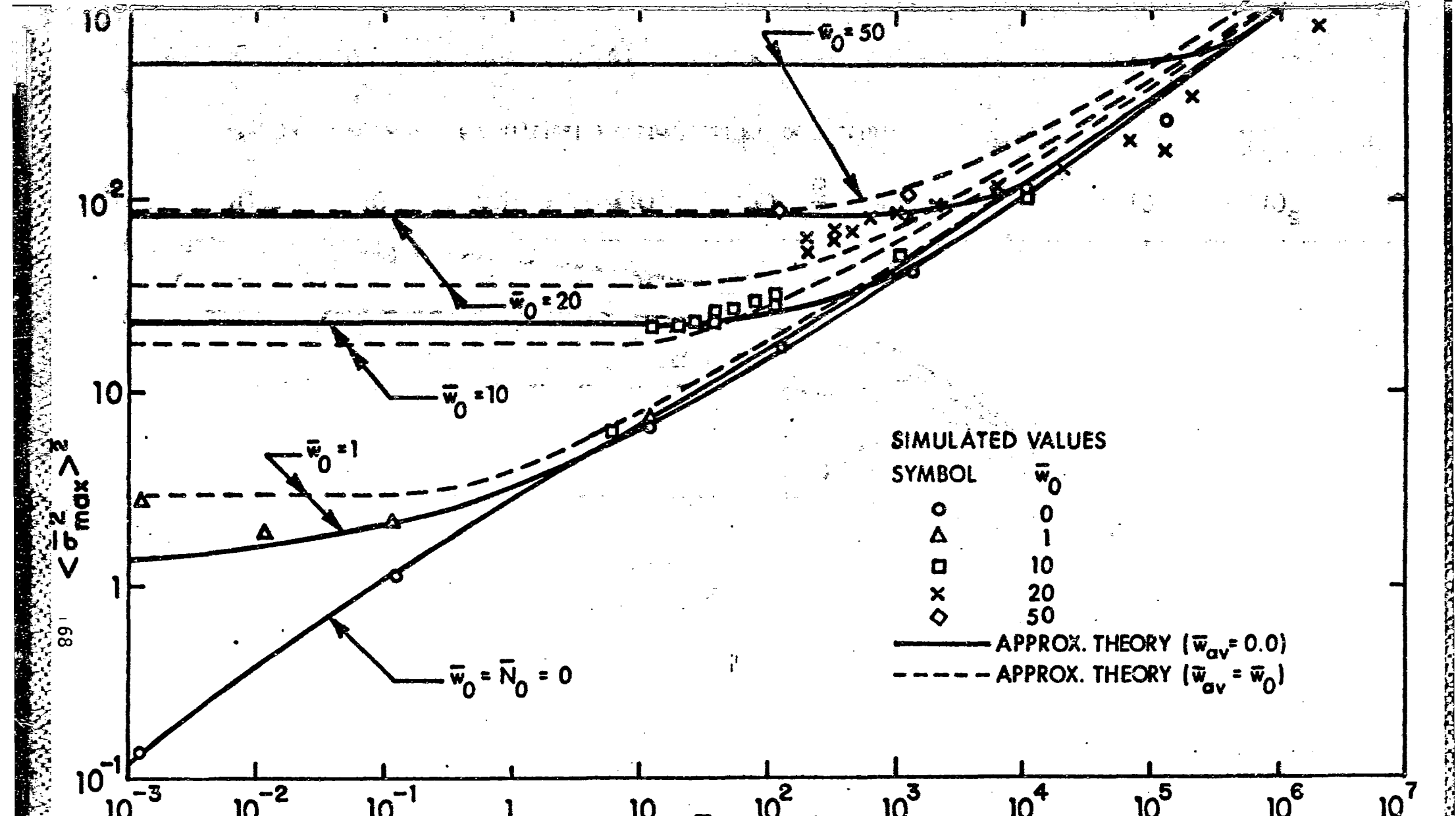

Fig. 19. Comparison of Analytical and Simulated RMS Results

parameter increases and to then increase. This phenomenon is explanable as the result of a shift in the average deflection from the buckled position to the unbuckled beam reference axis. THe mean position of the buckled beam would tend to shift toward the straight reference axis because of the softening spring characteristic for inward deflections and hardening spring characteristic for outward deflections exhibited in Fig. 2. Unfortunately the few results obtained for the variation of the average deflection with $\bar{S}$ are insufficient to define the shift. The stress behavior is not as consistent, however.

4.2 Approximate Analytical Investigation

The computation effort involved in these calculations is very great, so great as to motivate an approximate analytical treatment of the problem. The method of equivalent linearization (reference 18) which was used in reference 15 for unbuckled beams suggests itself as a possible means of obtaining an approximate solution which can be compared to the numerical integration results for an accuracy check. There are certain complications in the present case, however, The method of equivalent linearization has been applied successfully in cases of nonlinearities which imply a zero mean displacement. In the present case, however, the restoring force is reasonably symmetrical only for small motion about the buckled equilibrium position and for large snap-through motion about the straight reference position. Between these two extremes the mean displacement shifts from the buckled to the unbuckled position.

The two extreme cases are considered herein as providing possible bounds on the RMS displacements and stresses. The method of equivalent linearization involves replacing the nonlinear terms in each of Eqs.(3.1) by an equivalent linear term. The equivalent linear term is determined by requiring that the mean-square error be a minimum. For small motion about the buckled equilibrium position let the nonlinear terms in each of Eqs.(3.1) be replaced by a term of the form $k_m \bar{w}_m$. Then the errors are given by

$$e_m = (2m-1)^2 \left\{ \left[(2m-1)^2 - \bar{N}_0 + \frac{1}{2}\bar{w}_0\bar{w}_1 + \sum_{n=1}^{\infty} (2n-1)^2 \bar{w}_n^2 \right] \bar{w}_m + \bar{w}_0 \delta_{m1} \left[\frac{1}{2}\bar{w}_0\bar{w}_1 + \sum_{n=1}^{\infty} (2n-1)^2 \bar{w}_n^2 \right] \right\} - k_m \bar{w}_m \qquad m = 1,2,3,\ldots \qquad (4.4a)$$

Then

$$\frac{\partial \langle e_m^2 \rangle}{\partial k_m} = 0 = \left\langle e_m \frac{\partial e_m}{\partial k_m} \right\rangle = \langle e_m w_m \rangle \qquad m = 1,2,3,\ldots \qquad (4.4b)$$

yielding

$$k_m = (2m-1)^2 \left((2m-1)^2 - \bar{N}_0 + \frac{1}{\langle w_m^2 \rangle} \left\{ \frac{1}{2}\bar{w}_0 \langle \bar{w}_1 \bar{w}_m^2 \rangle + \sum_{n=1}^{\infty} (2n-1)^2 \langle \bar{w}_m^2 \bar{w}_n^2 \rangle + \bar{w}_0 \delta_{m1} \left[\frac{1}{2}\bar{w}_0 \langle \bar{w}_1 \bar{w}_m \rangle + \sum_{n=1}^{\infty} (2n-1)^2 \langle \bar{w}_m \bar{w}_n^2 \rangle \right] \right\} \right) \qquad m = 1,2,3,\ldots \qquad (4.4c)$$

Considerations similar to those of reference 12 lead to the following result for white noise

$$k_m = (2m-1)^2\left[(2m=1)^2 - \bar{N}_0 + \frac{1}{2}\bar{w}_0^2\delta_{m1} + \bar{S}\sum_{n=1}^{\infty}\left(\frac{1}{k_n} + \frac{32k_m}{D_{mn}^2}\right)\right] \qquad (4.5a)$$

with

$$D_{mn} = 2(k_m+k_n) + \frac{1}{\bar{\mu}^2}(k_m-k_n)^2 \qquad (4.5b)$$

The mean-square deflections are then given by

$$<\bar{w}_{max}^2> = \bar{w}_0^2 + 16\bar{S}\sum_{m=1}^{\infty}\sum_{n=1}^{\infty}\frac{(-1)^{m+n}}{(2m-1)(2n-1)D_{mn}} \qquad (.46)$$

which is the sum of the square of the "mean" deflection w_0 and the mean-square of the deflections with respect to that mean value. The mean-square stresses are given by

$$<(\bar{\sigma}_{max}^{\pm})> = \left(\bar{N}_0 \mp \bar{w}_0\frac{h}{r} - \bar{S}\sum_{n=1}^{\infty}\frac{1}{k_n}\right)^2$$

$$+ \bar{S}\left[\frac{\bar{w}_0^2}{k_1} + 16\left(\frac{h}{r}\right)^2\sum_{m=1}^{\infty}\sum_{n=1}^{\infty}\frac{(-1)^{m+n}(2m-1)(2n-1)}{D_{mn}}\right.$$

$$\left. \pm 16\bar{w}_0\frac{h}{r}\sum_{n=1}^{\infty}\frac{(-1)^{n-1}(2n-1)}{D_{1n}}\right]$$

$$+ 32\bar{S}^2\sum_{m=1}^{\infty}\sum_{n=1}^{\infty}\frac{1}{D_{mn}^2} \qquad (4.7)$$

The average stress is not equal to zero but is given by

$$\bar{\sigma}^{\pm}_{av} = \bar{N}_0 \mp \bar{w}_0 \frac{h}{r} - \bar{S} \sum_{n=1}^{\infty} \frac{1}{k_n} \tag{4.8}$$

Thus the mean-square stress given by Eq.(4.6b) is the sum of the square of the average stress and the mean-square stress with respect to the mean value, i.e.,

$$(\bar{\sigma}^{\pm}_{max} - \bar{\sigma}^{\pm}_{av})^2 = \bar{S}\left[\frac{\bar{w}_0^2}{k_1} + 16\left(\frac{h}{r}\right)^2 \sum_{m=1}^{\infty}\sum_{n=1}^{\infty} \frac{(-1)^{m+1}(2m-1)(2n-1)}{D_{mn}}\right.$$

$$\left. \pm 16\bar{w}_0 \frac{h}{r} \sum_{n=1}^{\infty} \frac{(-1)^{n-1}(2n-1)}{D_{1n}}\right] + 32\bar{S}^2 \sum_{m=1}^{\infty}\sum_{n=1}^{\infty} \frac{1}{D_{mn}^2} \tag{4.9}$$

When motion about a mean straight reference position is considered, the nonlinear terms in Eqs.(3.1) are replaced by equivalent linear expressions $k_m(\bar{w}_m + \bar{w}_0\delta_{m1})$. The error is then written as

$$e_m = \left\{(2m-1)^2\left[(2m-1)^2 - \tilde{N}_0 - \frac{1}{4}\bar{w}_0^2 + \sum_{n=1}^{\infty}(2n-1)^2(\bar{w}_n + \bar{w}_0\delta_{n1})^2\right] - k_m\right\}(\bar{w}_m + \bar{w}_0\delta_{m1})$$

$$m = 1,2,3,... \tag{4.10a}$$

so that the criteria for the determiniation of k_m are

$$\langle e_m(w_m + \bar{w}_0\delta_{m1})\rangle = 0 \qquad m = 1,2,3,... \tag{4.10b}$$

Thus

$$k_m = (2m-1)^2\left[(2m-1)^2 - \bar{N}_0 - \frac{1}{4}\bar{w}_0^2 + \sum_{n=1}^{\infty}(2n-1)^2 < (\bar{w}_m+\bar{w}_0\delta_{m1})^2(\bar{w}_n+\bar{w}_0\delta_{n1})^2 \times (\bar{w}_m+\bar{w}_0\delta_{m})^2 > \right] \quad m = 1,2,3,\ldots \tag{4.11a}$$

and for white noise is given by

$$k_m = (2m-1)^2\left[(2m-1)^2 - \bar{N}_0 - \frac{1}{4}\bar{w}_0^2 + \bar{S}\sum_{n=1}^{\infty}\left(\frac{1}{k_n} + \frac{32k_m}{D_{mn}^2}\right)\right] \tag{4.11b}$$

The mean square deflection is now

$$<\bar{w}_{max}^2> = 16\bar{S}\sum_{m=1}^{\infty}\sum_{n=1}^{\infty}\frac{(-1)^{m+n}}{(2m-1)(2n-1)D_{mn}} \tag{4.12}$$

while the mean square deflection is given by

$$<\bar{\sigma}_{max}^2> = \left(\bar{N}_0 + \frac{1}{4}\bar{w}_0^2 - \bar{S}\sum_{n=1}^{\infty}\frac{1}{k_n}\right)^2 + 16\bar{S}\left(\frac{h}{r}\right)^2\sum_{m=1}^{\infty}\sum_{n=1}^{\infty}\frac{(-1)^{m+n}(2m-1)(2n-1)}{D_{mn}} + 32\bar{S}^2\sum_{m=1}^{\infty}\sum_{n=1}^{\infty}\frac{1}{D_{mn}^2} \tag{4.13}$$

which is again the sum of square of the average stress

$$\bar{\sigma}_{av} = \bar{N}_0 + \frac{1}{4}\bar{w}_0^2 - \bar{S}\sum_{n=1}^{\infty}\frac{1}{k_n} \tag{4.14}$$

and the mean square stress about this average.

4.3 Comparison of Simulated and Equivalent Linearization Results

Equations (4.5) and (4.11b) were solved by a quadratic iteration process as in reference 15. The results were found to be quite insensitive to the viscous damping parameter $\bar{\mu}$ so that most calculations were made with this parameter taken equal to zero. In this case $1/D_{mn}$ vanishes if m is not equal to n and is equal to $1/4k_m$ if m and n are equal. Thus single summations are reduced to a single term while double summations are reduced to single summations, thereby simplifying the computations. Since the numerical integration results involved only three Fourier series terms, the number of terms in the approximate solutions were restricted to three for comparison purposes. The RMS deflections and stresses predicted by Eqs(4.5) and (4.11b) are shown in Figs. 18 and 19 by the solid and dashed curves together with the points obtained by numerical integration.

It will be noted that the deflections obtained by the numerical integration are reasonably bracketed by the two sets of approximate curves. The RMS deflections with respect to the straight reference position approach the static buckle deflection for small excitation and merge with the curve for large snap-through deflections about the straight reference position as the excitation increases. For an unbuckled beam ($\bar{w}_0 = \bar{N}_0 = 0$) the equivalent linearization results reduce to a single curve. In this case the numerical integration and equivalent linearization results are in very good agreement over a quite large range of the parameter $\bar{S}$.

The approximate calculations indicate similar RMS deflections from both equations as the spectral density parameter increases. In agreement with the numerical integration results, the deflection for all values of $\bar{w}_0$ tend to become equal. The equivalent linearization deflections appear to become increasingly larger than those obtained by numerical integration for large $\bar{S}$. This disagreement is possibly due to use of the method of equivalent linearization beyond its range of applicability (see, however ref.16). Certainly the beam is very highly nonlinear for large deformations. It is also possible that the constant time increment used in the simulation process for the random loading is too large. The average period of vibration about the straight position decreases as the excitation increases, whereas the time increment over which the loading remains constant was not decreased. This could conceivably result in decreased deflections. Additional calculations to prove or disprove this contention would be quite costly, however.

Also shown in Fig. 18 are the critical values of the spectral density parameter $\bar{S}$ given by Eq.(3.5). The RMS deflections appear to only first depart significantly from the static value at this point rather than an abrupt discontinuity of RMS deflection.

Similar agreement is found for simulated and equivalent linearization results in Fig. 19. There is again a transition of the simulated stresses from those given for vibrations about the buckled position to vibrations about the unbuckled position. The somewhat strange behavior of the appropriate theoretical results consisting of the stresses of the two approximate results crossing for large $\bar{w}_0$, but not for $\bar{w}_0$ of unity, is confirmed by

the simulated results. Again the stresses given by equivalent linearization deviate from the simulated results for large $\bar{S}$. The approximate results are conservative, however, and are thus useful. Indeed, they may be more reliable for the reasons discussed earlier.

Since convergent stresses require the consideration of a large number of terms, calculations for a parametric study were made with the use of 100 Fourier series terms. The results are presented in Table 9 for vibrations about the static buckled position while results for vibrations about the straight reference position are given in Table 10. The RMS deflection, average stress, and RMS stress with respect to the average are given for $\bar{S}$ stress with respect to the average are given for $\bar{S}$ ranging from 10^{-2} to 10^{6} for various values of $\bar{w}_0$. In Table 9 stress results are presented for both the top and bottom fibers of the beam under the assumption of h/r equal to $\sqrt{3}$ (a rectangular section). For vibrations about the straight position the RMS and average stresses at the top and bottom of a beam symmetrical about the centroidal axis are identical and are tabulated in Table 10 with h/r also equal to $\sqrt{3}$ for that case.

The calculated RMS deflections about the average position are shown graphically in Fig. 20 and exhibit a regular behavior. The results for vibrations about the buckled position indicate as expected that the beam becomes stiffer as the initial buckled amplitude increasing with constant excitation resulting in decreasing RMS deflection. The unbuckled beam becomes less stiff as the axial load increases and the RMS deflection becomes greater for constant excitation. This explains the results for beams of increasing $\bar{w}_0$ vibrating about the straight position since they can be considered to be unbuckled beams with axial load parameters $\bar{N}_0$ greater than unity and equal to $1 + \frac{1}{4}\bar{w}_0^2$.

Table 9: RMS Deflections and Stresses ($\bar{w}_{av} = \bar{w}_0$)

$\bar{w}_0$	$\bar{S}$	$\langle \bar{w}^2 \rangle^{1/2}$	$\bar{\sigma}^-_{av}$	$\langle \bar{\sigma}^{-2}_- \rangle^{1/2}$	$\bar{\sigma}^+_{av}$	$\langle \bar{\sigma}^{-2}_+ \rangle^{1/2}$
1.0	0.100000D-01	0.268756D+00	0.271385D+01	0.373970D+00	-0.750255D+00	0.624372D+00
	0.200000D-01	0.365241D+00	0.269841D+01	0.513587D+00	-0.765693D+00	0.851726D+00
	0.500000D-01	0.530451D+00	0.266098D+01	0.764346D+00	-0.803123D+00	0.124813D+01
	0.100000D+00	0.685166D+00	0.261324D+01	0.101662D+01	-0.850862D+00	0.163019D+01
	0.200000D+00	0.867016D+00	0.254125D+01	0.133986D+01	-0.922854D+00	0.209639D+01
	0.500000D+00	0.115424D+01	0.239192D+01	0.192009D+01	-0.107218D+01	0.287942D+01
	0.100000D+01	0.141327D+01	0.221886D+01	0.252561D+01	-0.124524D+01	0.364370D+01
	0.200000D+01	0.171569D+01	0.196920D+01	0.333832D+01	-0.149491D+01	0.461522D+01
	0.500000D+01	0.219665D+01	0.146195D+01	0.487069D+01	-0.200215D+01	0.635158D+01
	0.100000D+02	0.263536D+01	0.875811D+00	0.651981D+01	-0.258829D+01	0.814780D+01
	0.200000D+02	0.315251D+01	0.268660D-01	0.875456D+01	-0.343724D+01	0.105234D+02
	0.500000D+02	0.398263D+01	-0.170668D+01	0.129459D+02	-0.517078D+01	0.148947D+02
	0.100000D+03	0.474518D+01	-0.371199D+01	0.173968D+02	-0.717609D+01	0.194803D+02
	0.200000D+03	0.564830D+01	-0.660629D+01	0.233591D+02	-0.100704D+02	0.255785D+02
	0.500000D+03	0.710401D+01	-0.124693D+02	0.344605D+02	-0.159334D+02	0.368629D+02
	0.100000D+04	0.844534D+01	-0.191908D+02	0.462484D+02	-0.226549D+02	0.487921D+02
	0.200000D+04	0.100371D+02	-0.288198D+02	0.621064D+02	-0.322839D+02	0.647935D+02
	0.500000D+04	0.126077D+02	-0.481754D+02	0.918590D+02	-0.516395D+02	0.947383D+02
	0.100000D+05	0.149798D+02	-0.702225D+02	0.123732D+03	-0.736866D+02	0.126757D+03
	0.200000D+05	0.177979D+02	-0.101650D+03	0.166983D+03	-0.105114D+03	0.170155D+03
	0.500000D+05	0.223536D+02	-0.164498D+03	0.249050D+03	-0.167962D+03	0.252412D+03
	0.100000D+06	0.265611D+02	-0.235776D+03	0.337992D+03	-0.239240D+03	0.341494D+03
	0.200000D+06	0.315626D+02	-0.337048D+03	0.459970D+03	-0.340512D+03	0.463606D+03
	0.500000D+06	0.396523D+02	-0.538904D+03	0.694339D+03	-0.542368D+03	0.698145D+03
	0.100000D+07	0.471266D+02	-0.767220D+03	0.951395D+03	-0.770684D+03	0.955321D+03
2.0	0.100000D-01	0.141122D+00	0.445898D+01	0.200937D+00	-0.246923D+01	0.421787D+00
	0.200000D-01	0.198848D+00	0.445392D+01	0.284022D+00	-0.247428D+01	0.594741D+00
	0.500000D-01	0.311117D+00	0.443917D+01	0.448419D+00	-0.248903D+01	0.932442D+00
	0.100000D+00	0.432912D+00	0.441579D+01	0.632737D+00	-0.251241D+01	0.130166D+01
	0.200000D+00	0.595019D+00	0.437269D+01	0.891335D+00	-0.255552D+01	0.179958D+01
	0.500000D+00	0.880946D+00	0.426292D+01	0.139691D+01	-0.266529D+01	0.270300D+01
	0.100000D+01	0.115514D+01	0.411642D+01	0.195582D+01	-0.281179D+01	0.360926D+01
	0.200000D+01	0.148115D+01	0.388818D+01	0.273007D+01	-0.304002D+01	0.475067D+01

Table 9: Continued

$\bar{w}_0$	$\bar{S}$	$\langle \bar{w}^2 \rangle^{1/2}$	$\bar{\sigma}^-_{av}$	$\langle \bar{\sigma}^{-2}_- \rangle^{1/2}$	$\bar{\sigma}^+_{av}$	$\langle \bar{\sigma}^{-2}_+ \rangle^{1/2}$
2.0	0.500000D+01	0.199813D+01	0.340094D+01	0.422185D+01	-0.352726D+01	0.672967D+01
	0.100000D+02	0.246370D+01	0.282444D+01	0.584542D+01	-0.410377D+01	0.870945D+01
	0.200000D+02	0.300559D+01	0.198131D+01	0.805620D+01	-0.494689D+01	0.112615D+02
	0.500000D+02	0.386422D+01	0.250986D+00	0.122137D+02	-0.667722D+01	0.158501D+02
	0.100000D+03	0.464506D+01	-0.175427D+01	0.166349D+02	-0.868248D+01	0.205875D+02
	0.200000D+03	0.556385D+01	-0.464982D+01	0.225632D+02	-0.115780D+02	0.268277D+02
	0.500000D+03	0.703671D+01	-0.105156D+02	0.336134D+02	-0.174438D+02	0.382879D+02
	0.100000D+04	0.838871D+01	-0.172396D+02	0.453586D+02	-0.241678D+02	0.503413D+02
	0.200000D+04	0.998950D+01	-0.268712D+02	0.611713D+01	-0.337994D+02	0.664624D+02
	0.500000D+04	0.125698D+02	-0.462304D+02	0.908611D+02	-0.531586D+02	0.965587D+02
	0.100000D+05	0.149479D+02	-0.682801D+02	0.122684D+03	-0.752083D+02	0.128687D+03
	0.200000D+05	0.177711D+02	-0.997096D+02	0.165886D+03	-0.106638D+03	0.172191D+03
	0.500000D+05	0.223323D+02	-0.162560D+03	0.247887D+03	-0.169489D+03	0.254583D+03
	0.100000D+06	0.265432D+02	-0.233841D+03	0.336780D+03	-0.240769D+03	0.343762D+03
	0.200000D+06	0.315476D+02	-0.335115D+03	0.458709D+03	-0.342043D+03	0.465966D+03
	0.500000D+06	0.396403D+02	-0.536972D+03	0.693018D+03	-0.543901D+03	0.700619D+03
	0.100000D+07	0.471165D+02	-0.765290D+03	0.950030D+03	-0.772218D+03	0.957874D+03
5.0	0.100000D-01	0.571331D-01	0.965929D+01	0.177723D+00	-0.766122D+01	0.294957D+00
	0.200000D-01	0.807902D-01	0.965833D+01	0.251332D+00	-0.766218D+01	0.417101D+00
	0.500000D-01	0.127701D+00	0.965544D+01	0.397358D+00	-0.766506D+01	0.659347D+00
	0.100000D+00	0.180506D+00	0.965064D+01	0.561875D+00	-0.766987D+01	0.932109D+00
	0.200000D+00	0.255016D+00	0.964107D+01	0.794400D+00	-0.767944D+01	0.131722D+01
	0.500000D+00	0.402009D+00	0.961256D+01	0.125507D+01	-0.770795D+01	0.207813D+01
	0.100000D+01	0.565760D+00	0.956575D+01	0.177265D+01	-0.775476D+01	0.292841D+01
	0.200000D+01	0.792653D+00	0.947457D+01	0.250068D+01	-0.784584D+01	0.411309D+01
	0.500000D+01	0.122189D+01	0.921791D+01	0.392698D+01	-0.810260D+01	0.638399D+01
	0.100000D+02	0.166755D+01	0.883353D+01	0.549948D+01	-0.848698D+01	0.879843D+01
	0.200000D+02	0.223082D+01	0.817292D+01	0.765681D+01	-0.914759D+01	0.119582D+02
	0.500000D+02	0.316465D+01	0.663772D+01	0.117335D+02	-0.106828D+02	0.175306D+02
	0.100000D+03	0.402048D+01	0.473670D+01	0.160820D+02	-0.125838D+02	0.230702D+02
	0.200000D+03	0.501750D+01	0.191184D+01	0.219284D+02	-0.154087D+02	0.301110D+02
	0.500000D+03	0.658791D+01	-0.389951D+01	0.328622D+02	-0.212200D+02	0.425834D+02
	0.100000D+04	0.800552D+01	-0.106030D+02	0.445172D+02	-0.279235D+02	0.553549D+02
	0.200000D+04	0.966394D+01	-0.202260D+02	0.602395D+02	-0.375465D+02	0.721475D+02
	0.500000D+04	0.123086D+02	-0.395854D+02	0.898102D+02	-0.569059D+02	0.103062D+03

Table 9: Continued

$\bar{w}_0$	$\bar{S}$	$\langle \bar{w}^2 \rangle^{1/2}$	$\bar{\sigma}^-_{av}$	$\langle \bar{\sigma}^{-2}_- \rangle^{1/2}$	$\bar{\sigma}^+_{av}$	$\langle \bar{\sigma}^{-2}_+ \rangle^{1/2}$
5.0	0.100000D+05	0.147274D+02	-0.616406D+02	0.121544D+03	-0.789611D+02	0.135761D+03
	0.200000D+05	0.175851D+02	-0.930783D+02	0.164658D+03	-0.110399D+03	0.179795D+03
	0.500000D+05	0.221839D+02	-0155942D+03	0.246545D+03	-0.173262D+03	0.262831D+03
	0.100000D+06	0.264183D+02	-0.227232D+03	0.335355D+03	-0.244552D+03	0.352457D+03
	0.200000D+06	0.314424D+02	-0.328515D+03	0.457204D+03	-0.345836D+03	0.475075D+03
	0.500000D+06	0.395566D+02	-0.530385D+03	0.691412D+03	-0.547705D+03	0.710225D+03
	0.100000D+07	0.470461D+02	-0.758710D+03	0.948355D+03	-0.776031D+03	0.967819D+03
10.0	0.100000D-01	0.294082D-01	0.183201D+02	0.195556D+00	-0.163209D+02	0.256816D+00
	0.200000D-01	0.415890D-01	0.183198D+02	0.276554D+00	-0.163212D+02	0.363188D+00
	0.500000D-01	0.657560D-01	0.183187D+02	0.437247D+00	-0.163223D+02	0.574228D+00
	0.100000D+00	0.929884D-01	0.183169D+02	0.618307D+00	-0.163241D+02	0.812028D+00
	0.200000D+00	0.131492D+00	0.183133D+02	0.874266D+00	-0.163278D+02	0.114823D+01
	0.500000D+00	0.207846D+00	0.183024D+02	0.138162D+01	-0.163386D+02	0.181479D+01
	0.100000D+01	0.293794D+00	0.182844D+02	0.195224D+01	-0.163567D+02	0.256482D+01
	0.200000D+01	0.415082D+00	0.182485D+02	0.275624D+01	-0.163925D+02	0.362252D+01
	0.500000D+01	0.654423D+00	0.181424D+02	0.433694D+01	-0.164986D+02	0.570630D+01
	0.100000D+02	0.921260D+00	0.179706D+02	0.606767D+01	-0.166705D+02	0.802285D+01
	0.200000D+02	0.129175D+01	0.1764230+02	0.849667D+01	-0.169988D+02	0.112272D+02
	0.500000D+02	0.199736D+01	0.167478D+02	0.130342D+02	-0.178932D+02	0.173068D+02
	0.100000D+03	0.274028D+01	0.154499D+02	0.178115D+02	-0.191912D+02	0.237247D+02
	0.200000D+03	0.369738D+01	0.132624D+02	0.241193D+02	-0.213786D+02	0.321239D+02
	0.500000D+03	0.532300D+01	0.822356D+01	0.356511D+02	-0.264175D+02	0.470258D+02
	0.100000D+04	0.683973D+01	0.198781D+01	0.477153D+02	-0.326532D+02	0.619386D+02
	0.200000D+04	0.862104D+01	-0.728294D+01	0.637960D+02	-0.419240D+02	0.809677D+02
	0.500000D+04	0.114351D+02	-0.263316D+02	0.937626D+02	-0.609727D+02	0.114793D+03
	0.100000D+05	0.139745D+02	-0.482415D+02	0.125745D+03	-0.828825D+02	0.149570D+03
	0.200000D+05	0.169412D+02	-0.795885D+02	0.169071D+03	-0.114229D+03	0.195537D+03
	0.500000D+05	0.216644D+02	-0.142389D+03	0.251195D+03	-0.177030D+03	0.280879D+03
	0.100000D+06	0.259782D+02	-0.213659D+03	0.340159D+03	-0.248300D+03	0.372058D+03
	0.200000D+06	0.310704D+02	-0.314937D+03	0.462144D+03	-0.349578D+03	0.496070D+03
	0.500000D+06	0.392594D+02	-0.5168140+03	0.696511D+03	-0.551455D+03	0.732833D+03
	0.100000D+07	0.467956D+02	-0.745150D+03	0.953559D+03	-0.779791D+03	0.991487D+03

Table 9: Continued

$\bar{w}_0$	$\bar{S}$	$\langle \bar{w}^2 \rangle^{\frac{1}{2}}$	$\bar{\sigma}^-_{av}$	$\langle \bar{\sigma}^{-2}_- \rangle^{\frac{1}{2}}$	$\bar{\sigma}^+_{av}$	$\langle \bar{\sigma}^{-2}_+ \rangle^{\frac{1}{2}}$
20.0	0.100000D-01	0.162743D-01	0.356408D+02	0.208257D+00	-0.336412D+02	0.239222D+00
	0.200000D-01	0.230151D-01	0.356406D+02	0.294516D+00	-0.336414D+02	0.338308D+00
	0.500000D-01	0.363893D-01	0.356400D+02	0.465655D+00	-0.336421D+02	0.534898D+00
	0.100000D+00	0.514602D-01	0.356389D+02	0.658499D+00	-0.336453D+02	0.756428D+00
	0.200000D+00	0.727701D-01	0.356368D+02	0.931155D+00	-0.336453D+02	0.106966D+01
	0.500000D+00	0.115033D+00	0.356304D+02	0.147180D+01	-0.336516D+02	0.169084D+01
	0.100000D+01	0.162619D+00	0.356198D+02	0.208029D+01	-0.336622D+02	0.239019D+01
	0.200000D+01	0.229803D+00	0.355988D+02	0.293878D+01	-0.336833D+02	0.337740D+01
	0.500000D+01	0.362557D+00	0.355366D+02	0.463205D+01	-0.337454D+02	0.532717D+01
	0.100000D+02	0.510995D+00	0.354360D+02	0.651879D+01	-0.338461D+02	0.750533D+01
	0.200000D+02	0.718314D+00	0.352440D+02	0.913912D+01	-0.340380D+02	0.105430D+02
	0.500000D+02	0.111994D+01	0.347223D+02	0.141588D+02	-0.345597D+02	0.164093D+02
	0.100000D+03	0.155843D+01	0.339630D+02	0.195561D+02	-0.353191D+02	0.227856D+02
	0.200000D+03	0.215824D+01	0.326600D+02	0.268238D+02	-0.366221D+02	0.314639D+02
	0.500000D+03	0.329461D+01	0.294863D+02	0.403630D+02	-0.397958D+02	0.478142D+02
	0.100000D+04	0.450321D+01	0.252035D+02	0.546449D+02	-0.440785D+02	0.651792D+02
	0.200000D+04	0.609239D+01	0.182172D+02	0.735817D+02	-0.510649D+02	0.881930D+02
	0.500000D+04	0.887385D+01	0.228332D+01	0.108127D+03	-0.669987D+02	0.129680D+03
	0.100000D+05	0.115367D+02	-0.175203D+02	0.143897D+03	-0.868023D+02	0.171656D+03
	0.200000D+05	0.147088D+02	-0.471437D+02	0.191008D+03	-0.116426D+03	0.225457D+03
	0.500000D+05	0.197566D+02	-0.1082860+03	0.277803D+03	-0.177568D+03	0.321285D+03
	0.100000D+06	0.243180D+02	-0.1787030+03	0.369908D+03	-0.247985D+03	0.420023D+03
	0.200000D+06	0.296414D+02	-0.279390D+03	0.494658D+03	-0.348672D+03	0.551023D+03
	0.500000D+06	0.381000D+02	-0.480774D+03	0.732117D+03	-0.550056D+03	0.795957D+03
	0.100000D+07	0.458111D+02	-0.708887D+03	0.991118D+03	-0.778169D+03	0.105994D+04
50.0	0.100000D-01	0.984140D-02	0.876024D+02	0.216850D+00	-0.856027D+02	0.229274D+00
	0.200000D-01	0.139176D-01	0.876022D+02	0.306669D+00	-0.856029D+02	0.324239D+00
	0.500000D-01	0.220045D-01	0.876017D+02	0.484873D+00	-0.856034D+02	0.512655D+00
	0.100000D+00	0.311162D+01	0.876008D+02	0.685683D+00	-0.856042D+02	0.724973D+00
	0.200000D+00	0.439971D-01	0.875991D+02	0.969613D+00	-0.856060D+02	0.102518D+01
	0.500000D+00	0.695281D-01	0.875940D+02	0.153267D+01	-0.856111D+02	0.162056D+01
	0.100000D+01	0.982402D-01	0.875855D+02	0.216655D+01	-0.856196D+02	0.229089D+01
	0.200000D+01	0.138689D+00	0.975687D+02	0.306123D+01	-0.856364D+02	0.323722D+01
	0.500000D+01	0.218173D+00	0.875189D+02	0.482774D+01	-0.856861D+02	0.510668D+01

Table 9: Continued

$\bar{w}_0$	$\bar{s}$	$\langle \bar{w}^2 \rangle^{1/2}$	$\bar{\sigma}^{-}_{av}$	$\langle \bar{\sigma}^{-2}_{-} \rangle^{1/2}$	$\bar{\sigma}^{-+}_{av}$	$\langle \bar{\sigma}^{-2}_{+} \rangle^{1/2}$
50.0	0.100000D+02	0.306101D+00	0.874387D+02	0.680006D+01	-0.857663D+02	0.719601D+01
	0.200000D+02	0.426773D+00	0.872870D+02	0.954812D+01	-0.859181D+02	0.101118D+02
	0.500000D+02	0.652478D+00	0.868814D+02	0.148465D+02	-0.863237D+02	0.157516D+02
	0.100000D+03	0.887359D+00	0.863075D+02	0.205966D+02	-0.868976D+02	0.218994D+02
	0.200000D+03	0.119384D+01	0.853588D+02	0.284277D+02	-0.878463D+02	0.303110D+02
	0.500000D+03	0.174939D+01	0.831750D+02	0.432903D+02	-0.900301D+02	0.463683D+02
	0.100000D+04	0.233178D+01	0.803894D+02	0.593666D+02	-0.928157D+02	0.638340D+02
	0.200000D+04	0.311669D+01	0.760280D+02	0.813192D+02	-0.971771D+02	0.877976D+02
	0.500000D+04	0.460839D+01	0.662866D+02	0.123091D+03	-0.106918D+03	0.133639D+03
	0.100000D+05	0.623048D+01	0.539634D+02	0.168204D+03	-0.119242D+03	0.183373D+03
	0.200000D+05	0.844640D+01	0.345971D+02	0.229409D+03	-0.138608D+03	0.251045D+03
	0.500000D+05	0.125944D+02	-0.906432D+01	0.343982D+03	-0.182269D+03	0.377844D+03
	0.100000D+06	0.168827D+02	-0.644061D+02	0.464518D+03	-0.237611D+03	0.510867D+03
	0.200000D+06	0.223122D+02	-0.149987D+03	0.623176D+03	-0.323192D+03	0.684765D+03
	0.500000D+06	0.313743D+02	-0.333707D+03	0.910263D+03	-0.506912D+03	0.995258D+03
	0.100000D+07	0.397446D+02	-0.551206D+03	0.120713D+04	-0.724411D+03	0.131115D+04

Table 10: RMS Deflections and Stresses ($\bar{w}_{av} = 0.0$)

$\bar{S}$	$\bar{w}_0 = 0.0$ $\bar{N}_0 = 0.0$			$\bar{w}_0 = 0.0$ $\bar{N}_0 = 0.5$		
	$\langle \bar{w}^2_{max} \rangle^{1/2}$	$\bar{\sigma}_{av}$	$\langle \bar{\sigma}^2 \rangle^{1/2}$	$\langle \bar{w}^2_{max} \rangle^{1/2}$	$\bar{\sigma}_{av}$	$\langle \bar{\sigma}^2 \rangle^{1/2}$
0.100000D-01	0.197280D+00	-0.986204D-02	0.380132D+00	0.268751D+00	0.4818040+00	0.4957660+00
0.200000D-01	0.275314D+00	-0.192135D-01	0.532148D+00	0.365235D+00	0.4663740+00	0.677682D+00
0.500000D=01	0.420468D+00	-0.448569D=01	0.819591D+00	0.530446D+00	0.428966D+00	0.997867D+00
0.100000D+00	0.567818D+00	-0.819167D-01	0.112002D+01	0.685164D+00	0.381264D+00	0.131088D+01
0.200000D+00	0.750242D+00	-0.143324D+00	0.150811D+01	0.867019D+00	0.309342D+00	0.169940D+01
0.500000D+00	0.104739D+01	-0.280688D+00	0.218968D+01	0.115426D+01	0.160210D+00	01236847D+01
0.100000D+01	0.131750D+01	-0.446605D+00	0.287424D+01	0.141330D+01	-0.125417D-01	0.303968D+01
0.200000D+01	0.163182D+01	-0.690414D+00	0.376108D+01	0.171575D+01	-0.261647D+00	0.391400D+01
0.500000D+01	0.212788D+01	-0.119079D+01	0.537743D+01	0.219679D+01	-0.767461D+00	0.551869D+01
0.100000D+02	0.257687D+01	-0.177140D+01	0.707826D+01	0.263557D+01	-0.135168D+01	0.721537D+01
0.200000D+02	0.310312D+01	-0.261377D+01	0.935691D+01	0.315280D+01	-0.219772D+01	0.949335D+01
0.500000D+02	0.394349D+01	-0.433637D+01	0.136019D+02	0.398306D+01	-0.392579D+01	0.137405D+02
0.100000D+03	0.471252D+01	-0.633190D+01	0.180960D+02	0.474571D+01	-0.592595D+01	0.182363D+02
0.200000D+03	0.562114D+01	-0.921568D+01	0.241064D+02	0.564890D+01	-0.881460D+01	0.242479D+02
0.500000D+03	0.708280D+01	-0.150646D+02	0.352794D+02	0.710468D+01	-0.146700D+02	0.354208D+02
0.100000D+04	0.842778D+01	-0.217758D+02	0.471264D+02	0.844603D+01	-0.213858D+02	0.472670D+02
0.200000D+04	0.100226D+02	-0.313949D+02	0.630468D+02	0.100378D+02	-0.310094D+02	0.631861D+02
0.500000D+04	0.125964D+02	-0.507383D+02	0.928861D+02	0.126084D+02	-0.503584D+02	0.930230D+02
0.100000D+05	0.149705D+02	-0.727769D+02	0.124826D+03	0.149805D+02	-0.724008D+02	0.124961D+03
0.200000D+05	0.177902D+02	-0.104196D+03	0.168146D+03	0.177985D+02	-0.103824D+03	0.168279D+03
0.500000D+05	0.223476D+02	-0.167035D+03	0.250304D+03	0.223542D+02	-0.166666D+03	0.250433D+03
0.100000D+06	0.265562D+02	-0.238307D+03	0.339313D+03	0.265617D+02	-0.237941D+03	0.339440D+03
0.200000D+06	0.315586D+02	-0.339574D+03	0.461356D÷03	0.315631D+02	-0.339211D+03	0.461480D+03
0.500000D+06	0.396491D+02	-0.541423D+03	0.695808D+03	0.396527D+02	-0.541063D+03	0.695929D+03
0.100000D+07	0.471240D+02	-0.769735D+03	0.952922D+03	0.471270D+02	-0.769377D+03	0.953041D+03

Table 10: Continued

$\bar{S}$	$\bar{w}_0 = 0.0$ $\bar{N}_0 = 1.0$			$\bar{w}_0 = 1.0$		
	$\langle \bar{w}^2_{max} \rangle^{1/2}$	$\bar{\sigma}_{av}$	$\langle \bar{\sigma}^2 \rangle^{1/2}$	$\langle \bar{w}^2 \rangle^{1/2}$	$\bar{\sigma}_{av}$	$\langle \bar{\sigma}^2 \rangle^{1/2}$
0.100000D-1	0.480517D+00	0.942130D+00	0.853658D+00	0.671832D+00	0.113701D+01	0.118715D+01
0.200000D-01	0.571412D+00	0.918081D+00	0.102543D+01	0.730178D+00	0.111642D+01	0.130171D+01
0.500000D-01	0.718458D+00	0.870231D+00	0.131452D+01	0.841966D+00	0.107204D+01	0.152892D+01
0.100000D+00	0.854323D+00	0.816095D+00	0.159600D+01	0.956589D+00	0.101977D+01	0.177327D+01
0.200000D+00	0.101585D+01	0.739162D+00	0.195132D+01	0.110074D+01	0.944200D+00	0.209834D+01
0.500000D+00	0.127707D+01	0.585266D+00	0.257983D+01	0.134369D+01	0.791575D+00	0.269453D+01
0.100000D+01	0.151832D+01	0.409928D+00	0.322557D+01	0.156393D+01	0.617056D+00	0.331820D+01
0.200000D+01	0.180499D+01	0.158754D+00	0.408012D+01	0.185152D+01	0.367093D+00	0.414677D+01
0.500000D+01	0.226825D+01	-0.349556D+00	0.566797D+01	0.230526D+01	-0.136593D+00	0.567468D+01
0.100000D+02	0.269574D+01	-0.935908D+00	0.735842D+01	0.272725D+01	-0.712491D+00	0.727579D+01
0.200000D+02	0.320333D+01	-0.178463D+01	0.963446D+01	0.323078D+01	-0.153629D+01	0.939717D+01
0.500000D+02	0.402303D+01	-0.351730D+01	0.138824D+02	0.404751D+01	-0.318984D+01	0.132971D+02
0.100000D+03	0.477911D+01	-0.552165D+01	0.183794D+02	0.480338D+01	-0.507092D+01	0.173899D+02
0.200000D+03	0.567678D+01	-0.841484D+01	0.243913D+02	0.570291D+01	-0.774964D+01	0.228442D+02
0.500000D+03	0.712661D+01	-0.142763D+02	0.355636D+02	0.715903D+01	-0.131009D+02	0.329773D+02
0.100000D+04	0.846431D+01	-0.209966D+02	0.474085D+02	0.850507D+01	-0.191645D+02	0.437425D+02
0.200000D+04	0.100531D+02	-0.306245D+02	0.633260D+02	0.101060D+02	-0.277738D+02	0.582601D+02
0.500000D+04	0.126203D+02	-0.499788D+02	0.931603D+02	0.126964D+02	-0.449220D+02	0.856338D+02
0.100000D+05	0.149904D+02	-0.720250D+02	0.125096D+03	0.150905D+02	-0.643073D+02	0.115148D+03
0.200000D+05	0.178068D+02	-0.103451D+03	0.168411D+03	0.179376D+02	-0.917835D+02	0.155470D+03
0.500000D+05	0.223607D+02	-0.166298D+03	0.250562D+03	0.225442D+02	-0.146419D+03	0.232651D+03
0.100000D+06	0.265671D+02	-0.237576D+03	0.339567D+03	0.268016D+02	-0.208098D+03	0.317039D+03
0.200000D+06	0.315677D+02	-0.338847D+03	0.461604D+03	0.318644D+02	-0.295434D+03	0.433670D+03
0.500000D+06	0.396562D+02	-0.540703D+03	0.696050D+03	0.400562D+02	-0.468931D+03	0.659749D+03
0.100000D+07	0.471300D+02	-0.769018D+03	0.953160D+03	0.476269D+02	-0.664645D+02	0.909704D+03

Table 10: Continued

$\bar{S}$	$\bar{w}_0 = 2.0$			$\bar{w}_0 = 5.0$		
	$\langle \bar{w}_{max}^2 \rangle^{1/2}$	$\bar{\sigma}_{av}$	$\langle \bar{\sigma}^2 \rangle^{1/2}$	$\langle \bar{w}_{max}^2 \rangle^{1/2}$	$\bar{\sigma}_{av}$	$\langle \bar{\sigma}^2 \rangle^{1/2}$
0.100000D-01	0.117134D+01	0.165683D+01	0.209343D+01	0.288781D+01	0.516486D+01	0.581019D+01
0.200000D-01	0.118790D+01	0.164750D+01	0.212983D+01	0.288886D+01	0.516305D+01	0.581686D+01
0.500000D-01	0.122851D+01	0.162190D+01	0.222864D+01	0.289202D+01	0.515765D+01	0.583674D+01
0.100000D+00	0.128618D+01	0.158487D+01	0.236901D+01	0.289724D+01	0.514871D+01	0.586942D+01
0.200000D+00	0.137615D+01	0.152346D+01	0.259610D+01	0.290757D+01	0.513105D+01	0.593323D+01
0.500000D+00	0.155762D+01	0.138595D+01	0.308412D+01	0.293757D+01	0.507973D+01	0.611383D+01
0.100000D+01	0.175017D+01	0.121975D+01	0.364514D+01	0.298464D+01	0.499894D+01	0.638632D+01
0.200000D+01	0.199694D+01	0.975701D+00	0.442644D+01	0.306975D+01	0.485121D+01	0.685767D+01
0.500000D+01	0.241853D+01	0.476889D+00	0.591070D+01	0.327661D+01	0.447915D+01	0.795120D+01
0.100000D+02	0.282132D+01	-0.969592D-01	0.748892D+01	0.353273D+01	0.398808D+01	0.977892D+01
0.200000D+02	0.330909D+01	-0.919656D+00	0.959323D+01	0.389505D+01	0.323117D+01	0.112928D+02
0.500000D+02	0.410914D+01	-0.257266D+01	0.134769D+02	0.456236D+01	0.163953D+01	0.148737D+02
0.100000D+03	0.485490D+01	-0.445375D+01	0.175610D+02	0.522920D+01	-0.210897D+00	0.188561D+02
0.200000D+03	0.574601D+01	-0.713268D+01	0.230090D+02	0.605619D+01	-0.286907D+01	0.242306D+02
0.500000D+03	0.719313D+01	-0.124844D+02	0.331363D+02	0.743621D+01	-0.820386D+01	0.342928D+02
0.100000D+04	0.853366D+01	-0.185484D+02	0.438988D+02	0.873639D+01	-0.142604D+02	0.450238D+02
0.200000D+04	0.101299D+02	-0.271581D+02	0.584148D+02	0.102993D+02	-0.228657D+02	0.595193D+02
0.500000D+04	0.127154D+02	-0.443068D+02	0.857875D+02	0.128493D+02	-0.400115D+02	0.868778D+02
0.100000D+05	0.151064D+02	-0.636924D+02	0.115302D+03	0.152186D+02	-0.593963D+02	0.116388D+03
0.200000D+05	0.179510D+02	-0.911689D+02	0.155625D+03	0.180451D+02	-0.868727D+02	0.156712D+03
0.500000D+05	0.225548D+02	-0.145804D+03	0.232807D+03	0.226295D+02	-0.141509D+03	0.233899D+03
0.100000D+06	0.268105D+02	-0.207484D+03	0.317196D+03	0.268732D+02	-0.203189D+03	0.318295D+03
0.200000D+06	0.318719D+02	-0.294820D+03	0.433827D+03	0.319246D+02	-0.290526D+03	0.434934D+03
0.500000D+06	0.400622D+02	-0.468317D+03	0.569909D+03	0.401040D+02	-0.464024D+03	0.661026D+03
0.100000D+07	0.476319D+02	-0.664032D+03	0.909865D+03	0.476671D+02	-0.659739D+03	0.910990D+03

Table 10: Continued

$\bar{S}$	$\bar{w}_0 = 10.0$			$\bar{w}_0 = 20.0$		
	$\langle \bar{w}^2_{max} \rangle^{1/2}$	$\bar{\sigma}_{av}$	$\langle \bar{\sigma}^2 \rangle^{1/2}$	$\langle \bar{w}^2_{max} \rangle^{1/2}$	$\bar{\sigma}_{av}$	$\langle \bar{\sigma}^2 \rangle^{1/2}$
0.100000D-01	0.574856D+01	0.174495D+02	0.164124D 02	0.114282D+02	0.657671D+02	0.544501D+02
0.200000D-01	0.574868D+01	0.174490D+02	0.164141D+02	0.114282D+02	0.657670D+02	0.544505D+02
0.500000D-01	0.574906D+01	0.174474D+02	0.164192D+02	0.114282D+02	0.657666D+02	0.544515D+02
0.100000D+00	0.574969D+01	0.174448D+02	0.164276D+02	0.114283D+02	0.657569D+02	0.544533D+02
0.200000D+00	0.575095D+01	0.174396D+02	0.164443D+02	0.114285D+02	0.567646D+02	0.544669D+02
0.500000D+00	0.575472D+01	0.174241D+02	0.164940D+02	0.114289D+02	0.567606D+02	0.544676D+02
0.100000D+01	0.576100D+01	0.173985D+02	0.165749D+02	0.114297D+02	0.657540D+02	0.544854D+02
0.200000D+01	0.577353D+01	0.173480D+02	0.167312D+02	0.114313D+02	0.657408D+02	0.545207D+02
0.500000D+01	0.581071D+01	0.172021D+02	0.171[illegible]5D+02	0.114361D+02	0.657013D+02	0.546248D+02
0.100000D+02	0.587094D+01	0.169725D+02	0.178073D+02	0.114440D+02	0.656362D+02	0.547934D+02
0.200000D+02	0.598450D+01	0.165492D+02	0.189139D+02	0.114599D+02	0.655078D+02	0.551159D+02
0.500000D+02	0.627875D+01	0.154564D+02	0.215204D+02	0.115075D+02	0.651332D+02	0.560085D+02
0.100000D+03	0.666738D+01	0.139694D+02	0.247720D+02	0.115857D+02	0.645342D+02	0.573511D+02
0.200000D+03	0.724512D+01	0.116222D+02	0.295522D+02	1.177364D+02	0.634030D+02	0.597354D+02
0.500000D+03	0.835478D+01	0.659665D+01	0.390465D+02	0.121449D+02	0.603676D+02	0.656586D+02
0.100000D+04	0.949319D+01	0.703586D+00	0.494861D+02	0.127162D+02	0.560620D+02	0.734774D+02
0.200000D+04	0.109249D+02	-0.778547D+01	0.637804D+02	0.136116D+02	0.490289D+02	0.855145D+02
0.500000D+04	0.133383D+02	-0.248300D+02	0.909731D+02	0.154206D+02	0.335228D+02	0.110467D+03
0.100000D+05	0.156259D+02	-0.441657D+02	0.120412D+03	0.173403D+02	0.150371D+02	0.138743D+03
0.200000D+05	0.183851D+02	-0.716089D+02	0.160696D+03	0.198000D+02	-0.117852D+02	0.178227D+03
0.500000D+05	0.228981D+02	-0.126217D+03	0.237866D+03	0.240016D+02	-0.658375D+02	0.254745D+03
0.100000D+06	0.270892D+02	-0.187885D+03	0.322266D+03	0.280162D+02	-0.127226D+03	0.338864D+03
0.200000D+06	0.321133D+02	-0.275214D+03	0.438918D+03	0.328789D+02	-0.214361D+03	0.455361D+03
0.500000D+06	0.402537D+02	-0.448706D+03	0.665036D+03	0.408579D+02	-0.387686D+03	0.681397D+03
0.100000D+07	0.477928D+02	-0.644419D+03	0.915023D+03	0.482988D+02	-0.583317D+03	0.931382D+03

Table 10: Continued

$\bar{S}$	$\bar{w}_0 = 50.0$		
	$\langle \bar{w}_{max}^2 \rangle^{1/2}$	$\bar{\sigma}_{av}$	$\langle \bar{\sigma}^2 \rangle^{1/2}$
0.100000D-01	0.284097D+02	0.400650D+03	0.303298D+03
0.200000D-01	0.284097D+02	0.400649D+03	0.303298D+03
0.500000D-01	0.284097D+02	0.400649D+03	0.303298D+03
0.100000D+00	0.284097D+02	0.400649D+03	0.303298D+03
0.200000D+00	0.284097D+02	0.400649D+03	0.303299D+03
0.500000D+00	0.284098D+02	0.400648D+03	0.303300D+03
0.100000D+01	0.284098D+02	0.400647D+03	0.303302D+03
0.200000D+01	0.284099D+02	0.400645D+03	0.303306D+03
0.500000D+01	0.284102D+02	0.400639D+03	0.303319D+03
0.100000D+02	0.284108D+02	0.400629D+03	0.303340D+03
0.200000D+02	0.284118D+02	0.400608D+03	0.303381D+03
0.500000D+02	0.284150D+02	0.400546D+03	0.303504D+03
0.100000D+03	0.284202D+02	0.400443D+03	0.303704D+03
0.200000D+03	0.284308D+02	0.400239D+03	0.304093D+03
0.500000D+03	0.284626D+02	0.399632D+03	0.305202D+03
0.100000D+04	0.285154D+02	0.398635D+03	0.306952D+03
0.200000D+04	0.286202D+02	0.396680D+03	0.310256D+03
0.500000D+04	0.289259D+02	0.391044D+03	0.319342D+03
0.100000D+05	0.294064D+02	0.382239D+03	0.332933D+03
0.299999D+05	0.302743D+02	0.366260D+03	0.356704D+03
0.500000D+05	0.323752D+02	0.326410D+03	0.413635D+03
0.100000D+06	0.349629D+02	0.274313D+03	0.485549D+03
0.200000D+06	0.386086D+02	0.194638D+03	0.592654D+03
0.500000D+06	0.453007D+02	0.284514D+02	0.810177D+03
0.100000D+07	0.519756D+02	-0.163452D+03	0.105600D+04

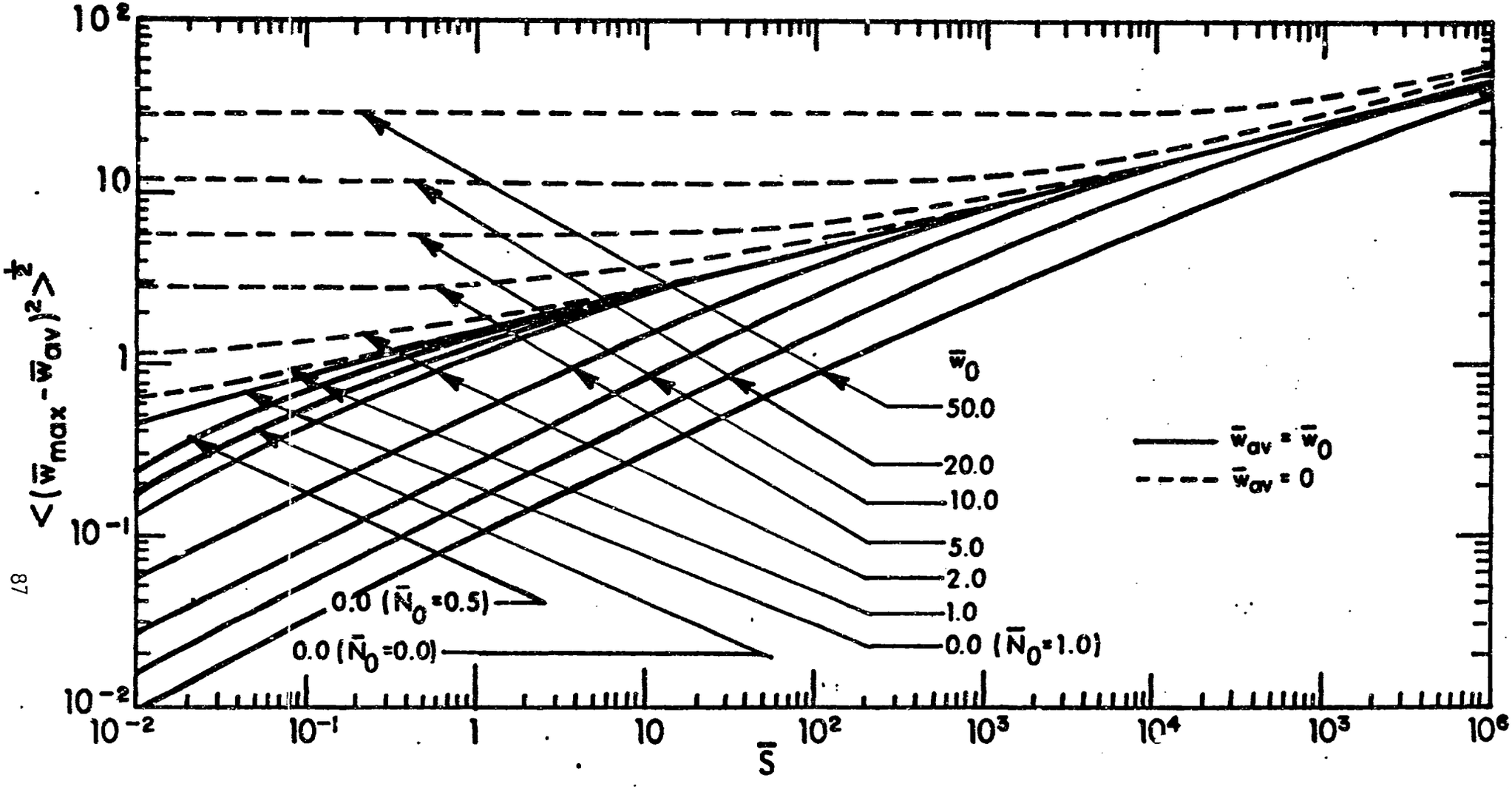

Fig. 20. RMS Deflections Obtained using Equivalent Linearization

The stress results are not shown graphically since there is no regular pattern that can be plotted without producing confusion.

Chapter 5

EXPERIMENTAL AND ANALYTICAL INVESTIGATION OF RMS RESPONSE OF CLAMPED BEAMS UNDER RANDOM LOADING

Experimental studies were performed to investigate the degree of agreement between analytical and experimental results. These experimental set-ups were guided by previous investigations of the effects of structural heating on aerospace vehicle structures loaded by random uniform pressure (reference 1).

5.1 Test Specimens

The material of the test specimens was aluminum Type 2024 Ducommun, which has a Young's modulus of 10.6×10^6 psi and 0.10 lb/in^3. The material was flexible enough to be snapped or excited by uniform sound pressure. The beam specimens were 8.125 in. long. and 1/4 in. wide, and had a thickness of 0.02 in.

5.2 Test Set-up

The overall test set-up for the nonlinear vibrations of the straight and buckled beam is shown in Fig. 21. The schematic set-up for measuring the strain response of the beam is shown in Fig. 22. A speaker with a 12 in. diameter was attached to one end of a tapered acoustic box. The other end is closed by a slotted board to which specimens were mounted (Figs. 23 and 24). The noise emitted by the speaker impinges on the beam specimen through the slot. A strain gage was installed at the beam center for measurement of the strain response of the beam. The box was made from one-

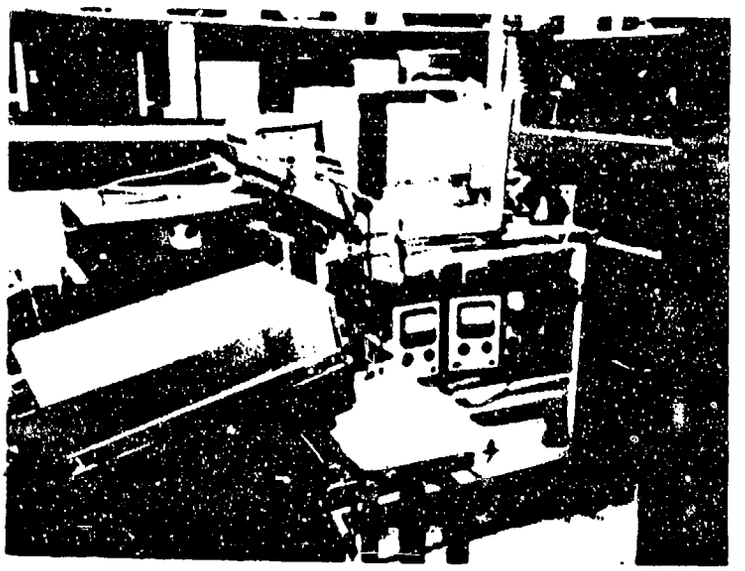

Fig. 21 Overall Experimental Set-Up

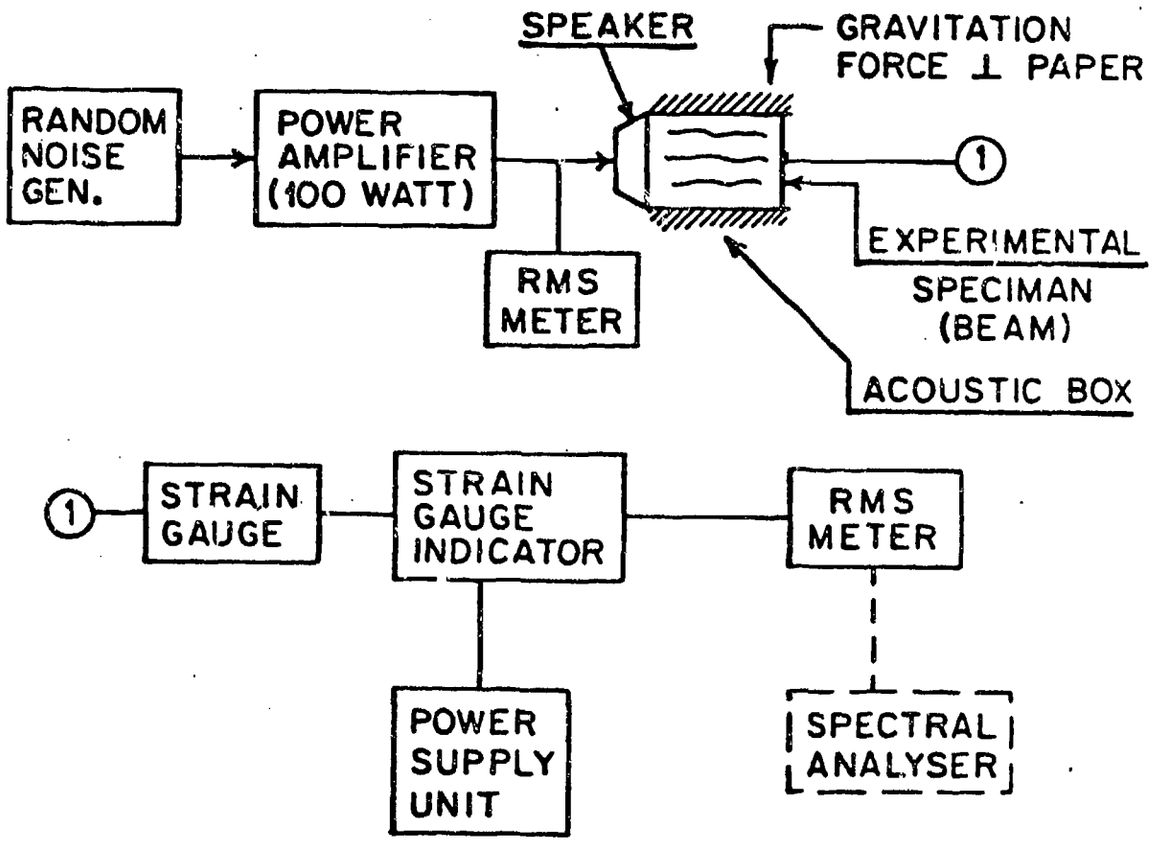

Fig. 22. Schematic Experimental Set-up for Measuring the Strain Response of Beam

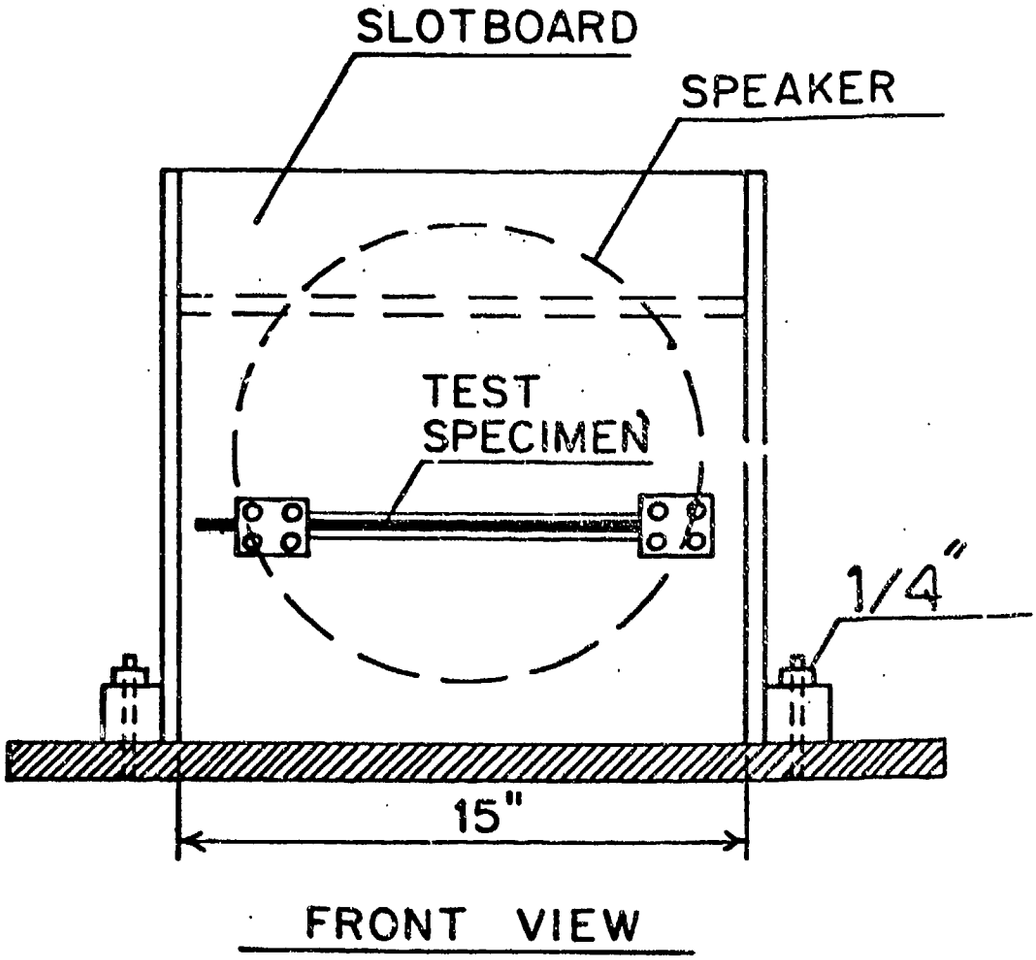

Fig. 23. Schematic Diagram of the Acoustic Box, Front View

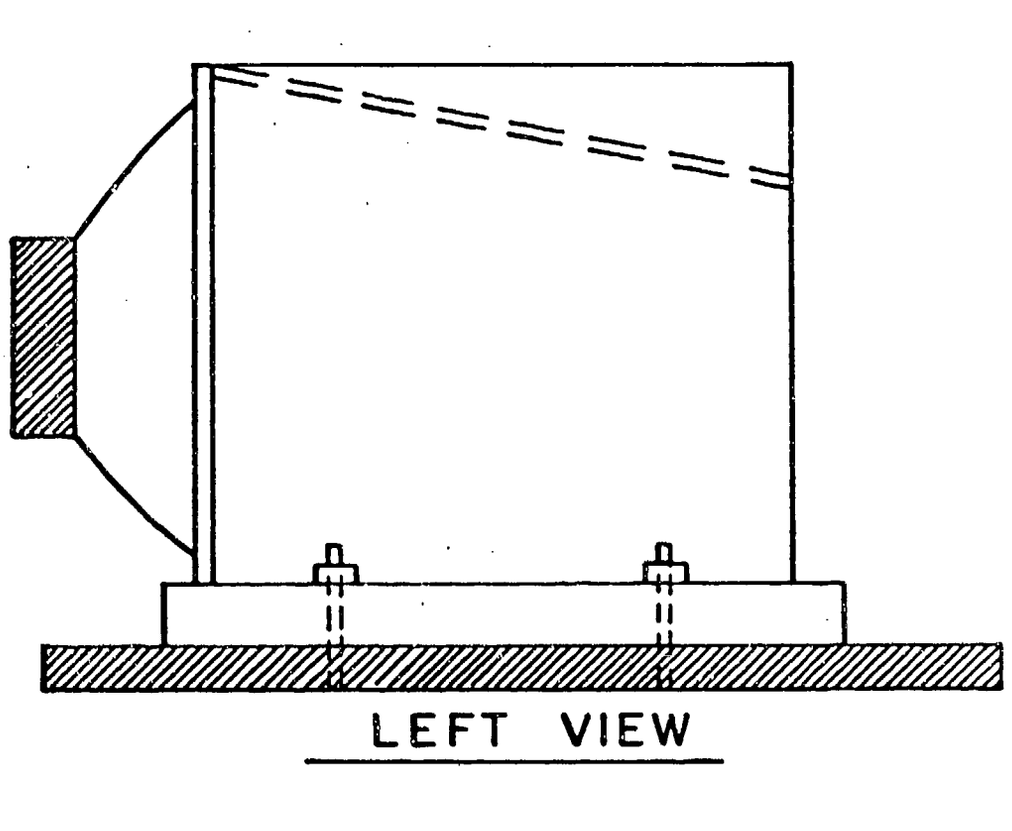

Fig. 24. Schematic Diagram of the Acoustic Box, Left View

inch and 3/4 in. plywood, so that it had the required rigidity to prevent vibration interaction with the speaker.

5.3 Sound Pressure Level Calibration

A calibration set up sketch for measuring sound pressure level vs. RMS values of input voltage for the speaker is shown in Fig. 25. The microphone supplied with the sound level meter was a prezoelectric ceramic microphone developed expressly for sound level meter use. To give a flat response to sound of random incidence from 20Hz to 12 KZ, a sound level meter was used of type 1551-C GenRad.

The sound level meter was first calibrated linearly. Then, the constant values of k_{nobe} for a different scale (NOBE) in terms of psi per volt was obtained using a sinusoidal signal. THe calibration curves are shown in Fig. 26.

To measure the power spectral density of the signal in terms of $(psi)^2 \cdot$ sec., a spectral analyzer was used (HP Type 3850) and the scope unit of the spectral analyzer was photographed. From those photographs, the power spectral density of output signal of the sound level meter S_0 in units of $(psi)^2 \cdot$sec. can be determined by squaring the amplitude of scope, dividing it by the bandwidth of spectral analyzer, and then multiplying by the square of the constant value of k_{nobe} and the square of the beam width. The bandwidth of the spectral analyzer was 30Hz and the time sweep was 10 seconds per division. The calibration curve of RMS input voltage versus $\bar{S}$, the nondimensional spectral density parameter, found by these measurements is shown in Fig. 27.

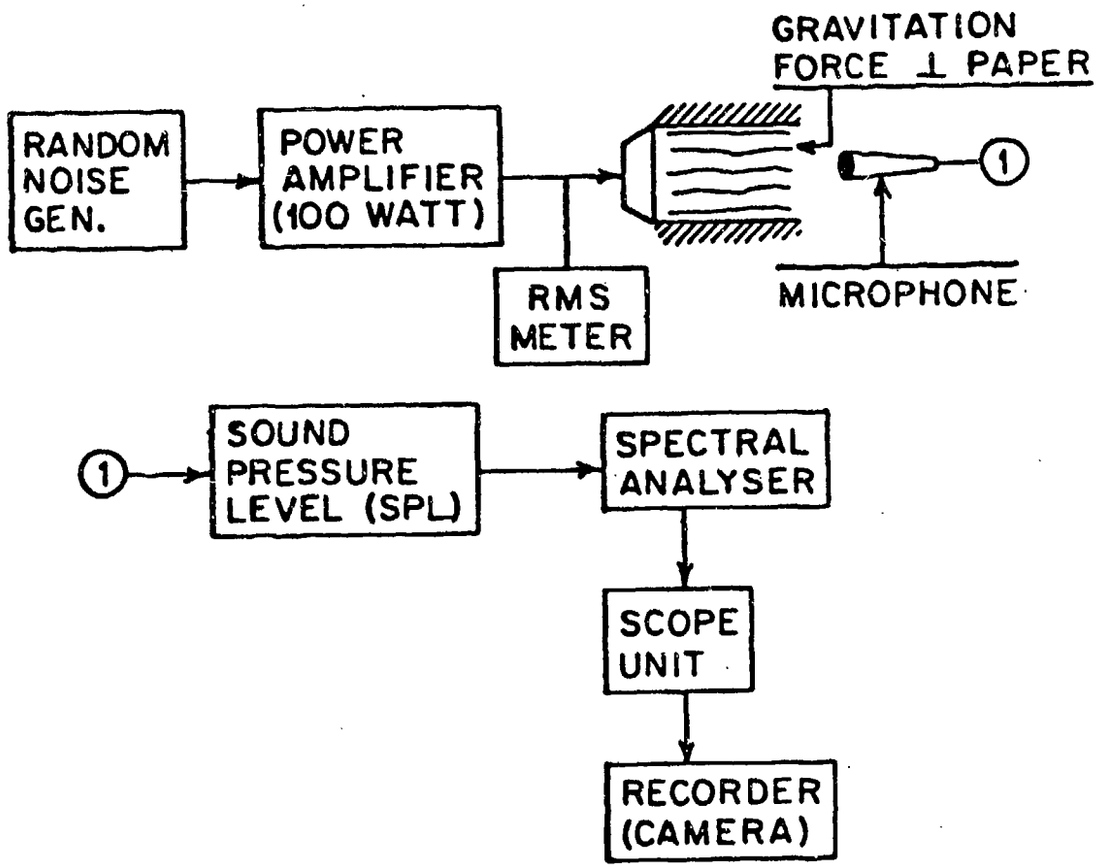

Fig. 25. Schematic Calibration Set-up for Measurement of Variation of Sount Pressure Level with Input Voltage of the Speaker

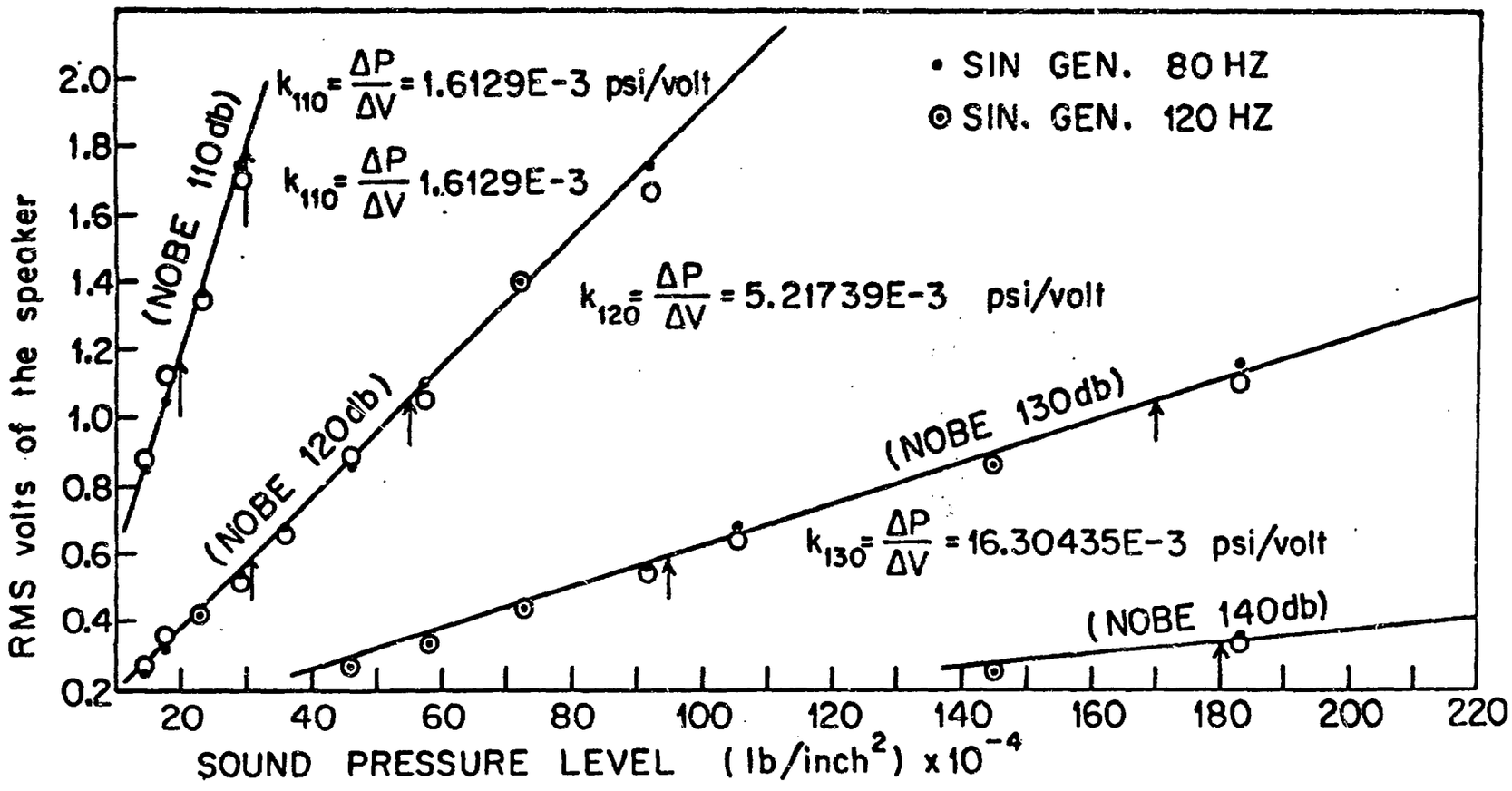

Fig. 26. Calibration Curves for Sound Pressure Level Meter

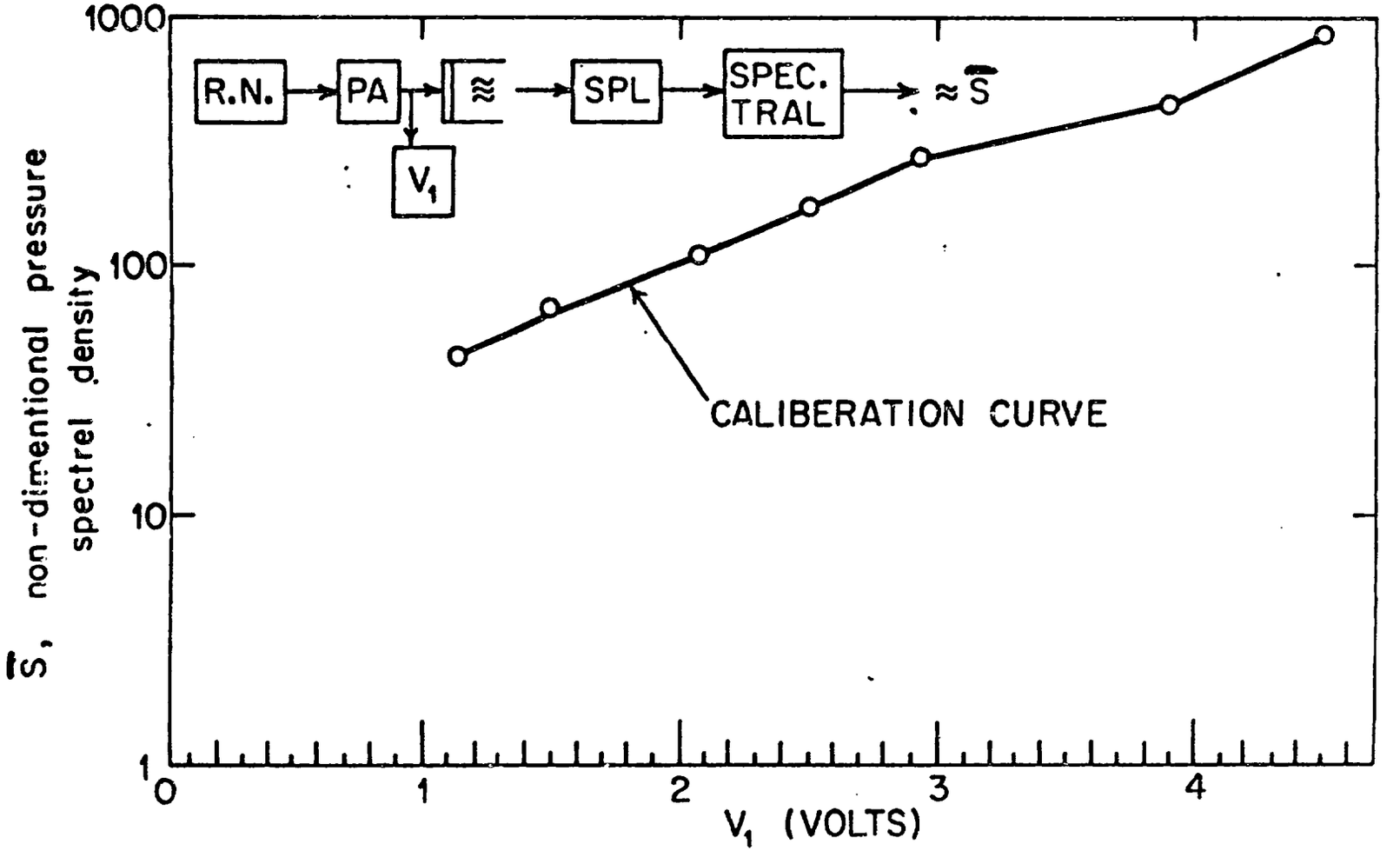

Fig. 27. Calibration of RMS Voltage of the Speaker vs the Power Spectral Density Parameter

The distribution of sound pressure level across the board slot of acoustic box for sinusoidal signal with frequency 115Hz is shown in Fig. 28. As can be seen from the figure, the pressure across the slot is almost uniform.

5.4 Test Procedure

The beam was mounted on the slotted board (see Fig. 29) and was subjected to pressure history which was generated by a random noise generator (General Radio Type 1381) with range of frequency from 2Hz to 2000Hz. The signal was amplified by a power amplifier with maximum power of about one hundred watts. THe RMS input voltage of the speaker was measured by an RMS meter (B&K Type 2409) with a bandwidth of 3Hz in 100 sec. The output of the strain gage was calibrated by using a dial gage indicator so that the calibration factor was 100 μin/in per 16.6 mv ($= \frac{100}{16.5} \frac{\mu \text{ in/in}}{\text{mv}}$). Then the RMS value of the dynamic strain of the beam, i.e., the RMS value of the total strain minus the static strain, was measured by using an RMS meter with a bandwidth of 3Hz in 100 sec. During a test run, the experimental data was collected within a period of about two to three minutes, in order to obtain almost constant value for the strain. The value of the excitation parameter $\bar{S}$ was obtained by using the calibration graph of RMS input voltage of the speaker versus the power spectral density of sound-pressure level (Fig.27).

The power spectral density of input voltage of the speaker was found to be relatively constant, approximating white noise (Fig. 30). The spectral density of the acoustic pressure was not uniform, however, due to the effects of the speaker distortion. A representative acoustic pressure

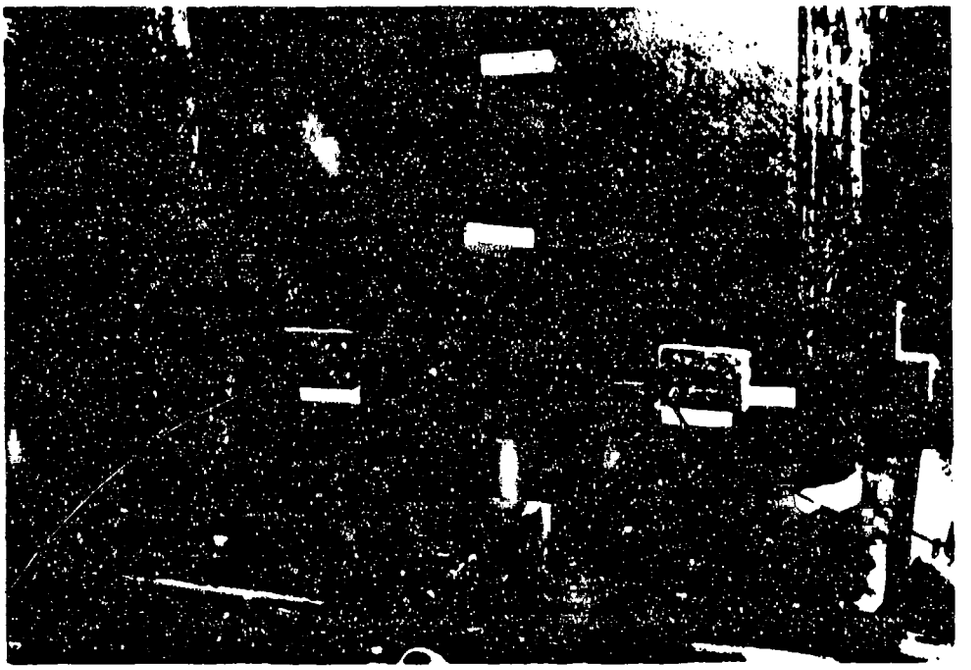

Fig. 28. Buckled Beam Mounted on Slot Board of Acoustic Box

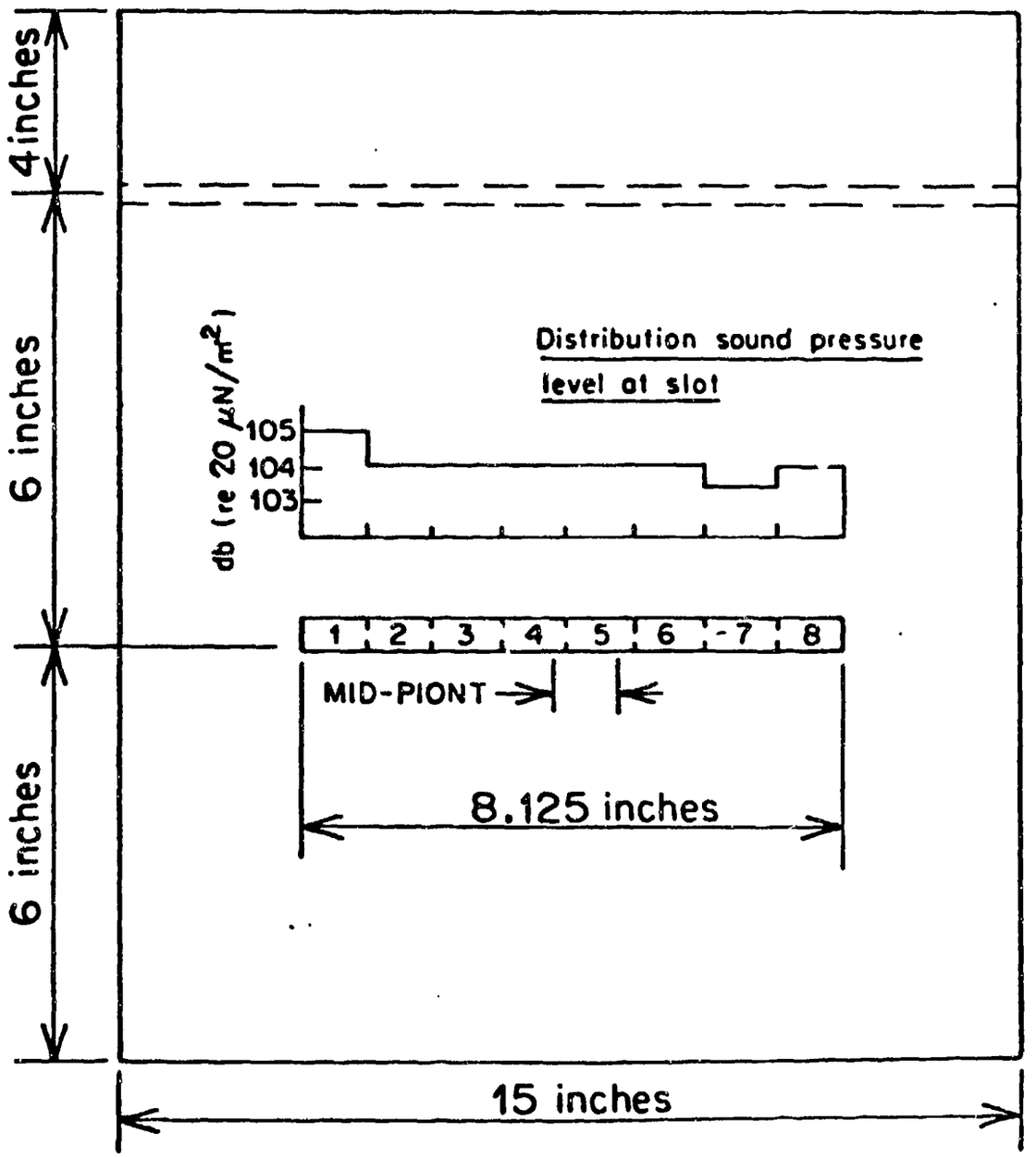

Fig. 29. Sound Pressure Distribution across the Slot of Acoustic Box

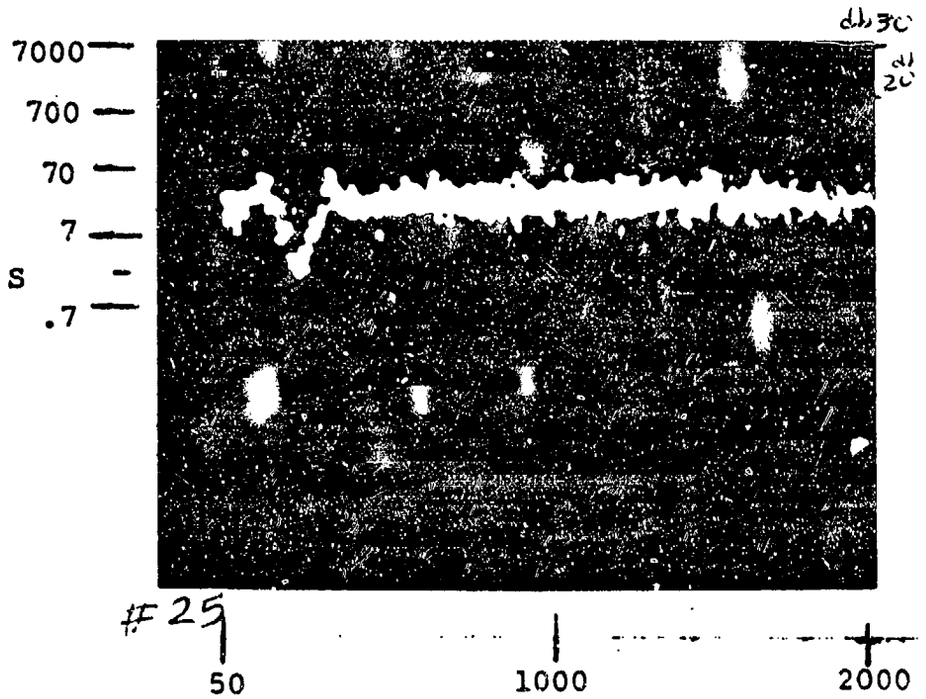

Fig. 30. Power Spectral Density of the Input Voltage of the Speaker

spectrum at the box opening during random loading test of beam specimens is shown in Fig. 31. In the spectral analysis shown in Fig. 31, the analysis bandwidth was 30 Hz and the sample being analyzed was of 50 sec. duration.

5.5 Measurement of Damping Coefficient

Probably the most frequently used experimental method is measurement of the decay of free vibrations. When a system has been set into free vibration by any means, the damping ratio can be determined from the ratio of two displacement amplitudes measured at an interval of m cycles. Thus, if v_n is the amplitude of vibration at any time and v_{n+m} is the amplitude m cycles later, the damping ratio is given by

$$\zeta = \frac{\delta_m}{2\pi m} \tag{5.1}$$

where

$$\delta_m = \ell n \frac{v_n}{v_{n+m}} \tag{5.2}$$

The response curve of aluminum beams for the critical damping ratio ζ, shown in Fig. 32, was measured by a strain gage at the center of the beam. The value of ζ calculated by using Eqs.(5.1) and (5.2) was found to be 0.05.

The damping per unit length β is equal to $2\rho A\omega_1\zeta$ where the first circular natural frequency of the beam ω_1 is given by

$$\omega_1 = 2\pi f_1 \tag{5.3a}$$

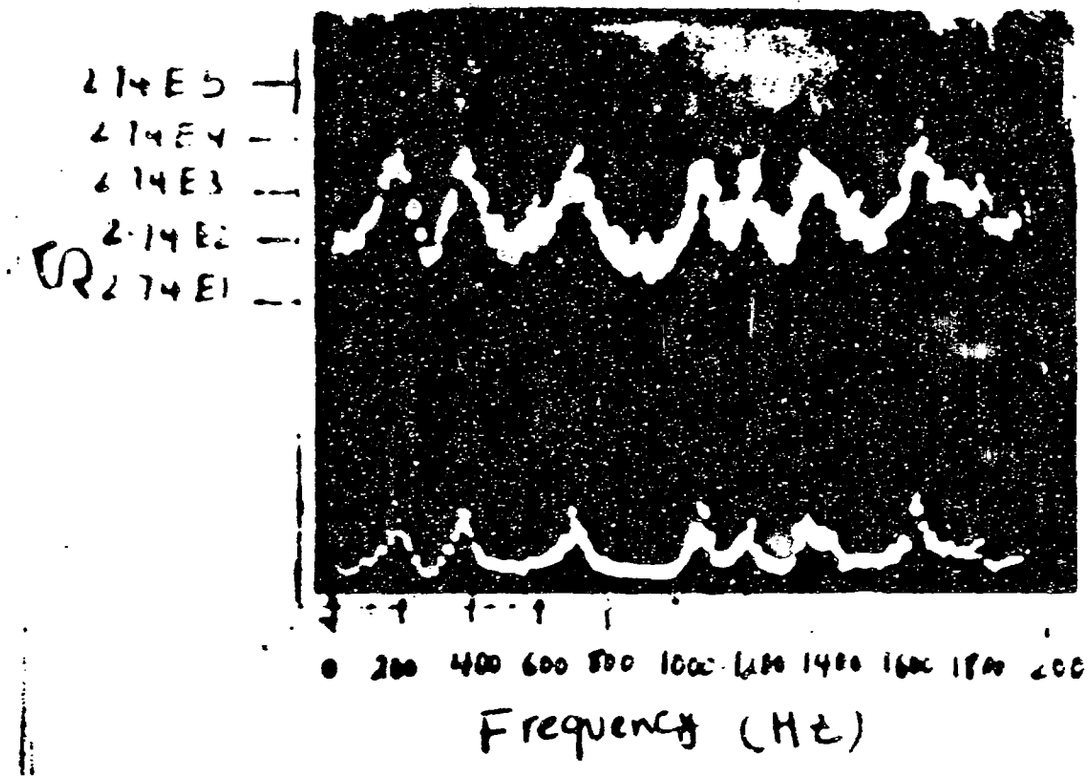

Fig. 31. Representative Acoustic Pressure Spectrum as Received at Box Opening: S≈274
(Bandwidth = 30Hz, RMS voltage input at speaker = 1.5 volts, 122 db)

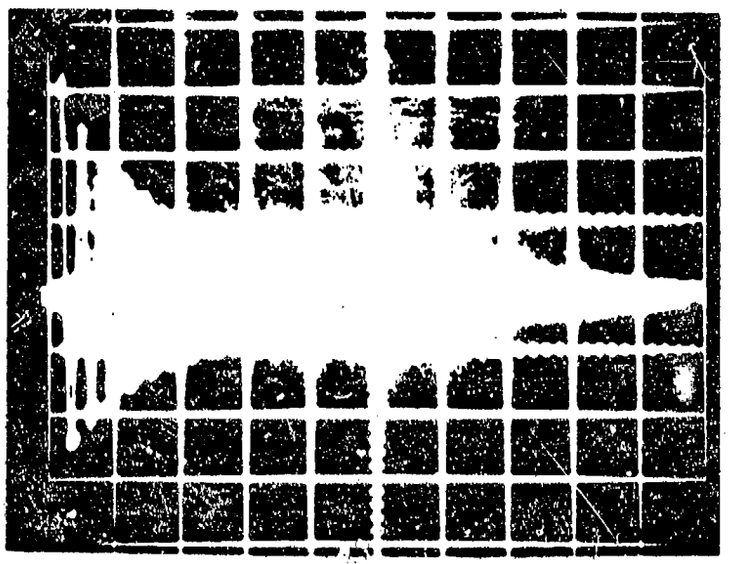

Fig. 32. Response Curve for Finding the Critical Damping Ratio ζ ($\xi = 0.05$, $E = 10.6 \times 10^6$ psi)

with

$$f_1 = 1.028 \frac{a}{L^2}\left(\frac{E}{\rho}\right)^{(1/2)} \tag{5.3b}$$

For aluminum

$$\beta = \frac{4\pi(0.1)(0.02)(0.25)(63)(0.05)}{(32.2\times 12)} = 5.12\times 10^{-5} \quad \text{lb-sec./in}^2 \tag{5.4a}$$

and

$$\bar{\mu} = \frac{\beta L^2}{\pi^2\sqrt{EI\rho A}} = 0.23 \tag{5.4b}$$

5.6 Beam Subjected to Random Loading

The beam was tested in the unstressed and unbuckled position and also was compressed to buckle with the non-dimensional initial static deflection $\bar{w}_0$ approximately equal to 21.6, 28.8 and 55.3. The values of $\bar{w}_0$ were obtained from the static strain measurements and the theoretical relationship for the maximum static strain of a buckled clamped beam.

$$\epsilon_{static} = \frac{\pi^2 r^2}{L^2}(4+\sqrt{12}\,\bar{w}_0) \tag{5.5}$$

The RMS dynamic strain $\epsilon_{dynamic}$ relative to the static strain was measured by another RMS meter (B&K Type 2419). A typical record of strain spectral density is shown in Fig. 33. The RMS values of the non-dimensional dynamic stress parameter at the center $<(\bar{\sigma}-\sigma_{sp})^2>^{1/2}$ which is equal to $\epsilon_{dynamic}(L/\pi r)^2$ are shown in Table 11. Unfortunately the power imparted to the beam was

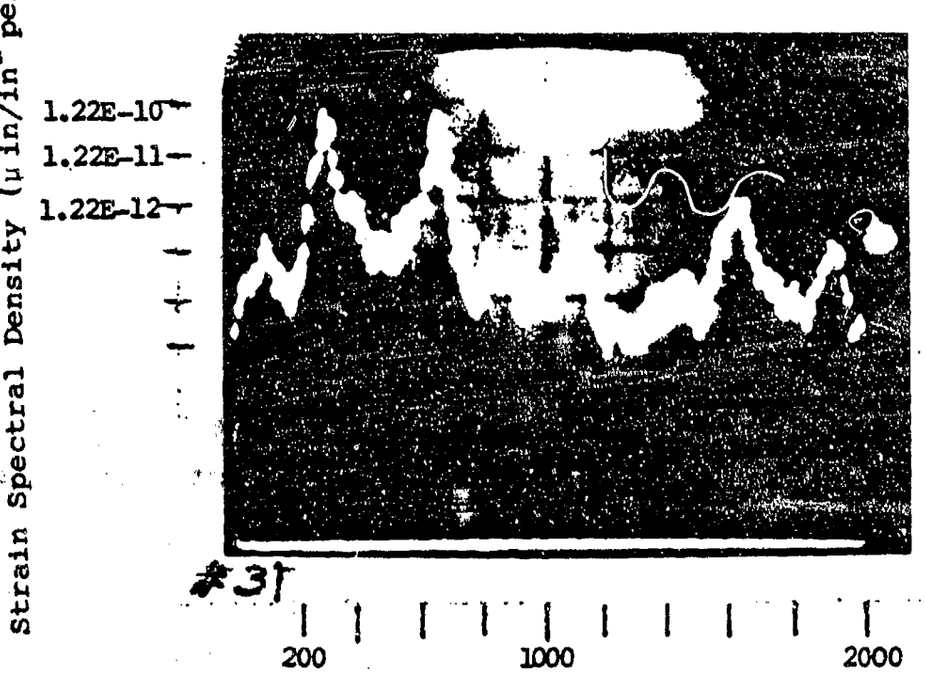

Fig. 33. Strain Spectral Density in the Absence of Oil Canning (Random Loading Case, S=846.687, W_o=55.3, Bandwidth=30 HZ, the Spectral Density is Plotted Logarithmically)

Table 11: Experimental Results of Non-dimensional Dynamic Stress for a Buckled Beam Under Random Loading

$\bar{S}$	Non-dimensional RMS Dynamic Stress			$<(\bar{\sigma}-\bar{\sigma}_{av})^2>^{\frac{1}{2}}$
	$\bar{w}_0 = 55.3$	$\bar{w}_0 = 28.8$	$\bar{w}_0 = 21.6$	$\bar{w}_0 = 0.0$ $(\bar{N}_0 = 0)$
50	2.01	2.21	2.21	1.20
110	3.21	3.01	3.01	2.01
172	4.21	3.61	3.61	2.61
240	4.12	4.21	4.21	3.01
434	6.42	5.22	5.22	7.83
850	6.82	6.22	6.42	15.65

insufficient to cause snap-through, a fact which was not ascertained until very late in the investigation.

5.7 Analytical Investigation

An approximate analytical investigation of the RMS stresses and deflections of a clamped beam which vibrates about the buckled equilibrium position was made by expanding the beam deflection function in a series of symmetric normal modes of vibration of the straight beam

$$W = \sum_m W_m \phi_m(\zeta) \tag{5.6}$$

where $\phi_m(\zeta)$ is the m^{th} vibration mode of the unstressed beam satisfying the relations

$$\frac{d^4\phi_m}{d\zeta^4} = \gamma_m^4 \phi_m \tag{5.7a}$$

$$\int_0^1 \phi_m \phi_n d\zeta = \delta_{mn} \tag{5.7b}$$

The modal functions and their derivatives are tabulated in reference 19. Various integrals involving the modal functions are evaluated in reference 20.

Equation (1.6) with the aid of Eqs.(1.4),(1.5a), and (5.7) and the use of the Galerkin method then yields the following equations for determining W_m

$$\frac{d^2w_m}{dt^2} + \frac{\beta}{\rho A}\frac{dw_m}{dt} + \omega_m^2 w_m + \frac{N_x}{L^2\rho A}\sum_m K_{mn}w_n - \left(\frac{2\pi^2 N_0 w_0}{L^2\rho A} + \frac{8EI\pi^4 w_0}{\rho A L^4}\right)G_m = \frac{Q_m}{\rho A}q(t) \qquad (m = 1,2,\ldots) \qquad (5.8)$$

with

$$N = -N_0 + \frac{EA}{2L^2}\left[\sum_m\sum_n K_{mn}w_m w_n - 2\pi^2 w_0 \sum_m G_m w_m\right] \qquad (5.9)$$

$$Q_m = \int_0^1 \phi_m(\zeta)d\zeta = \frac{4\alpha_m}{\gamma_m} \qquad (5.10)$$

$$K_{mn} = \int_0^1 \frac{d\phi_m}{d\zeta}\frac{d\phi_n}{d\zeta}d\zeta = K_{nm}$$

$$= \begin{cases} \alpha_m\gamma_m(\alpha_m\gamma_m - 2) & \text{if } m = n \\ \dfrac{8\gamma_m^2\gamma_n^2(\alpha_m\gamma_m - \alpha_n\gamma_n)}{\gamma_n^4 - \gamma_m^4} & \text{if } m \neq n \end{cases} \qquad (5.11)$$

$$G_m = \int_0^1 \phi_m(\zeta)\cos(2\pi\zeta)d\zeta$$

$$= \frac{4\alpha_m\gamma_m^4}{\gamma_m^4 - 16\pi^4} \qquad (5.12)$$

and α_m and γ_m are tabulated in reference 19.

The application of the method of equivalent linearization, whereby the terms in Eq.(5.8) involving the deflection coefficients are replaced by $k_m\omega_m^2 w_m$, then yields the following equations for k_m

$$k_m = 1 + \frac{256\bar{w}_0^2 k_m \gamma_m^4}{\gamma_m^4 - 16\pi^4} \sum_{n=1}^{\infty} \frac{\alpha_n^2 \gamma_n^2}{(\gamma_n^4 - 16\pi^4) D_{mn}}$$

$$- \frac{16\pi^2 \gamma_m k_m}{\alpha_m} \sum_{n=1}^{\infty} \frac{K_{mn}\alpha_n}{\gamma_n D_{mn}} + \frac{2\pi^6 \gamma_m k_m \bar{S}}{\alpha_m}$$

$$\sum_{n=1}^{\infty} \sum_{p=1}^{\infty} \sum_{q=1}^{\infty} \frac{\alpha_n \alpha_p \alpha_q}{\gamma_n \gamma_p \gamma_q} \frac{K_{mp}K_{nq} + 2K_{mn}K_{pq}}{D_{mp}D_{nq}} \qquad (5.13)$$

The RMS displacements are now given by

$$\langle \bar{w}_{max}^2 \rangle = \bar{w}_0^2 + 16\pi^6 \bar{S} \sum_{m=1}^{\infty} \sum_{n=1}^{\infty} \frac{\alpha_m \alpha_n \phi_m\left(\frac{1}{2}\right)\phi_n\left(\frac{1}{2}\right)}{\gamma_m \gamma_n D_{mn}} \qquad (5.14)$$

The average stresses are obtained from

$$\bar{\sigma}_{av}^{\pm} = \bar{N}_0 - 8\pi^4 \bar{S} \sum_{m=1}^{\infty} \sum_{n=1}^{\infty} \frac{\alpha_m \alpha_n K_{mn}}{\gamma_m \gamma_n D_{mn}} \qquad (5.15)$$

and the RMS stresses with respect to this mean are given by

$$\langle(\bar{\sigma}_{max}-\bar{\sigma}_{av})^2_{\pm}\rangle = 128\pi^8\bar{S}^2 \sum_{n=1}^{\infty}\sum_{n=1}^{\infty}\sum_{p=1}^{\infty}\sum_{q=1}^{\infty}\frac{\alpha_m\alpha_n\alpha_p\alpha_q K_{mn}K_{pq}}{\gamma_m\gamma_n\gamma_p\gamma_q D_{mp}D_{nq}}$$

$$+ 64\pi^6\bar{w}_0^2\bar{S}\sum_{m=1}^{\infty}\sum_{n=1}^{\infty}\frac{\alpha_m\alpha_n G_m G_n}{\gamma_m\gamma_n D_{mn}}$$

$$+ 64\pi^4\bar{w}_0\frac{h}{r}\bar{S}\sum_{m=1}^{\infty}\sum_{n=1}^{\infty}\frac{d^2\phi_m}{d\zeta^2}\frac{\alpha_n\gamma_n G_n}{\gamma_m\gamma_n D_{mn}}$$

$$+ 16\pi^4\left(\frac{h}{r}\right)^2\bar{S}\sum_{m=1}^{\infty}\sum_{n=1}^{\infty}\frac{d^2\phi_m}{d\zeta^2}\frac{d^2\phi_n}{d\zeta^2}\frac{\alpha_m\alpha_n}{\gamma_m\gamma_n D_{mn}} \qquad (5.16)$$

Some calculations were made of the RMS stress with respect to the static stress

$$\bar{\sigma}_{static} = -\bar{N}_0 \pm 2\frac{h}{r}\bar{w}_0 \qquad (5.17)$$

Then

$$\langle(\bar{\sigma}_{max}-\bar{\sigma}_{static})^2\rangle = \langle\bar{\sigma}_{max}\rangle - 2\bar{\sigma}_{av}\sigma_{static} + \bar{\sigma}^2_{static}$$

$$= \langle(\bar{\sigma}_{max}-\bar{\sigma}_{av})^2\rangle + (\bar{\sigma}_{av}-\bar{\sigma}_{static})^2 \qquad (5.18)$$

The results with $\bar{\mu}$ taken equal to zero for convenience are compared with the experimental results in Fig. 34. The experimental results are seen to be considerably lower than the theoretical results. One cause of this discrepancy may be conjectured to be the effect of the center strain gage which tends to stiffen the beam yielding smaller deflections and stresses. Another source of error is the nature of the random loading which is not white noise when it impinges on the beam. The effect of a non-constant loading spectrum is unexplored, however.

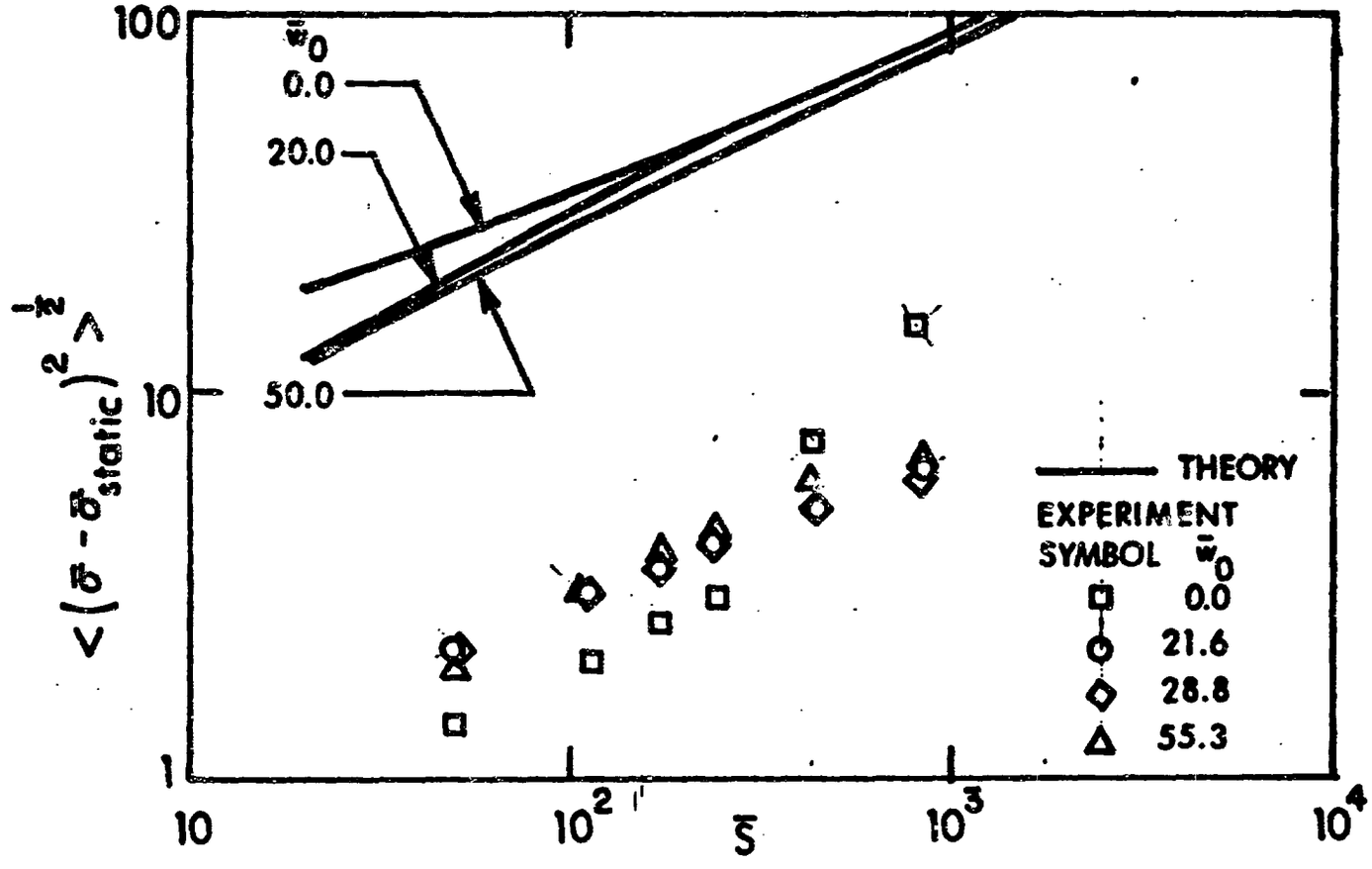

Fig. 34. Comparison of Theory and Experiment for Center RMS Stress

CONCLUSIONS

The present investigation serves to cast some light in the behavior of initially buckled beams under random loading. A reasonable indication of the critical spectral density of loading required for beam snap-through appears to be the vanishing of the average zero-crossing frequency of the beam. While this criterion does not lead to a completely precise value, due to the lengthy calculations required, an estimate of the critical power spectral density parameter has been obtained as

$$\bar{S} = 0.001\,\bar{w}_0^4$$

An investigation of the RMS response of initially buckled simply supported beams does not reveal any drastic change in the vicinity of the critical spectral density. The onset of snap-through does herald the possibility of stress reversal, however.

Bounds in the RMS response have been obtained by considering vibrations about the initial buckled position as an average and about the straight reference position as an average, together with the method of equivalent linearization. The results obtained by numerical simulation of random loading indicate a smooth transition from the first to the second type of behavior and in the limit are in good agreement with the approximate analytical values. The agreement between theory and experiment for clamped beams is reasonable, but not conclusive.

The results obtained suggest the need for better experimental as well as better analytical techniques to furnish the required data. While useful results have been obtained by numerical load simulation and integration of the differential equations of motion, the calculations are quite costly and time consuming. Further studies on methods for estimating the response of highly nonlinear structures for random loading are thus required. These results are needed, to some extent, prior to experimentation to help delineate the type of data to be measured and the power requirements for the loading. the present experimental investigation would have profited from a delay until analytical results were obtained.

REFERENCES

1. Jacobson, M.J. and Finwall., "Effects of Structural Heating on the Sonic Fatigue of Aerospace Vehicle Structures," Report No. AFFDL-TR-73-56, 1974, Air Froce Flight Dynamics Laboratory, Wright-Patterson AFB, Ohio.

2. Pi. H.N., Ariaratnam, S.T., and Lennox, W.C., "First-Passage Time for the Snap-through of a Shell-type Structure," J. Sound Vib., Vol. 14, No. 3, Feb. 8, 1971, pp. 375-384.

3. Huddleston, J.V., "Behavior of a Steep Prestressed Arch Made from a Buckled Strut," J. Appl. Mech., Vol. 37, No. 4, Dec. 1970, pp. 984-994.

4. Tseng, W.-Y. and Dugundji, J., "Nonlinear Vibrations of a Buckled Beam under Harmonic Excitation," J. Appl. Mech., Vol. 38, No. 2, June 1971, pp. 467-476.

5. Burgreen, D., "Free Vibrations of a Pin Ended Column with Constant Distance between Ends," J. Appl. Mech., Vol. 18, No. 1, March 1951, pp. 135-139.

6. Bisplinghoff, R.L. and Pian, T.H.H., "On the Vibration of Thermally Buckled Bars and Plates," Proc. IX Int. Cong. Appl. Mech., Vol. 7, 1957, pp. 307-318.

7. Eisley, J.G., "Nonlinear Vibrations of Beams and Rectangular Plates," Z. Agnew. Math. Phys., Vol. 15, 1964, pp. 167-174.

8. Eisley, J.G., "Large Amplitude Vibration of Buckled Beams and Rectangular Plates," AIAA J., Vol. 2, No. 12, Dec. 1964, pp. 2207-2209.

9. Seide, P., "An Investigation of the Dynamic Stability of Structures in a Combined Thermal-Acoustic Environment," Annual Report, October 1978-September 1979, AFOSR Grant No. 79-0013.

10. Hoff, N.J. and Bruce, V.G., "Dynamic Analysis of the Buckling of Laterally Loaded Flat ARches," J. Math. Phys., Vol. 32, 1954, pp. 276-288.

11. Humphreys, J.S., "On the Adequacy of Energy Criteria for Dynamic Buckling of Arches," AIAA J., Vol. 4, No. 5, May 1966, pp. 921-923.

12. Humphreys, J.S., "On Dynamic Snap Buckling of Shallow Arches," AIAA J., Vol. 4, No. 5, May 1966, pp. 878-886.

13. Greenberg, M.D., Foundations of Applied Mathematics, Prentice-Hall, Inc., Englewood Cliffs, NJ, 1978, pp. 476-485.

14. Stott, S.J. and Sasri, S.F., "Random Vibration of a Nonlinear Two-Degree-of-Freedom Oscillator," Report No. NUREG/CR-0361, CE 78-08, 1978, U.S. Nuclear Regulatory Commission, Washington, D.C.

15. Seide, P.,"Nonlinear Stresses and Deflections of Beams Subjected to Random Time Dependent Uniform Pressure," J. Eng. Ind., Vol. 98, No. 3, Aug. 1976, pp. 1014-1020.

16. Lin, Y.K., Probabilistic Theory of Structural Dynamics, McGraw-Hill Book Company, New York, 1967, pp. 293-299.

17. Abramowitz, M. and Stegun, I.A., Handbook of Mathematical Functions, National Bureau of Standards, Applied Mathematics Series 55, June 1964, p. 886.

18. Caughey, T.K., "Equivalent Linearization Techniques," J. Acoust. Soc. Am., Vol. 35, No. 11, Nov. 1963, pp. 1606-1711.

19. Young, D. and Felgar, R.P.,Jr., "Tables of Characteristic Functions Representing Normal Modes of Vibration of a Beam," Engineering Research Series, No. 44, Bureau of Engineering Research, University of Texas, Austin, July 1, 1949.

20. Felgar, R.P.,Jr., "Formulas for Integrals Containing Characteristic Functions of a Vibrating Beam," Circular No. 14, Bureau of Engineering Research, University of Texas, Austin, 1950.

APPENDIX A

PROGRAM DRIBB3 FOR THE DETERMINATION OF SNAP-THROUGH PROBABILITY

```
C   PROGRAM DR1833 - DYNAMIC RESPONSE OF INITIALLY BUCKLED BEAMS
C   CALCULATES PROBABILITY OF SNAP-THROUGH IN A GIVEN TIME BY A MONTE-
C   CARLO PROCESS FOR SIMPLY SUPPORTED BEAMS
C
C     BMU = DAMPING COEFFICIENT PARAMETER (CL**2/(PI**2*SQRT(RHO*AE)))
C     WO = INITIAL BUCKLE AMPLITUDE/RADIUS OF GYRATION RATIO
C     NT = NUMBER OF FOURIER SERIES TERMS USED
C     W(I) = ITH FOURIER SERIES AMPLITUDE/RADIUS OF GYRATION RATIO
C       (I = 1,NT)
C     T = FUNDAMENTAL FREQUENCY OF UNCOMPRESSED BEAM * TIME (PI**2*
C       SQRT(EI/(RHO*A))*TIME/L**2)
C     P = LOAD PARAMETER (4*LOAD*L**4*SQRT(A/I)/(PI**5*EI))
C     BN = AXIAL STRESS PARAMETER (AVERAGE STRESS*AL**2/(PI**2*EI))
C     WC = CENTER DEFLECTION/RADIUS OF GYRATION RATIO
C     A = BEAM CROSS-SECTIONAL AREA
C     E = YOUNG'S MODULUS OF BEAM MATERIAL
C     I = CENTROIDAL MOMENT OF INERTIA OF BEAM CROSS SECTION
C     L = BEAM LENGTH
C     C = DAMPING COEFFICIENT (UNITS OF FORCE*TIME/LENGTH**2)
C     RHO = DENSITY OF BEAM MATERIAL
C     RADIUS OF GYRATION = SQRT(I/A)
C     JJT = NUMBER OF INTERVALS FOR SNAP-THROUGH COUNT
C
      IMPLICIT REAL*8(A-H,O-Z)
      DIMENSION W(200),WP(200),WW(200,2),JT(500),PT(500)
      COMMON /B1/W,WP,P,WO,BMU,NT,T,BN
      OPEN(UNIT=5,TYPE='OLD',NAME='DRBIN3')
      OPEN(UNIT=6,TYPE='NEW',NAME='DRBOUT3')
      READ(5,1)BMU,WO,NT,JJT
    1 FORMAT(2D10.6,2I4)
      WRITE(6,2)WO,BMU
    2 FORMAT('  THE INITIAL CENTER DEFLECTION RATIO =',D13.6,'; THE
     1 DAMPING COEFFICIENT PARAMETER =',D13.6)
      WRITE(6,30)NT
   30 FORMAT('  ',I4,' FOURIER SERIES TERMS ARE USED.')
      DO 50 I=1,JJT
   50 JT(I)=0
      JJ=1
   37 DO 3 I=1,NT
      W(I)=0.D0
    3 W(NT+I)=0.D0
      T=0.D0
      IF(JJ.GT.1)GO TO 15
C
C   INTEGRATION OF THE SYSTEM OF DIFFERENTIAL EQUATIONS BY THE RUNGE-
C   KUTTA METHOD (FIXED STEP-SIZE)
C
C   DT=TIME INTERVAL FOR CONSTANT RANDOM PRESSURE
C   NI=NUMBER OF INTERVALS OF DT FOR INTEGRATION STEP SIZE
C   TMAX=MAXIMUM TIME CONSIDERED
C   IX=AN INTEGER HAVING NINE DIGITS OR LESS
C   S=THE DESIRED STANDARD DEVIATION OF THE GAUSSIAN NORMAL DISTRIBUTION
C   AM=THE DESIRED MEAN OF THE NORMAL DISTRIBUTION
C   JJO=TOTAL SAMPLE SIZE (NUMBER OF DIFFERENT LOADING HISTORIES)
C
      NEQ=2*NT
      READ(5,4)TMAX,DT,NI
    4 FORMAT(2D10.6,I4)
      READ(5,6)S,AM,IX,JJO
    6 FORMAT(2D10.3,2I10)
      WRITE(6,7)S,AM,IX
```

```
 6200       7 FORMAT('  THE LOAD IS RANDOM, THE STANDARD DEVIATION = ',D13.6,
 6300        1  ' ,THE MEAN VALUE = ',D13.6,' ,THE SEED VALUE = ',I10)
 6400         WRITE(6,100)DT,NI
 6500     100 FORMAT('  DT = ',D13.6,', THE INTEGRATION TIME STEP = DT/ ',I2)
 6600         DJ=JJT
 6700         DTJ=TMAX/DJ
 6800         DI=NI
 6900         DT=DT/DI
 7000        15 CALL GAUSS1(IX,S,AM,P)
 7100         II=1
 7200        16 CALL RSIDE
 7300         DO 17 I=1,NEQ
 7400        17 WW(I,1)=W(I)
 7500         DTO2=DT/2.DO
 7600         DTO6=DT/6.DO
 7700         DO 18 I=1,NEQ
 7800         WW(I,2)=WP(I)
 7900        18 W(I)=W(I)+DTO2*WP(I)
 8000         T=T+DTO2
 8100         DO 20 J=1,2
 8200         CALL RSIDE
 8300         DO 19 I=1,NEQ
 8400         WW(I,2)=WW(I,2)+2.DO*WP(I)
 8500         IF(J.EQ.2)GO TO 19
 8600         W(I)=WW(I,1)+DTO2*WP(I)
 8700        19 CONTINUE
 8800        20 CONTINUE
 8900         T=T+DTO2
 9000         DO 21 I=1,NEQ
 9100        21 W(I)=WW(I,1)+DT*WP(I)
 9200         CALL RSIDE
 9300         DO 22 I=1,NEQ
 9400         WW(I,2)=WW(I,2)+WP(I)
 9500        22 W(I)=WW(I,1)+DTO6*WW(I,2)
 9600         WC=W0
 9700         DO 25 I=1,NT
 9800        25 WC=WC-(-1)**I*W(I)
 9900         IF(WC.LT.0.00)GO TO 101
10000         II=II+1
10100         IF(II.LE.NI)GO TO 16
10200         IF(T-TMAX)15,101,101
10300    101  DO 51 I=1,JJT
10400     51  IF(T.LE.DTJ*I.AND.T.GT.DTJ*(I-1))JT(I)=JT(I)+1
10500         JJ=JJ+1
10600         IF(JJ.LE.JJO)GO TO 37
10700         WRITE(6,52)(JT(I),I=1,JJT)
10800         DO 102 I=2,JJT
10900    102  JT(I)=JT(I-1)+JT(I)
11000         CN=JJO
11100         DO 103 I=1,JJT
11200    103  PT(I)=JT(I)/CN
11300         WRITE(6,53)(PT(I),I=1,JJT)
11400     52  FORMAT(2015)
11500     53  FORMAT(5D13.6)
11600     29  STOP
11700         END
11800    C
11900    C SUBROUTINE RSIDE CALCULATES THE RIGHT SIDE OF THE EQUATIONS DW/DT=F(W,P)
12000    C
12100         SUBROUTINE RSIDE
12200         IMPLICIT REAL*8 (A-H,O-Z)
```

```
      COMMON /B1/W,WP,P,WO,BMU,NT,T,BN
      DIMENSION W(200),WP(200)
      DO 1 I=1,NT
    1 WP(I)=W(I+NT)
      SO=2.DO
      DO 5 I=1,NT
    5 SO=SO+((2*I-1)*W(I))**2
      BN=1.DO-0.5DO*WO*W(1)-0.25DO*SO
      WP(NT+1)=-P/(BN-1.DO)*(WO+W(1))-BMU*W(NT+1)
      DO 8 I=2,NT
    8 WP(NT+I)=-P/((2*I-1)+((2*I-1)**2*BN-(2*I-1)**4)*W(I)-BMU*W(NT+I)
      RETURN
      END
C
C   SUBROUTINES GAUSS1 & RANDOM GENERATE RANDOM NUMBERS AS DESIRED
C
      SUBROUTINE GAUSS1(IX,S,AM,V)
      IMPLICIT REAL*8 (A-H,O-Z)
      A=0.DO
      DO 1 I=1,12
      CALL RANDOM(IX,IY,Y)
      IX=IY
    1 A=A+Y
      V=(A-6.DO)*S+AM
      RETURN
      END
C
      SUBROUTINE RANDOM(IX,IY,YFL)
      IMPLICIT REAL*8 (A-H,O-Z)
      IY=IDINT(DMOD(7.DO**5*DFLOAT(IX),DFLOAT(2147483647)))
      YFL=DFLOAT(IY)/2.DO**31
      RETURN
      END
```

APPENDIX B

PROGRAM DRIBB2 FOR NUMERICAL INTEGRATION OF THE EQUATIONS OF MOTION

```
C   PROGRAM DRIBB2 - DYNAMIC RESPONSE OF INITIALLY BUCKLED BEAMS
C    (APPROXIMATE THEORY FOR SIMPLY SUPPORTED BEAMS)
C
C    BMU = DAMPING COEFFICIENT PARAMETER (CL**2/(PI**2*SQRT(RHO*A*E*I))
C    WO = INITIAL BUCKLE AMPLITUDE/RADIUS OF GYRATION RATIO
C    NT = NUMBER OF FOURIER SERIES TERMS USED
C    W(I) = ITH FOURIER SERIES AMPLITUDE/RADIUS OF GYRATION RATIO
C     (I = 1,NT)
C    T = FUNDAMENTAL FREQUENCY OF UNCOMPRESSED BEAM * TIME (PI**2*
C     SQRT(E*I/(RHO*A))*TIME/L**2)
C    P = LOAD PARAMETER (4*LOAD*L**4*SQRT(A/I)/(PI**5*E*I))
C    BN = AXIAL STRESS PARAMETER (AVERAGE STRESS*AL**2/(PI**2*E*I))
C    BNO = INITIAL AXIAL STRESS PARAMETER IF WO = 0. (POSITIVE IF
C     COMPRESSION, BNO < 1.0)
C    BM = MOMENT STRESS PARAMETER (MAXIMUM STRESS*AL**2/(PI**2*E*I)*
C     SQRT(I/A)/MAXIMUM DISTANCE TO OUTER FIBER)
C    WC = CENTER DEFLECTION/RADIUS OF GYRATION RATIO
C    A = BEAM CROSS-SECTIONAL AREA
C    E = YOUNG'S MODULUS OF BEAM MATERIAL
C    I = CENTROIDAL MOMENT OF INERTIA OF BEAM CROSS SECTION
C    L = BEAM LENGTH
C    C = DAMPING COEFFICIENT (UNITS OF FORCE*TIME/LENGTH**2)
C    RHO = DENSITY OF BEAM MATERIAL
C    RADIUS OF GYRATION = SQRT(I/A)
C
      IMPLICIT REAL*8(A-H,O-Z)
      DIMENSION W(10),WP(10),WW(10,2),WC(2),WS(2),SS1(2),SS2(2),
     1 SAV1(2),SAV2(2),WAV(2)
      COMMON /B1/W,WP,P,AAA,BEE,CEE,DEE,EEE,IP,WO,BMU,NT,T,BN,BNO
      OPEN(UNIT=5,TYPE='OLD',NAME='DRBIN2')
      OPEN(UNIT=6,TYPE='NEW',NAME='DRBOUT2')
  111 READ(5,1)BMU,WO,NT
    1 FORMAT(2D10.6,I4)
      IF(NT.EQ.0)GO TO 152
      WRITE(6,2)WO,BMU
    2 FORMAT('  THE INITIAL CENTER DEFLECTION RATIO =',D13.6,'; THE
     1 DAMPING COEFFICIENT PARAMETER =',D13.6)
      WRITE(6,30)NT
   30 FORMAT('  ',I4,' FOURIER SERIES TERMS ARE USED.')
      IF(WO)37,33,37
   33 READ(5,34)BNO
   34 FORMAT(1D10.6)
   37 IF(BNO.GT.0.00)BNO=1.00
      WRITE(6,35)BNO
   35 FORMAT('  THE INITIAL AXIAL LOAD PARAMETER = ',D13.6)
      DO 3 I=1,NT
      W(I)=0.00
    3 W(NT+I)=0.DO
      T=0.DO
C
C   INTEGRATION OF THE SYSTEM OF DIFFERENTIAL EQUATIONS BY THE RUNGE-
C   KUTTA METHOD (FIXED STEP-SIZE)
C
C   DT=INTEGRATION STEP SIZE
C   TMAX=MAXIMUM TIME CONSIDERED
C
C   IP=1 IF UNIFORM PRESSURE LOADING IS RANDOM
C     =2 IF UNIFORM PRESSURE LOADING IS LINEAR TIME FUNCTION
C     =3 IF UNIFORM PRESSURE LOADING IS SINUSOIDAL
C
C   IF IP=1 THE FOLLOWING ARE REQUIRED:
```

```
C     IX=AN INTEGER HAVING TEN DIGITS OR LESS
C     S=THE DESIRED STANDARD DEVIATION OF THE GAUSSIAN NORMAL DISTRIBUTION
C     AM=THE DESIRED MEAN OF THE NORMAL DISTRIBUTION
C     JJ1=0 IF ONLY RMS VALUES ARE DESIRED, =1 OTHERWISE
C
C   IF IP=2 THE FOLLOWING ARE REQUIRED:
C     AAA=CONSTANT RATE OF CHANGE OF PRESSURE
C     BEE=INITIAL PRESSURE AT T=0
C     P=AAA*T+BEE
C
C   IF IP=3 THE FOLLOWING ARE REQUIRED:
C     CEE=AMPLITUDE OF SINUSOIDAL PRESSURE LOADING
C     DEE=CIRCULAR FREQUENCY
C     EEE=PHASE SHIFT
C     P=CEE*SIN(DEE*T+EEE)
C
      NEQ=2*NT
      READ(5,4)IP,TMAX,DT
    4 FORMAT(I2,2D10.6)
      WRITE(6,139)DT,TMAX
  139 FORMAT('  THE TIME INCREMENT = ',D13.6,': TMAX = ',D13.6)
      IF(IP-2)5,8,11
    5 READ(5,6)S,AM,IX,JJ1,NI,NTT
    6 FORMAT(2D10.6,I10,3I4)
      WRITE(6,7)S,AM,IX
    7 FORMAT('  THE LOAD IS RANDOM. THE STANDARD DEVIATION = ',D13.6,
     1  ' ,THE MEAN VALUE = ',D13.6,' ,THE SEED VALUE = ',I10)
      WRITE(6,77)NI,NTT
   77 FORMAT('  THE INTEGRATION STEP IS EQUAL TO DT /',I4,': RMS VALUES
     1 ARE CALCULATED AT TMAX/',I4,' TIME INTERVALS')
      GO TO 14
    8 READ(5,9)AAA,BEE
    9 FORMAT(2D10.6)
      WRITE(6,10)AAA,BEE
   10 FORMAT('  THE LOAD IS LINEAR. P = ',D13.6,' *T + ',D13.6)
      GO TO 16
   11 READ(5,12)CEE,DEE,EEE
   12 FORMAT(3D10.6)
      WRITE(6,13)CEE,DEE,EEE
   13 FORMAT('  THE LOAD IS SINUSOIDAL. P = ',D13.6,' *SIN( ',D13.6,
     1 ' *T + ',D13.6,' )')
      GO TO 16
   14 M=1
      NC=0
      WS(1)=W0**2
      SS1(1)=(BN0-W0*DSQRT(3.D0))**2
      SS2(1)=(BN0+W0*DSQRT(3.D0))**2
      WAV(1)=W0
      SAV1(1)=0.D0
      SAV2(1)=0.D0
      DTI=DT
      DI=NI
      DT=DT/DI
      DTT=NTT
      DT2=TMAX/DTT
      T2=DT2
   15 CALL GAUSSI(IX,S,AM,P)
      DO 333 II=1,NI
   16 CALL RSIDE
      DO 17 I=1,NEQ
   17 WW(I,1)=W(I)
```

```
      DT02=DT/2.D0
      DT06=DT/6.D0
      DO 18 I=1,NEQ
      WW(I,2)=WP(I)
   18 W(I)=W(I)+DT02*WP(I)
      T=T+DT02
      DO 20 J=1,2
      CALL RSIDE
      DO 19 I=1,NEQ
      WW(I,2)=WW(I,2)+2.D0*WP(I)
      IF(J.EQ.2)GO TO 19
      W(I)=WW(I,1)+DT02*WP(I)
   19 CONTINUE
   20 CONTINUE
      T=T+DT02
      DO 21 I=1,NEQ
   21 W(I)=WW(I,1)+DT*WP(I)
      CALL RSIDE
      DO 22 I=1,NEQ
      WW(I,2)=WW(I,2)+WP(I)
   22 W(I)=WW(I,1)+DT06*WW(I,2)
      IF(IP-2)141,142,142
  141 IF(JJ1.EQ.0)GO TO 143
  142 WRITE(6,23)T,P
   23 FORMAT('   TIME= ',D13.6,', LOAD PARAMETER P = ',D13.6)
      WRITE(6,24)(W(I),I=1,NT)
   24 FORMAT('  ',8D13.6)
C
C CALCULATION OF CENTER DEFLECTION AND CENTER MOMENT PARAMETERS
C
  143 WC(1)=W0
      BM=-W0
      DO 25 I=1,NT
      WC(1)=WC(1)-(-1)**I*W(I)
   25 BM=BM+(2*I-1)**2*(-1)**I*W(I)
      IF(IP-2)144,145,145
  144 IF(JJ1.EQ.0)GO TO 146
  145 WRITE(6,26)WC(1)
   26 FORMAT('   THE CENTER DEFLECTION PARAMETER = ',D13.6)
      WRITE(6,31)BN
   31 FORMAT('   THE AXIAL LOAD PARAMETER = ',D13.6)
      WRITE(6,32)BM
   32 FORMAT('   THE BENDING MOMENT PARAMETER = ',D13.6)
      IF(IP-2)146,147,147
  146 WS(1)=WS(1)+(3.D0-(-1)**M)*WC(1)**2
      SS1(1)=SS1(1)+(BN+BM*DSQRT(3.D0))**2*(3.D0-(-1)**M)
      SS2(1)=SS2(1)+(BN-BM*DSQRT(3.D0))**2*(3.D0-(-1)**M)
      WAV(1)=WAV(1)+(3.D0-(-1)**M)*WC(1)
      SAV1(1)=SAV1(1)+(BN+BM*DSQRT(3.D0))*(3.D0-(-1)**M)
      SAV2(1)=SAV2(1)+(BN-BM*DSQRT(3.D0))*(3.D0-(-1)**M)
      IF(M.EQ.1)GO TO 150
      IF(WC(1).LT.0.D0.AND.WC(2).GT.0.D0)NC=NC+1
      IF(WC(1).GT.0.D0.AND.WC(2).LT.0.D0)NC=NC+1
  150 WC(2)=WC(1)
  333 M=M+1
      IF(T-T2)15,334,334
  334 WS(2)=WS(1)
      SS1(2)=SS1(1)
      SS2(2)=SS2(1)
      WAV(2)=WAV(1)
      SAV1(2)=SAV1(1)
```

```
      SAV2(2)=SAV2(1)
      WS(2)=WS(2)-WC(1)**2
      SS1(2)=SS1(2)-(BN+BM*DSQRT(3.D0))**2
      SS2(2)=SS2(2)-(BN-BM*DSQRT(3.D0))**2
      WAV(2)=WAV(2)-WC(1)
      SAV1(2)=SAV1(2)-(BN+BM*DSQRT(3.D0))
      SAV2(2)=SAV2(2)-(BN-BM*DSQRT(3.D0))
      WRMS=DSQRT(WS(2)/(3.D0*(M-1)))
      S1RMS=DSQRT(SS1(2)/(3.D0*(M-1)))
      S2RMS=DSQRT(SS2(2)/(3.D0*(M-1)))
      DAV=WAV(2)/(3.D0*(M-1))
      S1AV=DSQRT(SAV1(2)/(3.D0*(M-1)))
      S2AV=DSQRT(SAV2(2)/(3.D0*(M-1)))
      WRITE(6,200)T,T2,WRMS,S1RMS,S2RMS
  200 FORMAT(2D13.6,'  THE RMS DEFLECTION = ',D13.6,'  THE RMS STRESSES
     1    = ',2D13.6)
      WRITE(6,300)DAV,S1AV,S2AV
      ANC=NC/T
  300 FORMAT('THE AVERAGE DEFLECTION =',D13.6,';THE AVERAGE STRESSES ='
     1 ,2D13.6)
      WRITE(6,151)NC,ANC
  151 FORMAT(' NUMBER OF CROSSINGS =',I9,';CROSSINGS/UNIT TIME =',D13.6)
      T2=T2+DT2
      IF(T.LT.TMAX)GO TO 15
  149 GO TO 111
  147 IF(T-TMAX)16,111,111
  152 STOP
      END
C
CC  SUBROUTINE RSIDE CALCULATES THE RIGHT SIDE OF THE EQUATIONS DW/DT=F(W,P)
C
      SUBROUTINE RSIDE
      IMPLICIT REAL*8 (A-H,O-Z)
      COMMON /B1/W,WP,P,AAA,BEE,CEE,DEE,EEE,IP,WO,BMU,NT,T,BN,BNO
      DIMENSION W(10),WP(10)
      DO 1 I=1,NT
    1 WP(I)=W(I+NT)
      IF(IP-2)4,2,3
    2 P=AAA*T+BEE
      GO TO 4
    3 P=CEE*DSIN(DEE*T+EEE)
    4 SO=0.DO
      DO 5 I=1,NT
    5 SO=SO+((2*I-1)*W(I))**2
      BN=BNO-0.5D0*WO*W(1)-0.25D0*SO
      WP(NT+1)=-P+(BN-1.D0)*(WO+W(1))-BMU*W(NT+1)
      DO 8 I=2,NT
    8 WP(NT+I)=-P/(2*I-1)+((2*I-1)**2*BN-(2*I-1)**4)*W(I)-BMU*W(NT+I)
      RETURN
      END
C
C   SUBROUTINES GAUSS1 & RANDOM GENERATE RANDOM NUMBERS AS DESIRED
C
      SUBROUTINE GAUSS1(IX,S,AM,V)
      IMPLICIT REAL*8 (A-H,O-Z)
      A=0.D0
      DO 1 I=1,12
      CALL RANDOM(IX,IY,Y)
      IX=IY
    1 A=A+Y
      V=(A-6.D0)*S+AM
```

```
24500            RETURN
24600            END
24700      C
24800            SUBROUTINE RANDOM(IX,IY,YFL)
24900            IMPLICIT REAL*8 (A-H,O-Z)
25000            IY=IDINT(DMOD(7.D0**5*DFLOAT(IX),DFLOAT(2147483647)))
25100            YFL=DFLOAT(IY)/2.D0**31
25200            RETURN
25300            END
```

DEPARTMENT OF THE AIR FORCE
AIR FORCE RESEARCH LABORATORY
WRIGHT-PATTERSON AIR FORCE BASE OHIO 45433

9-14-99

MEMORANDUM FOR: Defense Technical Information Center/OMI
8725 John J. Kingman Rd, Suite 0944
Ft Belvoir, VA 22060-6218

FROM: Det 1 AFRL/WST
Bldg 640 Rm 60
2331 12th Street
Wright-Patterson AFB OH 45433-7950

SUBJECT: Notice of Changes in Technical Report(s) (See below)

Please change subject report(s) as follows:

The following have all been approved for public release; distribution is unlimited:

AFWAL-TR-83-3072,
WRDC-TR-90-3081,
WL-TR-96-3043,
WL-TR-96-3074,
WL-TR-97-3059,

AD B955 265
AD B166 585
AD B212 813 - OK ST-A
AD B212 361 ST-A
AD B232 172 ~~ST-A~~

B212361

Joseph A. Burke

JOSEPH A. BURKE, Team Leader
STINFO and Technical Editing
Technical Information Division